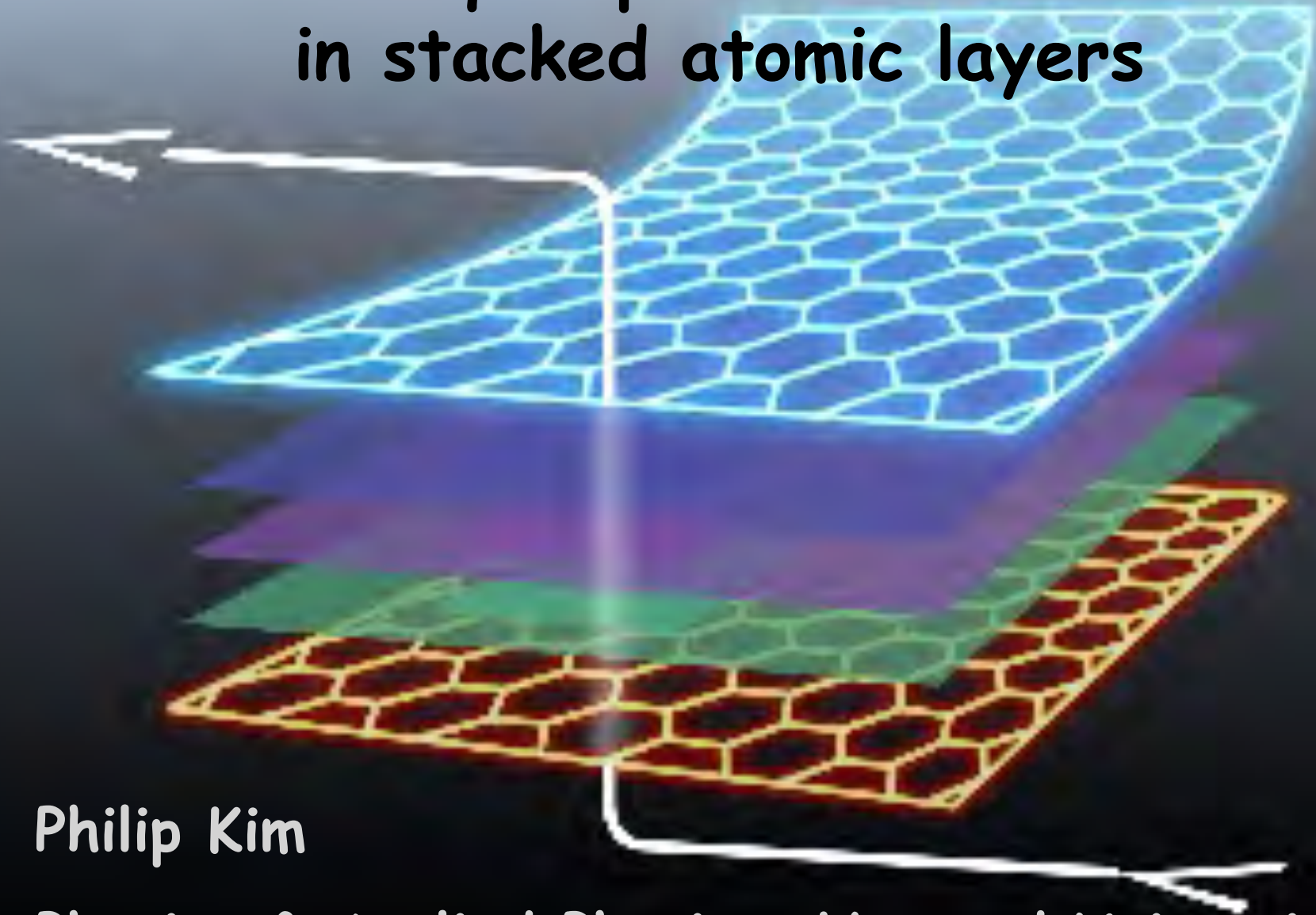


Unusual quasiparticle correlation in stacked atomic layers

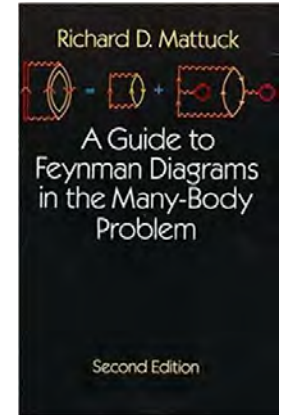


Philip Kim

Physics & Applied Physics, Harvard University

'Real' Particles and 'Quasi' Particles

R. Mattuck, "A guide to Feynman diagrams in the many-body problem"



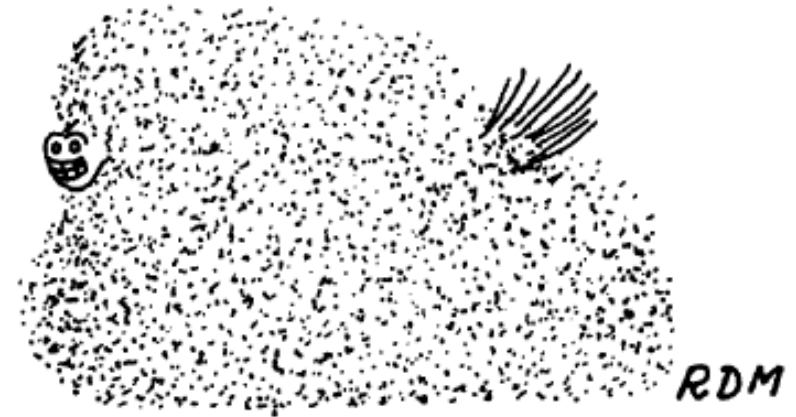
real particle



quasi particle



real horse

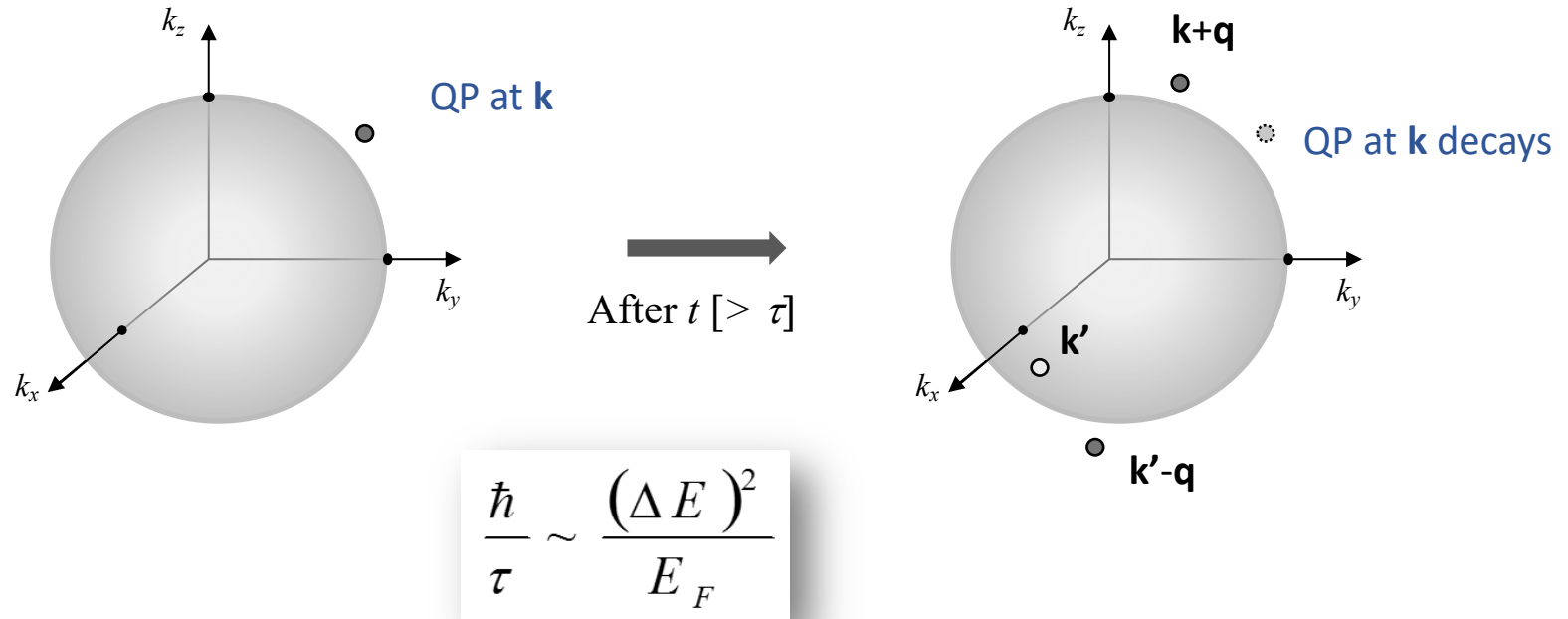


quasi horse

RDM

Landau Theory of Fermi Liquid

L. D. Landau (1957).



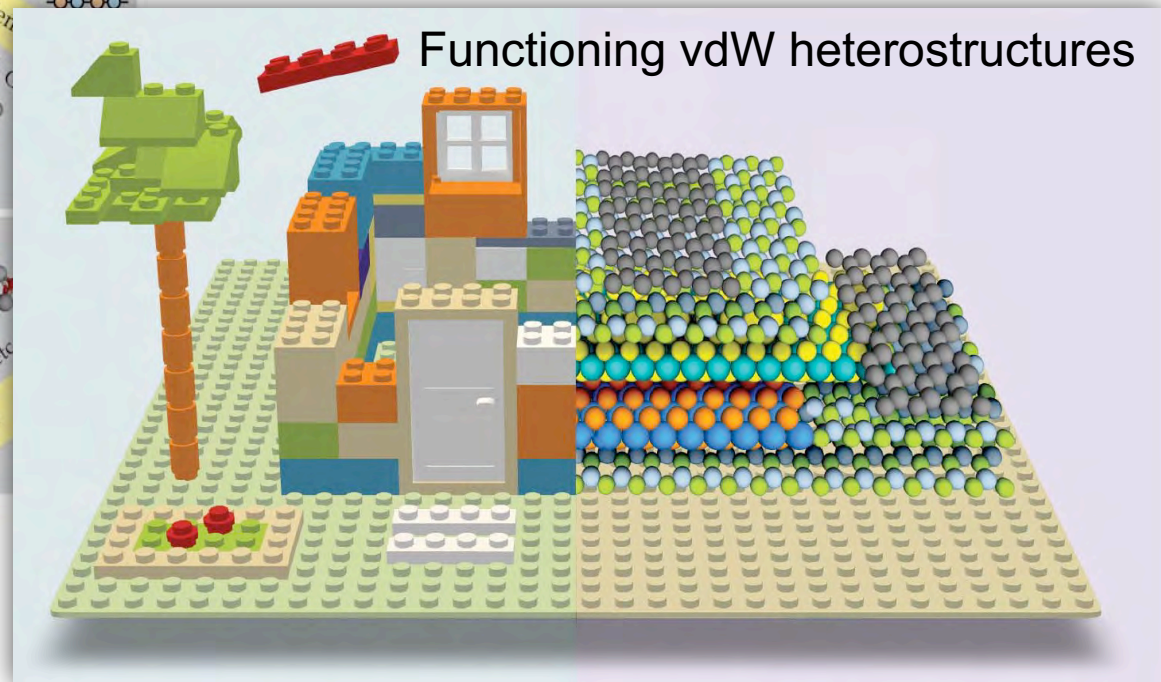
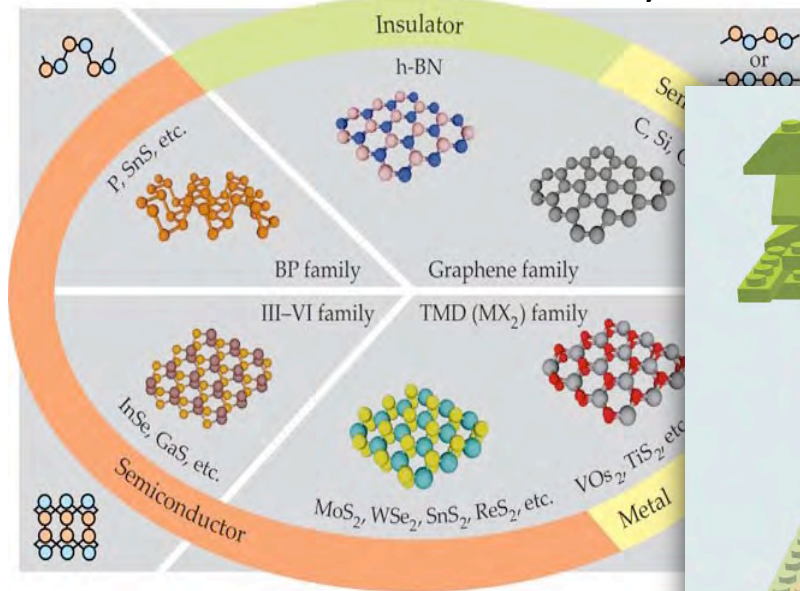
Fermi liquid: Weakly interacting quasiparticles

Non-Fermi liquid: Luttinger liquid (1D),
Strongly correlated system near the quantum criticality,
...

Assembling van der Waals Materials

2D van der Waals Materials Family

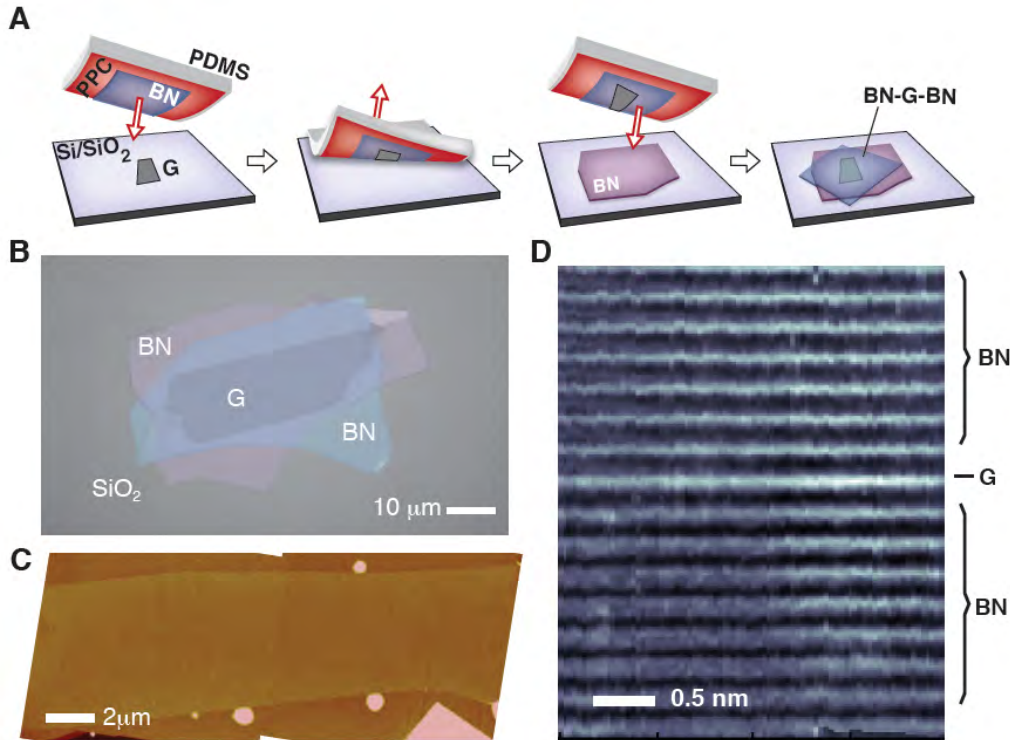
Ajayan, Kim and Banerjee, Physics Today (2016)



vdW Materials (partial list)

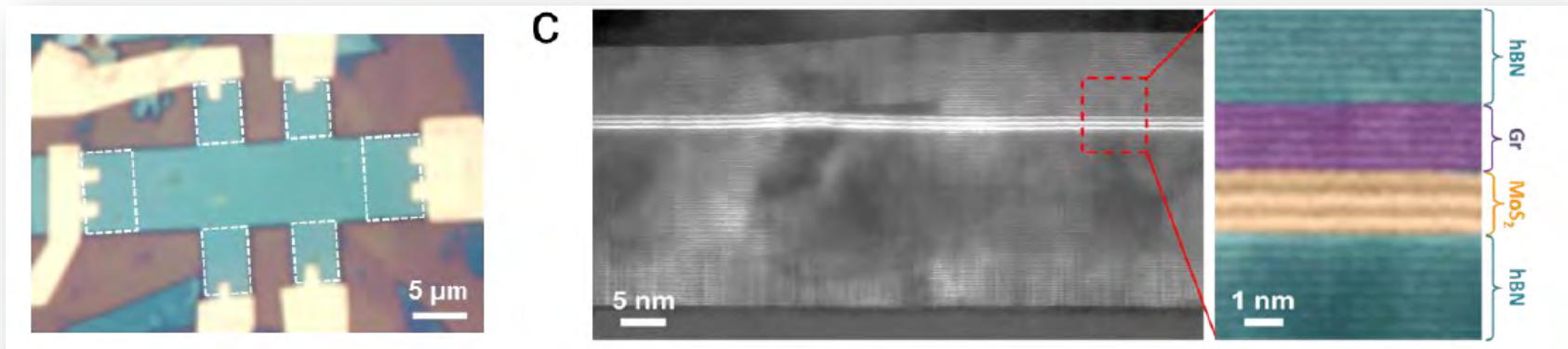
- **Semiconducting materials:** WSe_2 , $MoSe_2$, MoS_2 , WS_2 , BP...
- **Complex-metallic compounds :** $TaSe_2$, TaS_2 , ...
- **Magnetic materials:** Fe- TaS_2 , $CrSiTe_3$, CrI_3 ...
- **Superconducting:** $NbSe_2$, $Bi_2Sr_2CaCu_2O_{8-x}$, ...
- **Topological Insulator/Wyle SM:** Bi_2Se_3 , $MoTe_2$

Atomic Layer-by-Layer Stacking Up of VdW Materials



L. Wang *et al*, Science (2013)

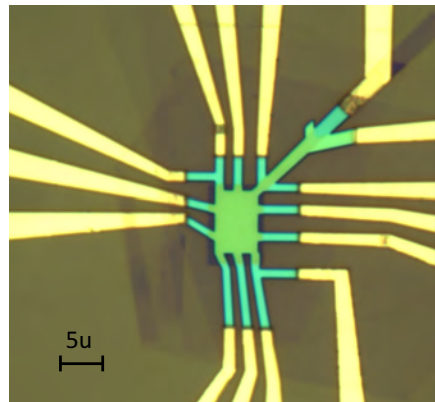
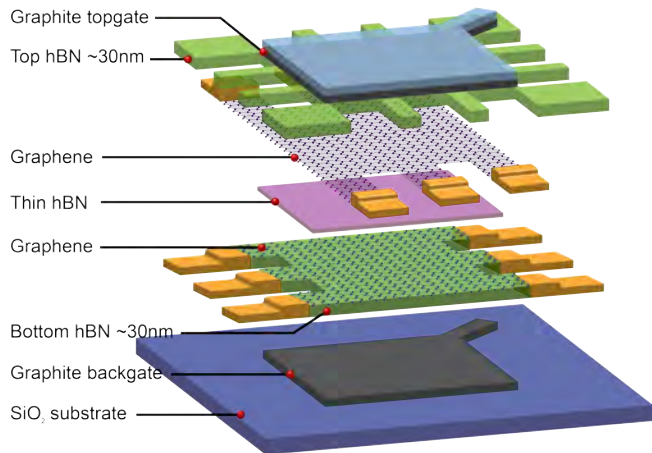
- Creation of multilayer systems with co-lamination techniques
- Encapsulated graphene in hBN
- Completely ballistic at low temperature



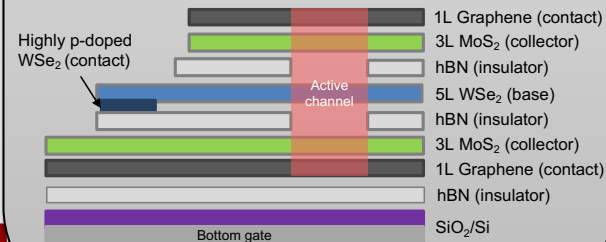
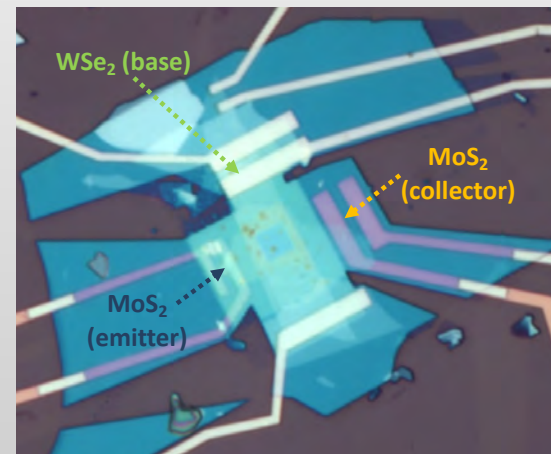
Xu *et al.*, Nature Nano (2015) (Hone group collaboration)

vdW Heterostructure Devices

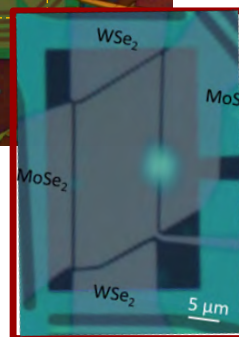
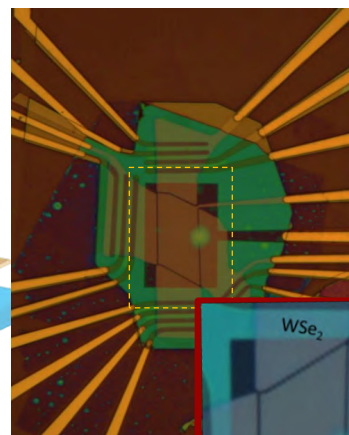
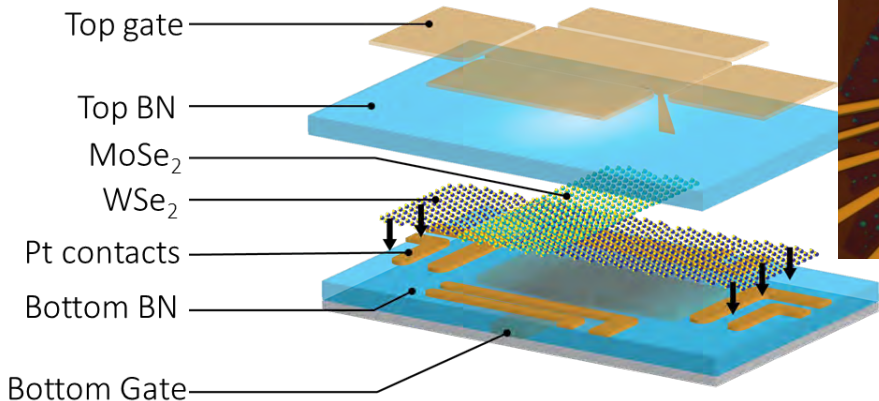
Coulomb Drag in Graphene



vdW Bipolar Transistor



WSe₂/MoSe₂ Optoelectric Device



Van der Waal Heterostructures

	Graphene	hBN	MoS ₂	WSe ₂	NbSe ₂	TaS ₂	Cr ₂ Ge ₂ Te ₆	Bi ₂ Se ₃
Graphene (semimetal)	Twisted stacking	Hofstadter Butterfly; tunneling	Schottky diode	Schottky diode	Andreev reflection	Super lattice potential	Magnetic insulating	Contacting surface states
hBN (insulator)		Twisted stacking	Encapsulation	Encapsulation	Encapsulation, tunneling	Encapsulating, tunneling	Control exchange interaction	Encapsulating, tunneling
MoS₂ (n-semicond)			Twisted stacking	Atomic pn junction	Supercond /Semicond junction	Super lattice modulation	Magnetic semiconductor	Valley trionics
WSe₂ (p-semicond)				Twisted stacking	Supercond /Semicond junction	Super lattice modulation	Magnetic semiconductor	Valley trionics
NbSe₂ (supercond.)					Josephson coupling	Competing order parameters	Triplet superconductor	Majorana
TaS₂ (CDW)						C-axis CDW orders	Competing order parameters	Super lattice modulation
Cr₂Ge₂Te₆ (magnetic)							C-axis magnetic orders	Creating gap in TI surface
Bi₂Se₃ (T. I.)								Annihilation of TI surface states

performed

in-progress

Planned

~ 5 years ago

Outline

- Electron and hole interaction near the Dirac point:
Dirac Fluid in graphene
- Electron and hole correlation across the vdW interface:
Long lived interlayer excitons
- Electron and hole correlation across the Landau levels:
Magnetoexciton condensation in Quantum Hall bilayer
- Ferromagnetic Superconductors in Flat bands:
Twisted Double Bilayers
- Electron and hole correlation by superconducting proximitized quantum Hall edge: **Crossed Andreev reflection**

Observation of the Dirac fluid and the breakdown of the Wiedemann-Franz law in graphene



Jess Crossno



Kin Chung Fong

J. Crossno, J. K. Shi, K. Wang, X. Liu, A. Harzheim, A. Lucas, S. Sachdev, P. Kim, T. Taniguchi, K. Watanabe, T. A. Ohki, K. C. Fong
Science **351**, 1058-1061 (2016).



Jing K. Shi



Ke Wang



Achim Harzheim



Thomas Ohki



Andrew Lucas



Subir Sachdev



T. Taniguchi, K. Watanabe



Jonah Weissman



Artem Talanov



Zhonging Yan



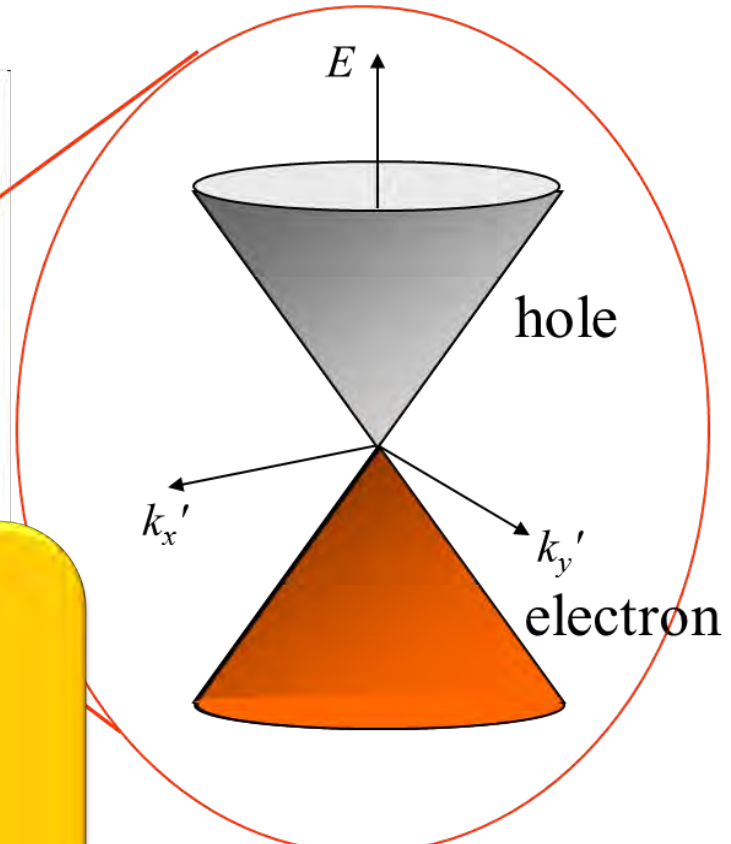
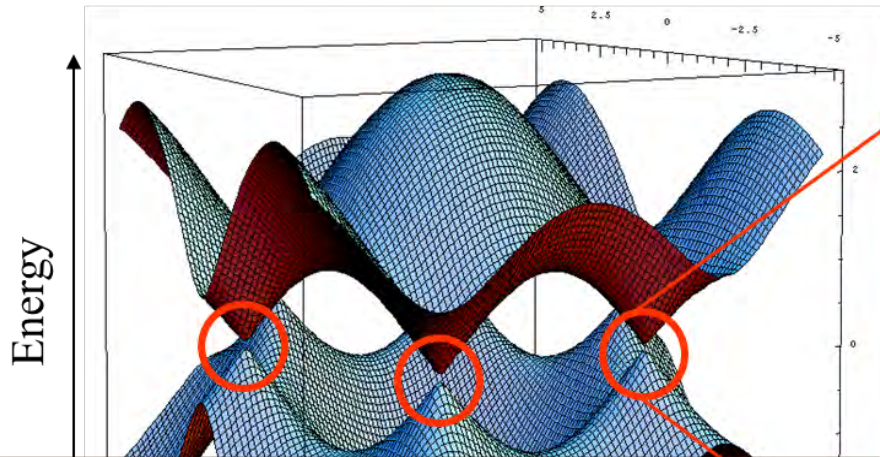
Sang-Jin Sin



Matt Forster

Dirac Point in Graphene

Band structure of graphene (Wallace 1947)



Physics at Dirac Point

- Symmetry protected degeneracy
- Charge Neutral
- Strong electro-electron interaction
- Quantum Criticality

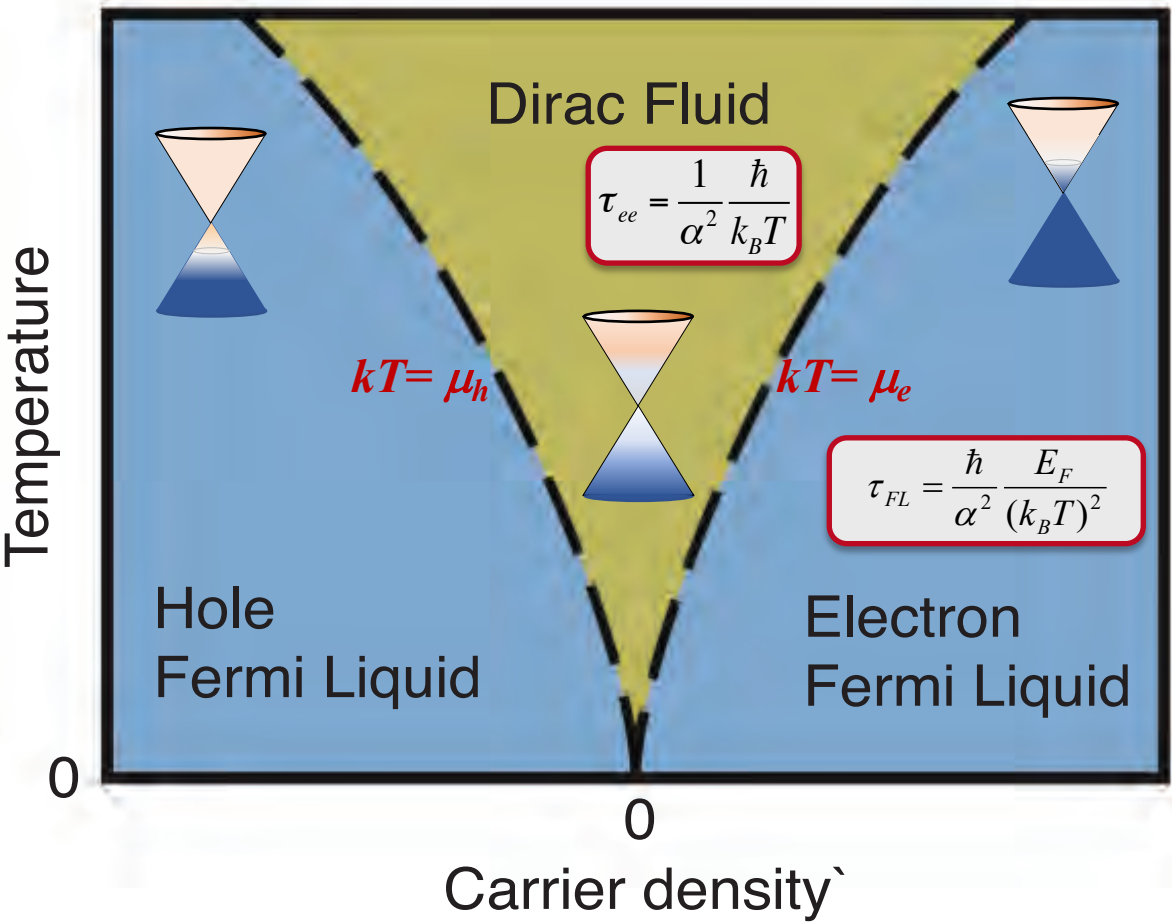
$$E \approx \hbar v_F |\vec{k}'_{\perp}|$$

speed v_F

Effective Fine Structure Constant $\alpha = \frac{e^2}{\epsilon_r \hbar v_F} \sim 1$

Effective Dirac Hamiltonian: $H_{eff} = \pm \hbar v_F \vec{\sigma} \cdot \vec{k}'_{\perp}$

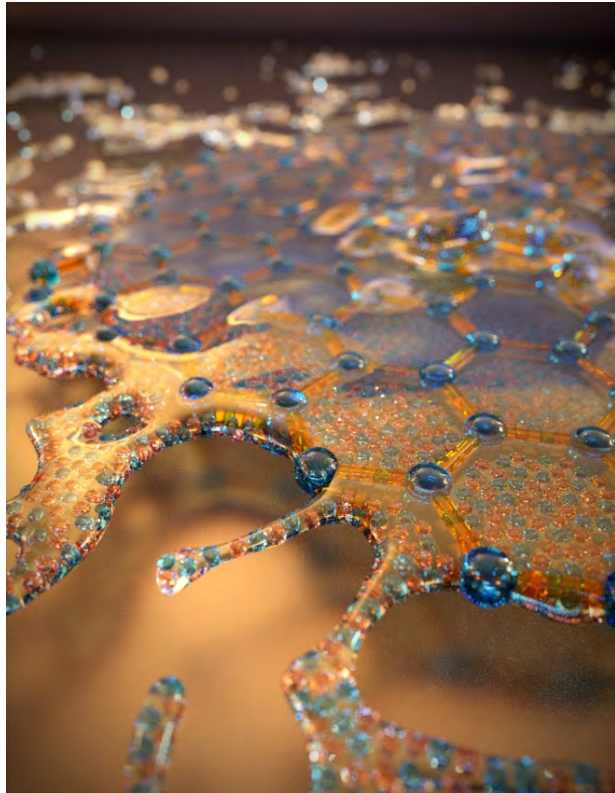
Hydrodynamic Transport in Dirac Point in Graphene



Condition of hydrodynamic description:

$$\tau_{ee} \ll \tau_{imp}$$

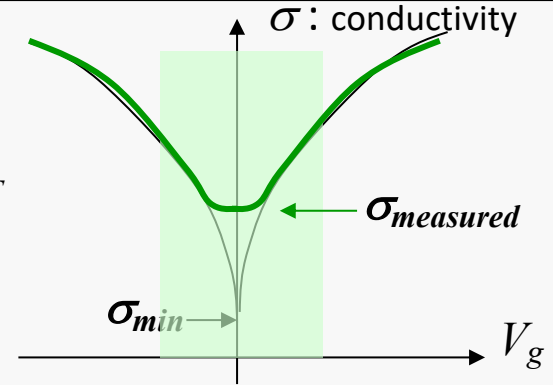
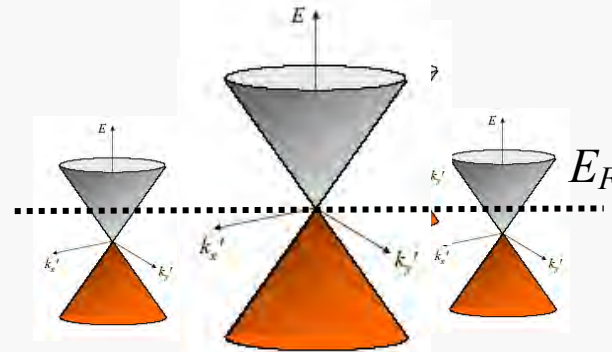
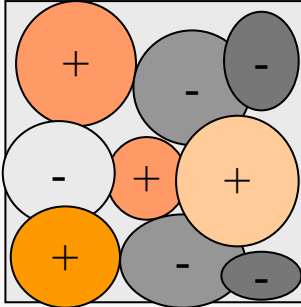
Sheehy and Schmalian, PRL 99, 226803 (2007)
 Fritz, Schmalian, Muller, and Sachdev, PRB (2008).
 Mueller, Fritz, and Sachdev, PRB (2008).
 Foster and Aleiner, PRL (2009).
 Mueller, Schmalian, Fritz, PRL (2009)



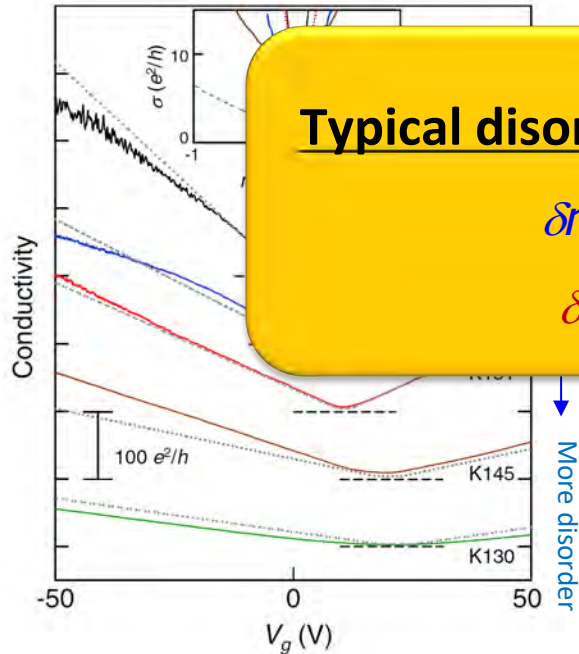
Dirac Fluid at the CNP of graphene

Disorder and Charge Puddles Near the Neutrality

Graphene sample



Conductivity of Graphene on SiO₂ Substrate



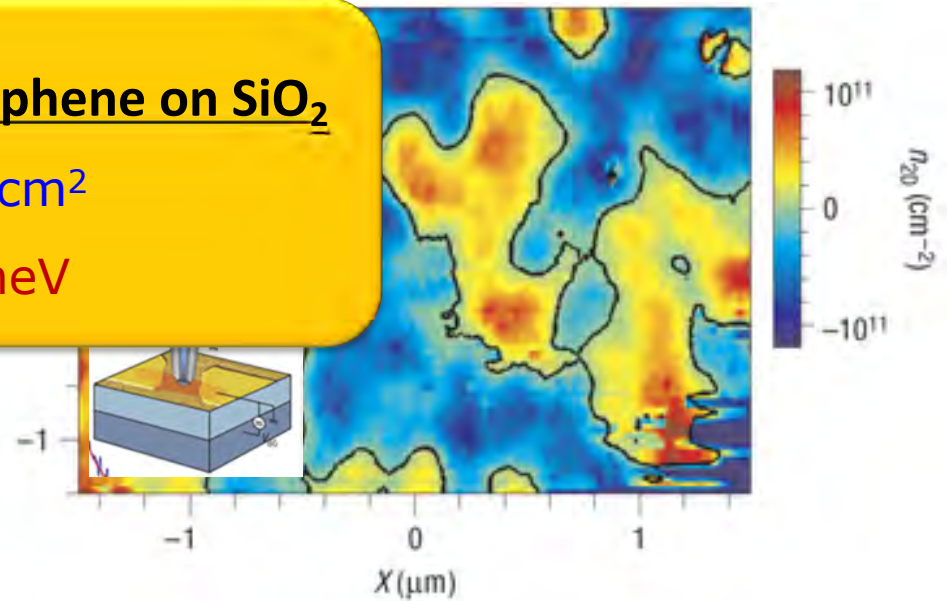
Typical disorder in graphene on SiO₂

$\delta n \sim 10^{11} / \text{cm}^2$

$\delta E_f \sim 40 \text{ meV}$

Tan et al., PRL (2008)

Potential Mapping by Scanning Single Electron Transistor



Martin et al., Nature Physics 4, 144 (2008)

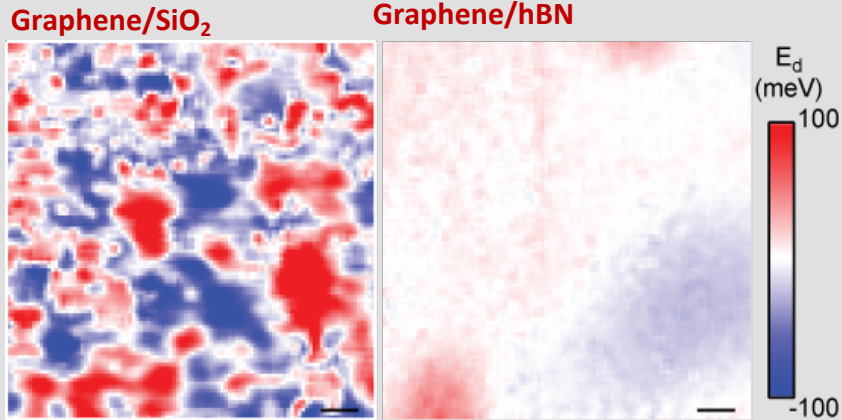
Stacking graphene on hBN

Dean et al. Nature Nano (2009)

Hone, Kim and Shepard groups collaboration

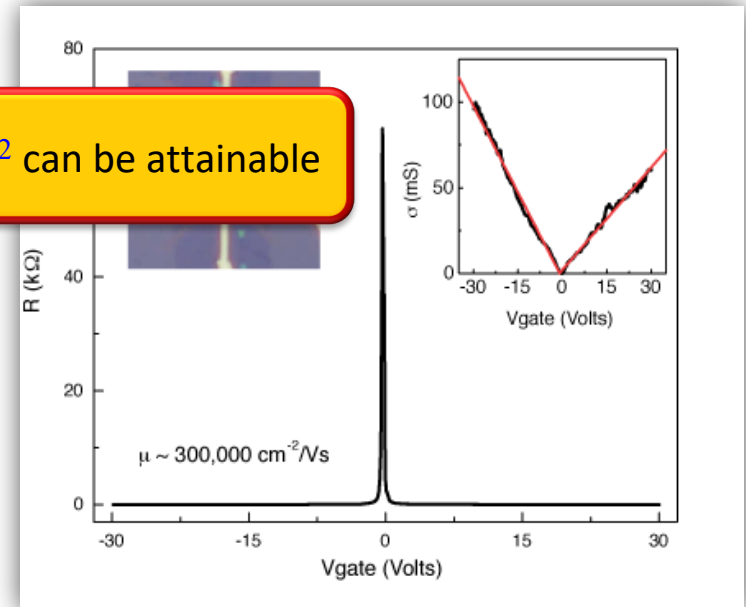
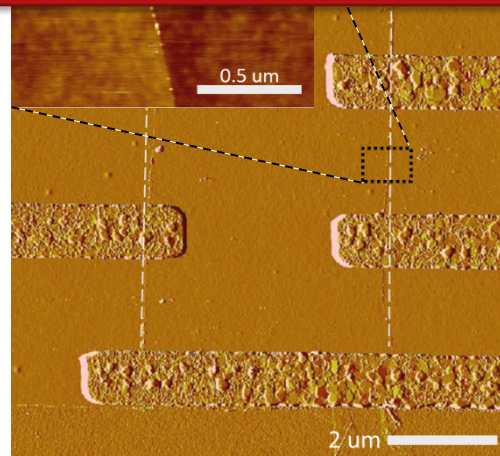
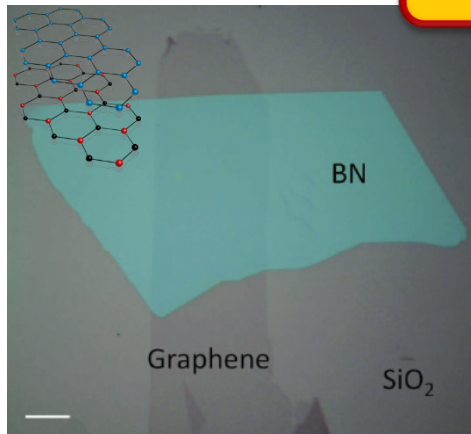
- Co-lamination techniques
- Submicron size precision
- Atomically smooth interface

Potential Fluctuation Measured by STM



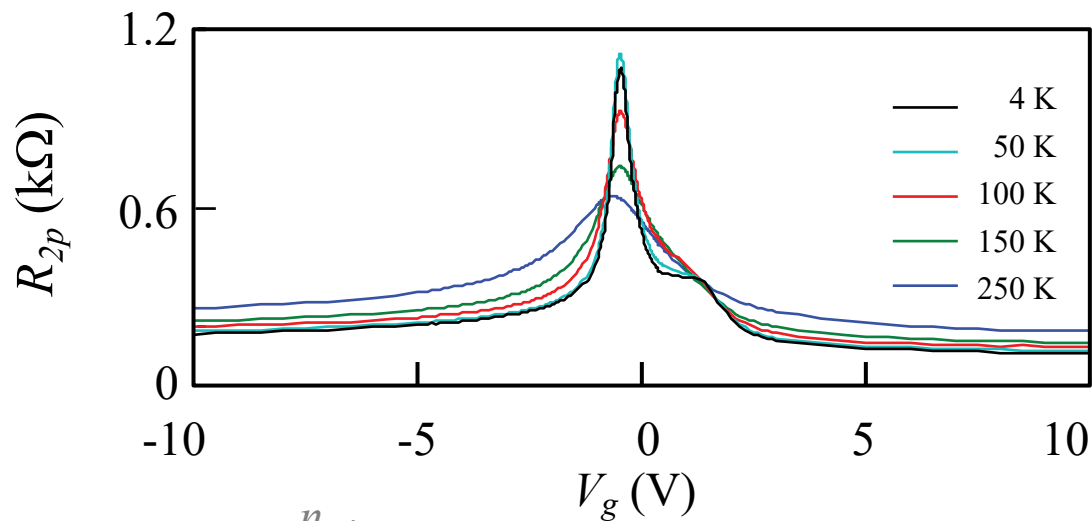
J. Xue *et al.* Nature Materials 10, 282 (2011)

Density fluctuation: $\delta n < 10^{10} / \text{cm}^2$ can be attainable

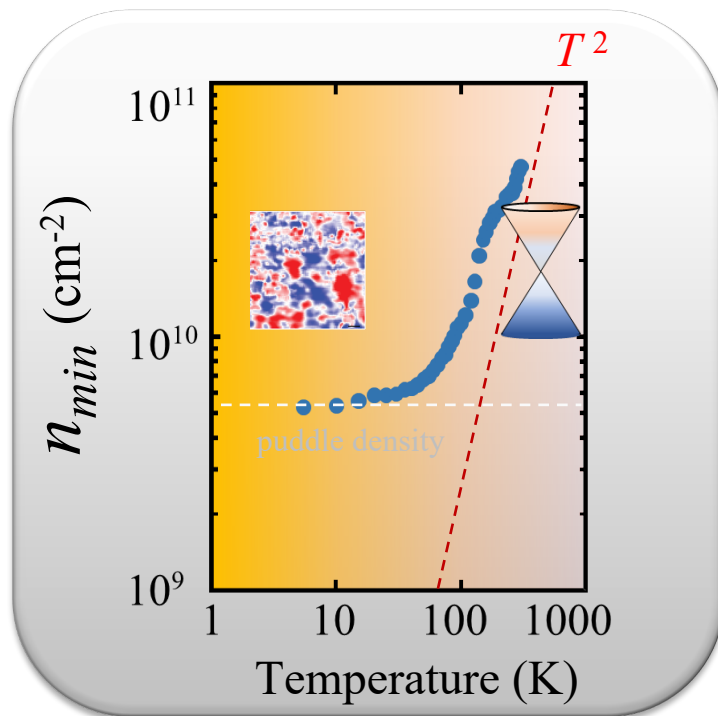
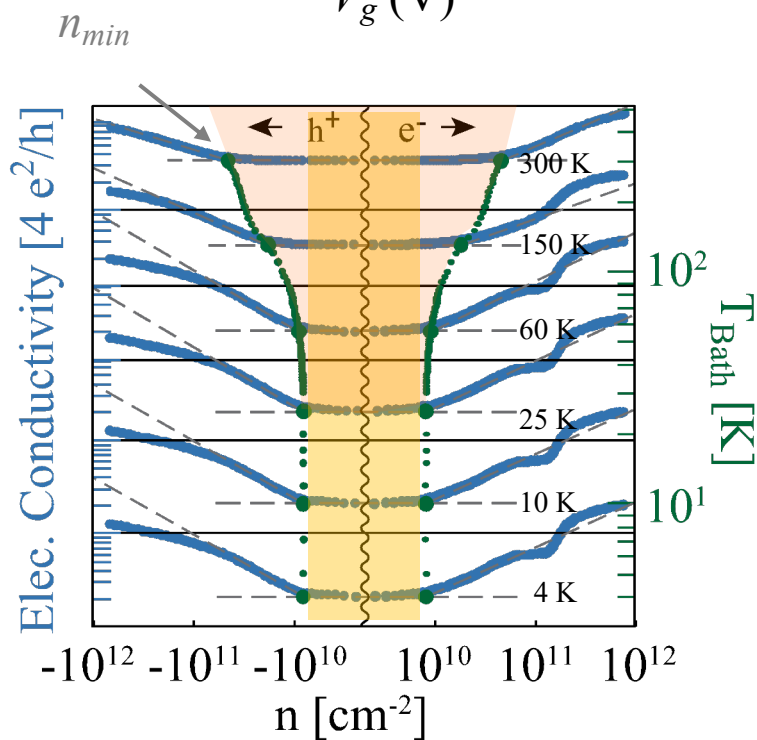
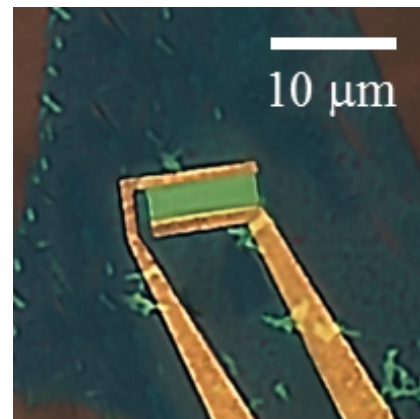


LT Mobility : $\sim 1,000,000 \text{ cm}^2 \text{V}^{-1} \text{s}^{-1}$
RT Mobility : $\sim 100,000 \text{ cm}^2 \text{V}^{-1} \text{s}^{-1}$

Non-Degenerate Electron Gas at Dirac Point



hBN encapsulated single layer graphene



Wiedemann Franz Law in Fermi Liquid

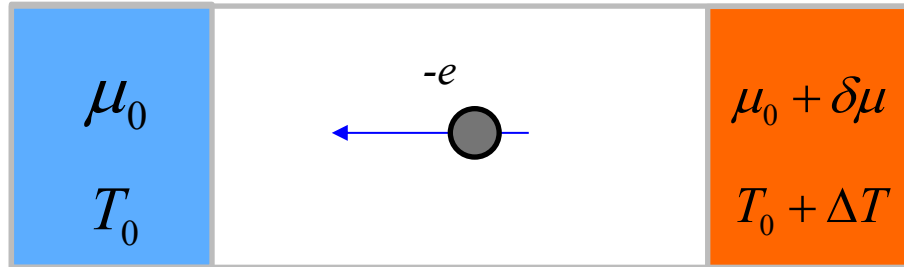
Thermal conductivity
versus electrical conductivity

$$\frac{\kappa}{\sigma T} = \frac{\pi^2}{3} \left(\frac{k_B}{e} \right)^2 = L_0 : \text{Sommerfeld value}$$

Relaxation of charge current and heat current

$$j = -en_e \langle v_e \rangle$$

$$j_Q = u_e n_e \langle v_e \rangle$$



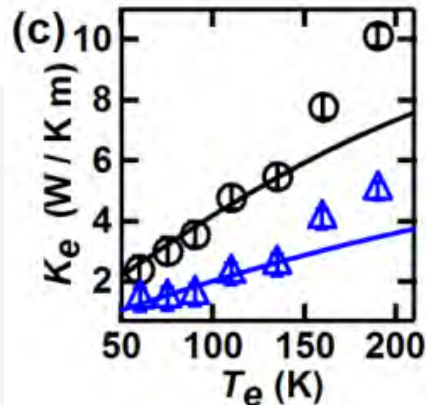
Works well for graphene in the degenerate limit...

NANO LETTERS

Wiedemann–Franz Relation and Thermal-Transistor Effect in
Suspended Graphene

S. Yiğen and A. R. Champagne*

Department of Physics, Concordia University, Montréal, Québec, H4B 1R6 Canada



PHYSICAL REVIEW X 3, 041008 (2013)

Measurement of the Electronic Thermal Conductance Channels
and Heat Capacity of Graphene at Low Temperature

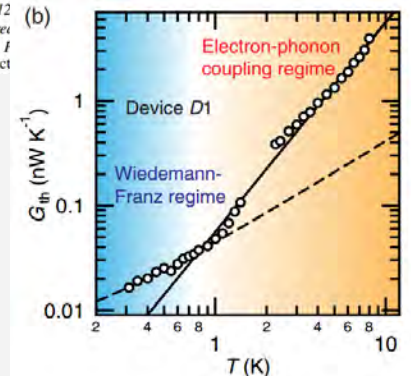
Kin Chung Fong,¹ Emma E. Wollman,¹ Harish Ravi,¹ Wei Chen,² Aashish A. Clerk,²
M. D. Shaw,³ H. G. Leduc,³ and K. C. Schwab^{1,*}

¹Kavli Nanoscience Institute, California Institute of Technology, MC 12

²Department of Physics, McGill University, Montreal

³Jet Propulsion Laboratory, California Institute of Technology, I

(Received 29 June 2013; published 29 Oct



Wiedemann Franz in Non Fermi Liquid

ARTICLE

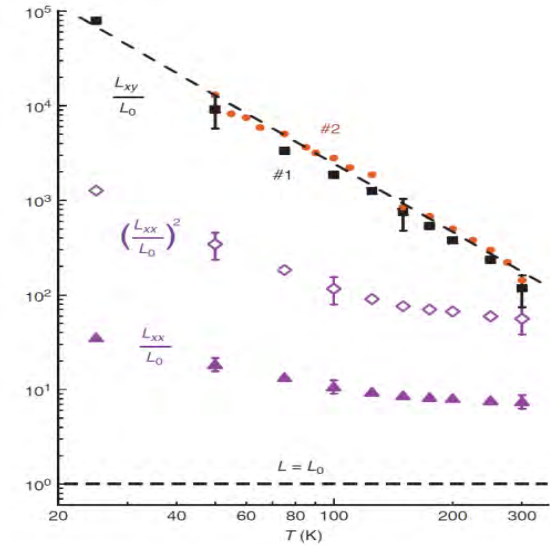
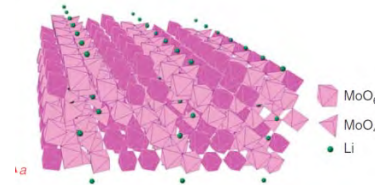
NATURE COMMUNICATIONS | 2:396 | DOI: 10.1038/ncomms1406

Received 25 Feb 2011 | Accepted 20 Jun 2011 | Published 19 Jul 2011

DOI: 10.1038/ncomms1406

Gross violation of the Wiedemann-Franz law in a quasi-one-dimensional conductor

Nicholas Wakeham¹, Alimamy F. Bangura^{1,2}, Xiaofeng Xu^{1,3}, Jean-Francois Mercure¹, Martha Greenblatt⁴ & Nigel E. Hussey¹



REPORT

Lee et al., *Science* **355**, 371–374 (2017) 27 January 2017

SOLID-STATE PHYSICS

Anomalously low electronic thermal conductivity in metallic vanadium dioxide

Sangwook Lee,^{1,2*} Kedar Hippalgaonkar,^{3,4*} Fan Yang,^{3,5*} Jiawang Hong,^{6,7*} Changhyun Ko,¹ Joonki Suh,¹ Kai Liu,^{1,8} Kevin Wang,¹ Jeffrey J. Urban,⁵ Xiang Zhang,^{3,8,9} Chris Dames,^{3,8} Sean A. Hartnoll,¹⁰ Olivier Delaire,^{7,11†} Junqiao Wu^{1,8†}

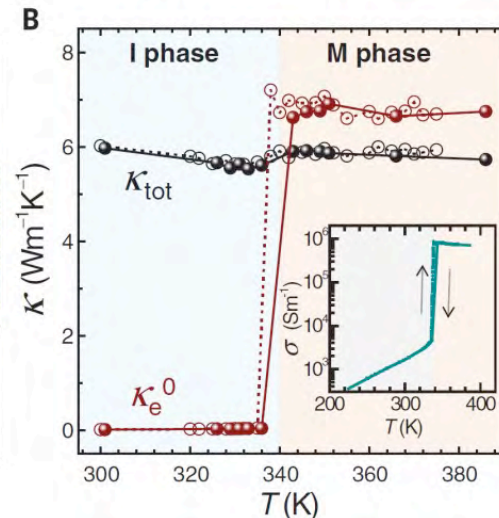
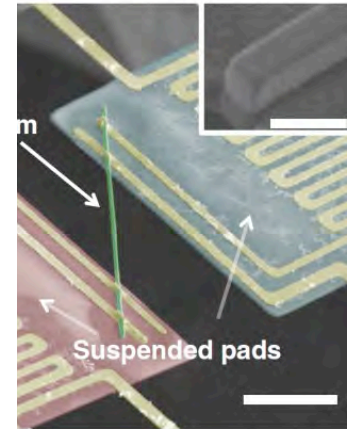
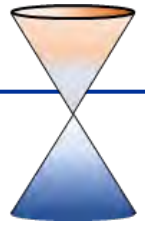


Fig. 1. Thermal conductivity of VO₂ across the metal-insulator transition. (A) False-color scanning

Charge and Heat Transport at Dirac Point



For a Dirac fluid at chemical potential $\mu = 0$;

Density: $n_e = n_h$

Energy density: $u_e = u_h$

Drift velocity: $|\langle v_e \rangle| = |\langle v_h \rangle|$

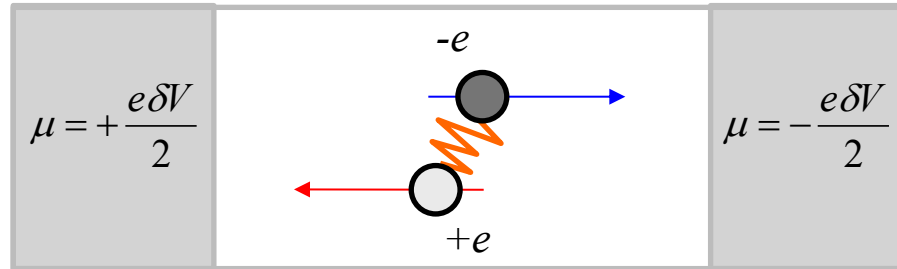
Charge current: $j = en_h \langle v_h \rangle + (-e)n_e \langle v_e \rangle$

Heat current: $j_Q = u_h n_h \langle v_h \rangle + u_e n_e \langle v_e \rangle$

Electric Transport

$$j \neq 0$$

$$j_Q = 0$$

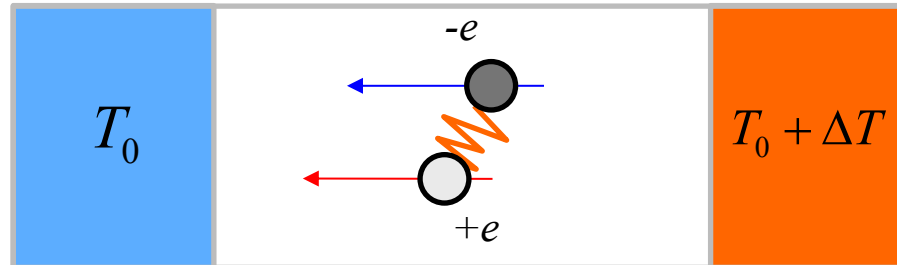


e-h interaction provides a **friction** to electric current!

Thermal Transport

$$j = 0$$

$$j_Q \neq 0$$



e-h interaction provides **no friction** to heat current!

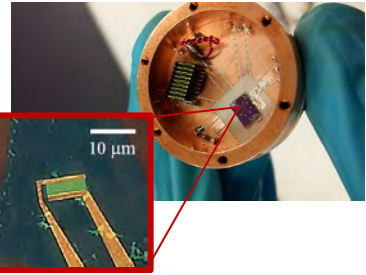
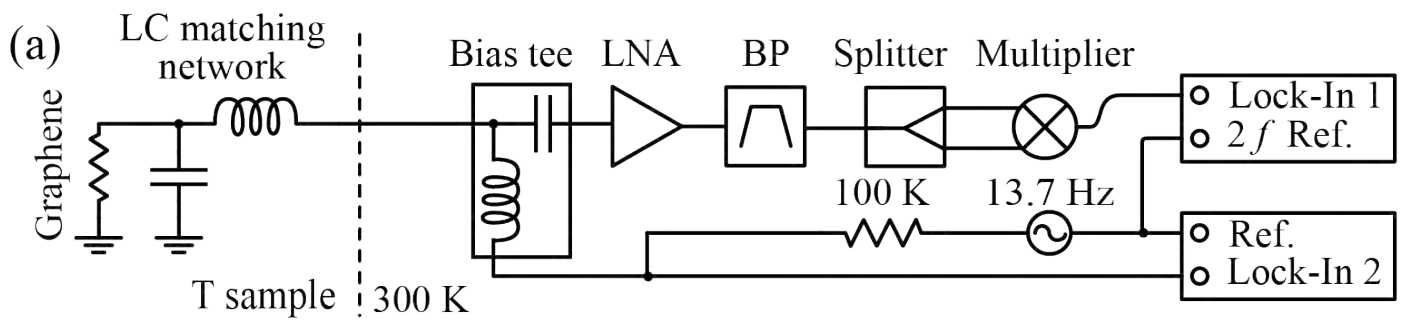
Near the charge neutrality,

$$\frac{\kappa}{\sigma T} > \frac{\pi^2}{3} \left(\frac{k_B}{e} \right)^2 = L_0$$

- L. Fritz, J. Schmalian, M. Müller, and S. Sachdev, Phys. Rev. B 78, 085416 (2008).
- M. Müller, L. Fritz, and S. Sachdev, Phys. Rev. B 78, 115406 (2008); M. Müller and S. Sachdev, *ibid.* 78, 115419 (2008).
- M. S. Foster and I. L. Aleiner, Phys. Rev. B 77, 195413 (2008).

Johnson Noise Thermometry for Thermal Conductivity Measurement

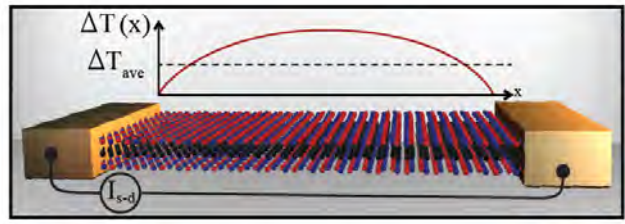
J. Crossno *et al.*, APL (2015)



$$\sqrt{4k_b T \Delta f R} = V_{RMS}$$

Electron temperature can be measured in the range of 1-300 K @ 100 MHz

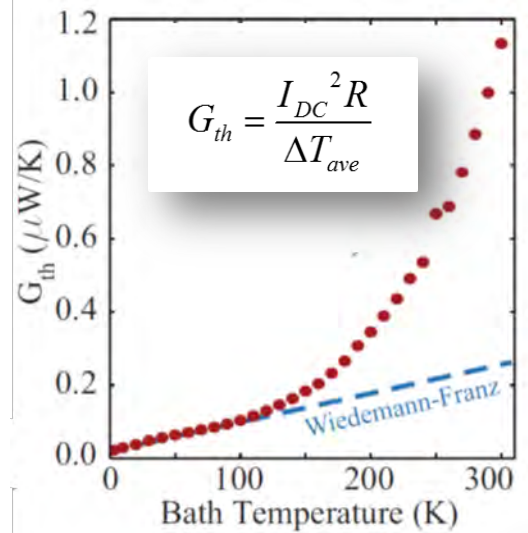
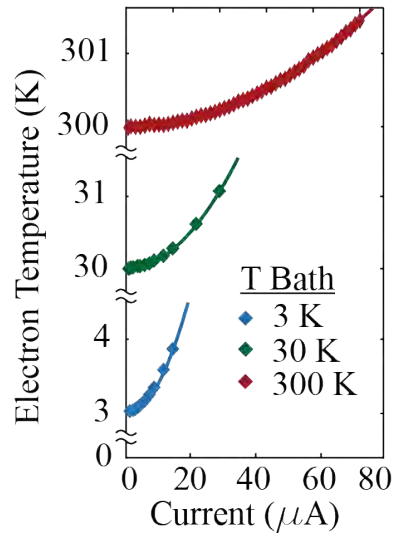
Joule heating by DC bias through bias T



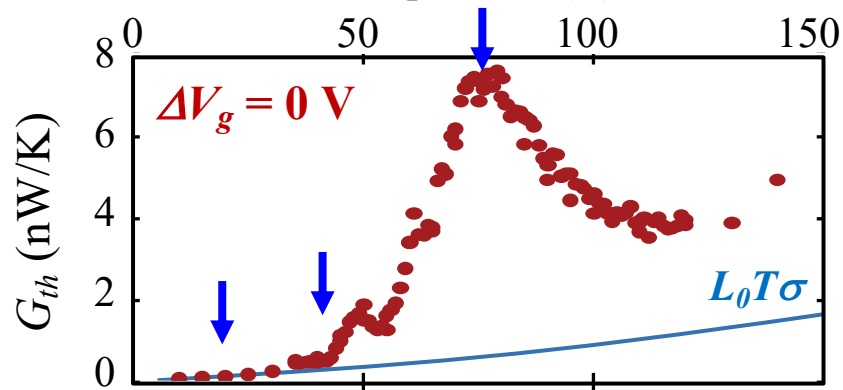
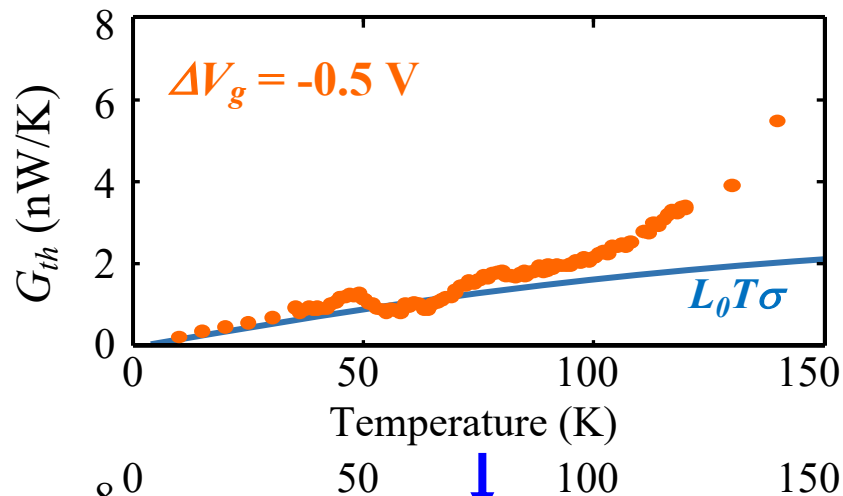
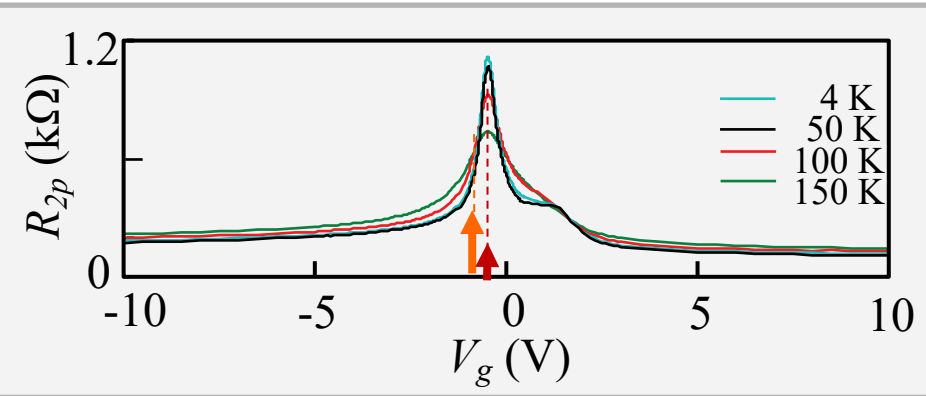
Johnson Noise Temperature

$$T_{JN} = \frac{\int \dot{q}(x, y) * T(x, y) dA}{\int \dot{q}(x, y) dA}$$

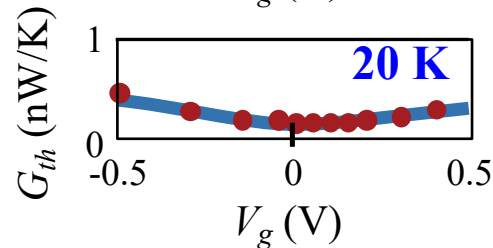
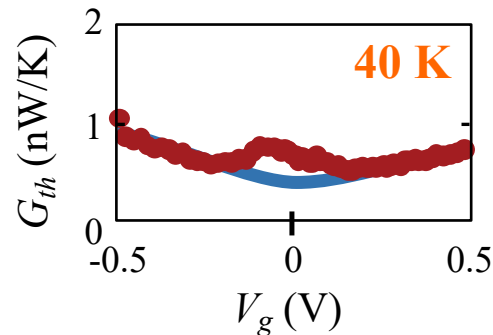
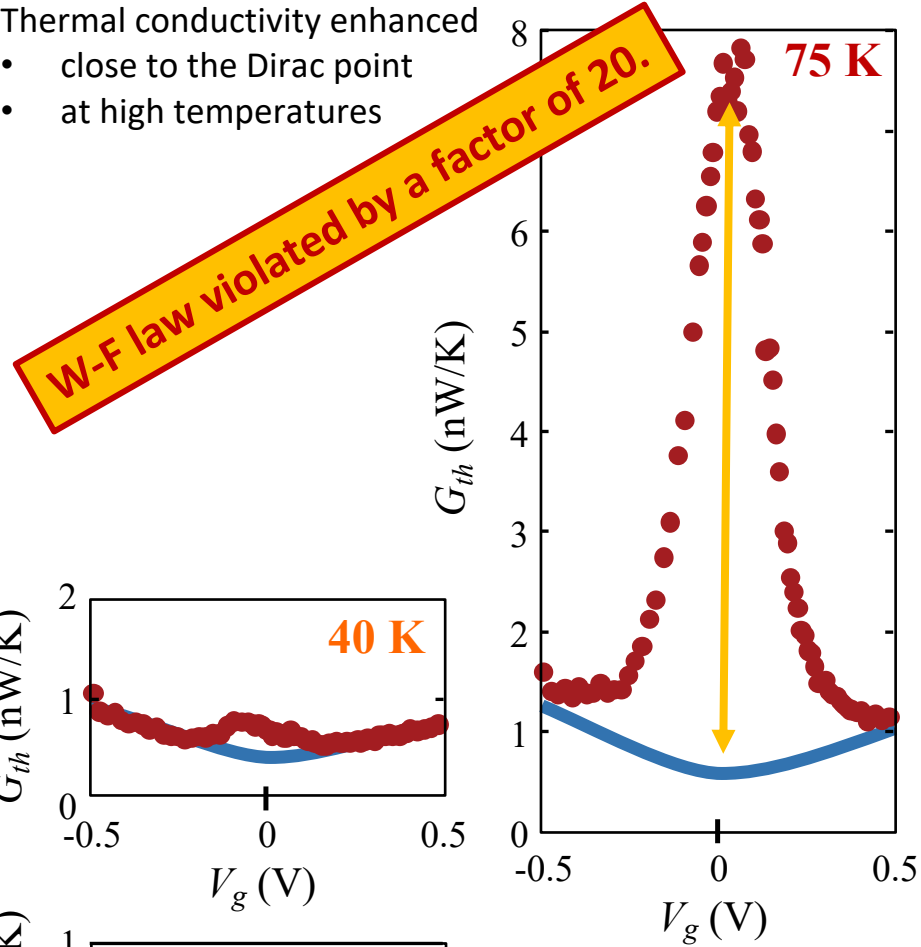
Local heat dissipation



Electronic Thermal Conductance Near the Neutrality



- Thermal conductivity enhanced
- close to the Dirac point
 - at high temperatures



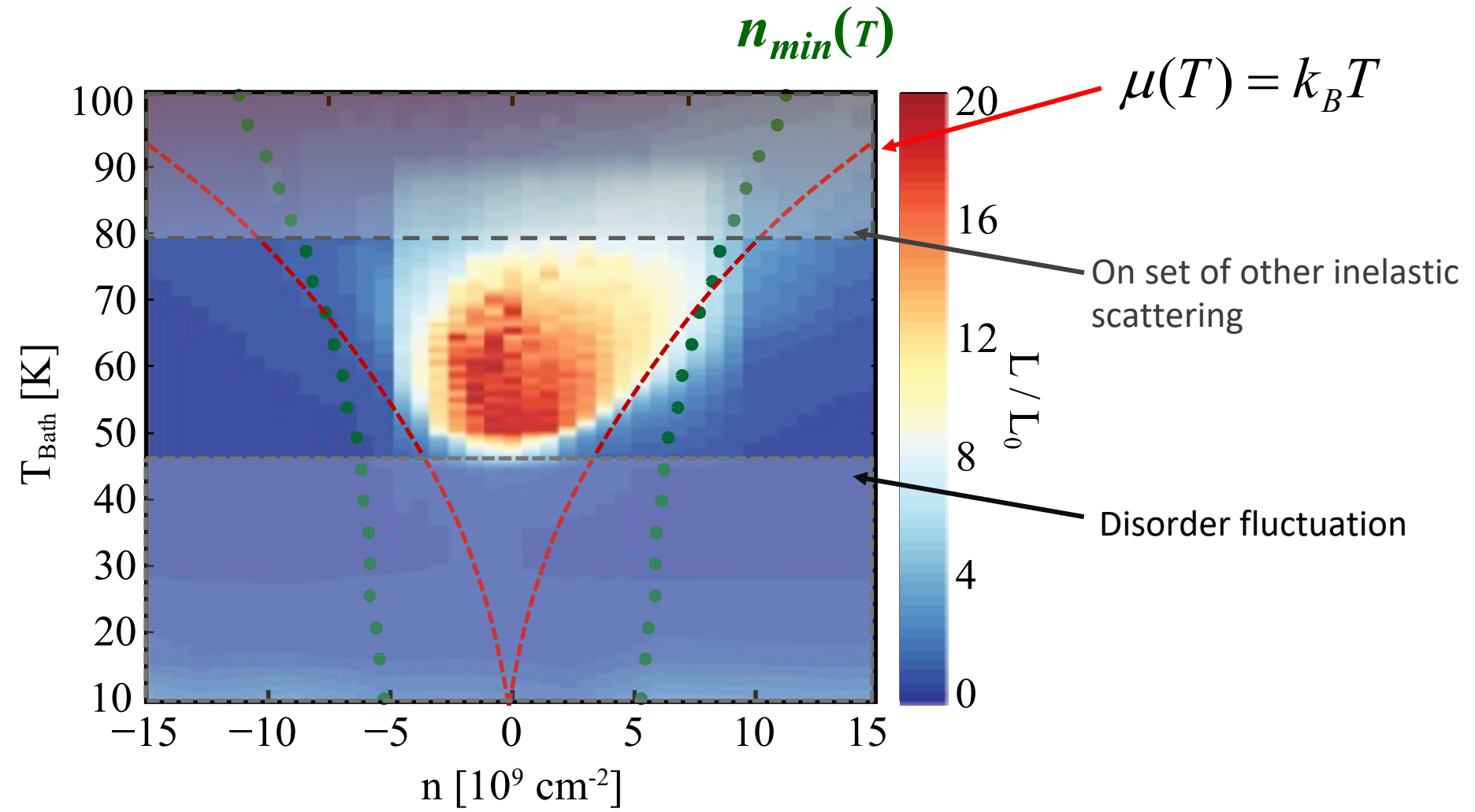
Lorentz Number as Function of Temperature and Density

Experimentally obtained Lorentz value:

$$L = \frac{\kappa}{\sigma T} \approx \frac{G_{th} R}{12T}$$

Sommerfeld value:

$$L_0 = \frac{\pi^2}{3} \left(\frac{k_B}{e} \right)^2$$



Relativistic Hydrodynamics Analysis

Muller *et al*, PRB (2008) & Foster *et al.*, PRB (2009)

Lorentz number for Dirac fluid

$$L = \frac{1}{((n/n_0)^2 + 1)} L_c$$

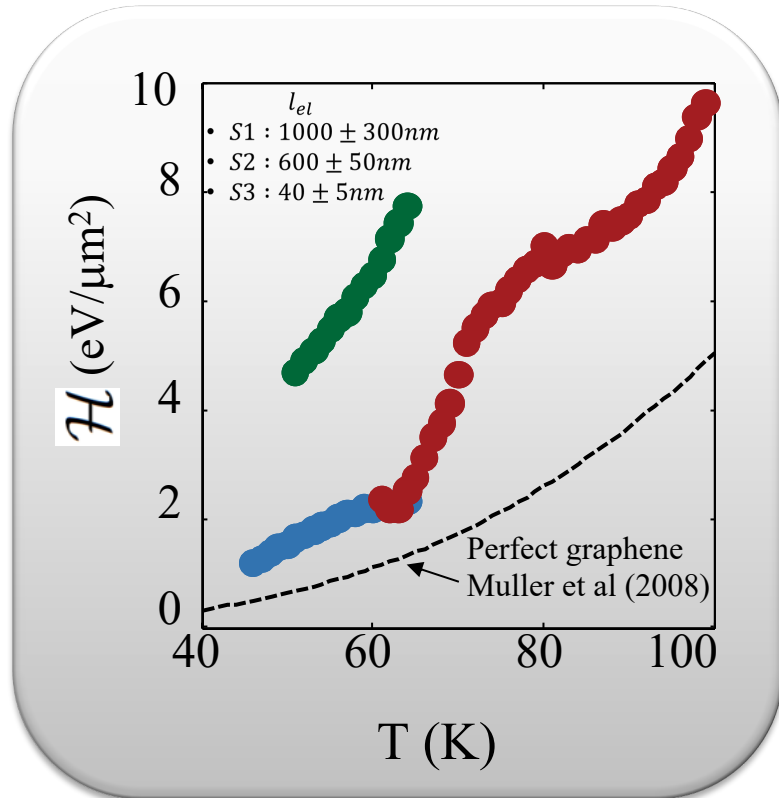
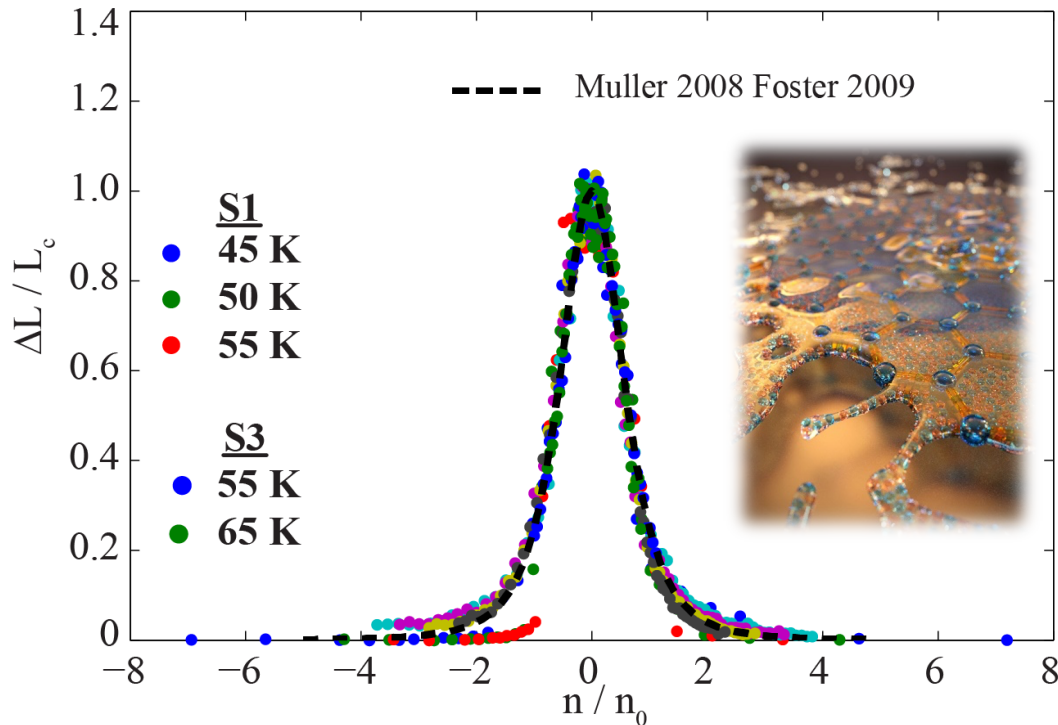
$$L_c = \frac{v_F}{\sigma_{min} T^2} \mathcal{H} \ell_{el}$$

$$n_0^2 = \frac{\sigma_{min}}{e^2 v_F} \frac{\mathcal{H}}{\ell_{el}}$$

\mathcal{H} : Fluid enthalpy density

ℓ_{el} : elastic mean free path

$\eta/s \sim 10 > 1/4\pi$ (Kovtun-Son-Starinets limit)
See A. Lucas arXiv: 1510.01738 for detail



Electrical and Thermal Conductance

Effect of Disorder

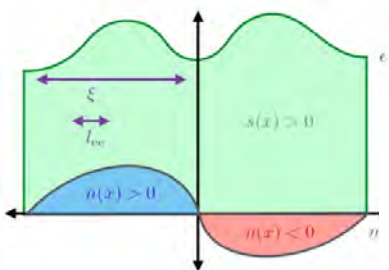
Lucas et al, PRB (2016).

$$\partial_\mu T^{\mu\nu} = e F^{\mu\nu} J_\nu \quad \text{and} \quad \partial_\mu J^\mu = 0$$

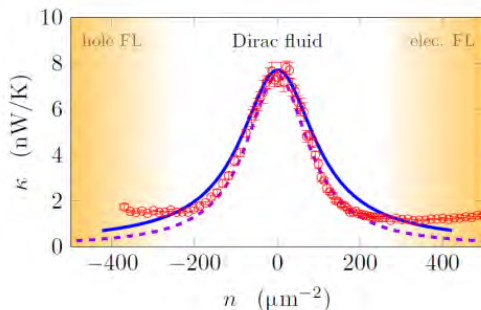
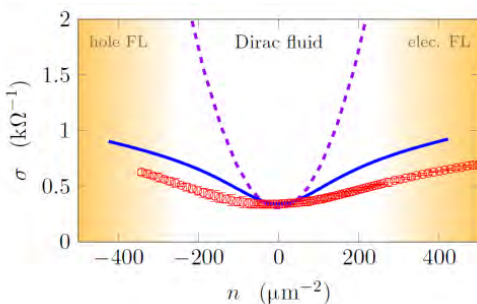
$$T^{ti} = (\varepsilon + P) v^i$$

$$T^{ij} = P \delta^{ij} - \eta (\partial^i v^j + \partial^j v^i) - (\zeta - \eta) \delta^{ij} \partial_k v^k$$

$$J^i = n v^i - \sigma_Q [\partial_i (\mu - \mu_0) - (\mu/T) \partial_i T]$$



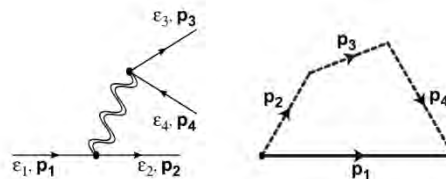
$$F_{\text{ext}}^{ti} = -F_{\text{ext}}^{it} = \partial_i \mu_0$$



Disorder affect charge current more than energy current

Slow Imbalance

Foster and Aleiner PRB (2012);



$$e^- \leftrightarrow e^- + e^- + h^+,$$

$$h^+ \leftrightarrow h^+ + h^+ + e^-.$$

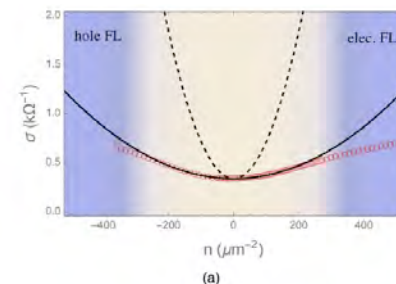
Kinematical constraint of the Dirac cone make the electron and hole current are nearly conserved separately.

Holography of the Dirac Fluid in Graphene with two currents

Yunseok Seo¹, Geunho Song¹, Philip Kim^{2,3}, Subir Sachdev^{2,4} and Sang-Jin Sin¹

PRL (2017)

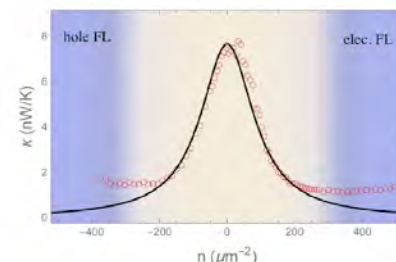
$$\sigma = W_0 + Z_0 + \frac{Q^2}{k^2 r_0^2}, \quad \kappa = \frac{(4\pi r_0^2)^2 T}{r_0^2 k^2 + (Q^2 + Q_n^2)/2Z_0}$$



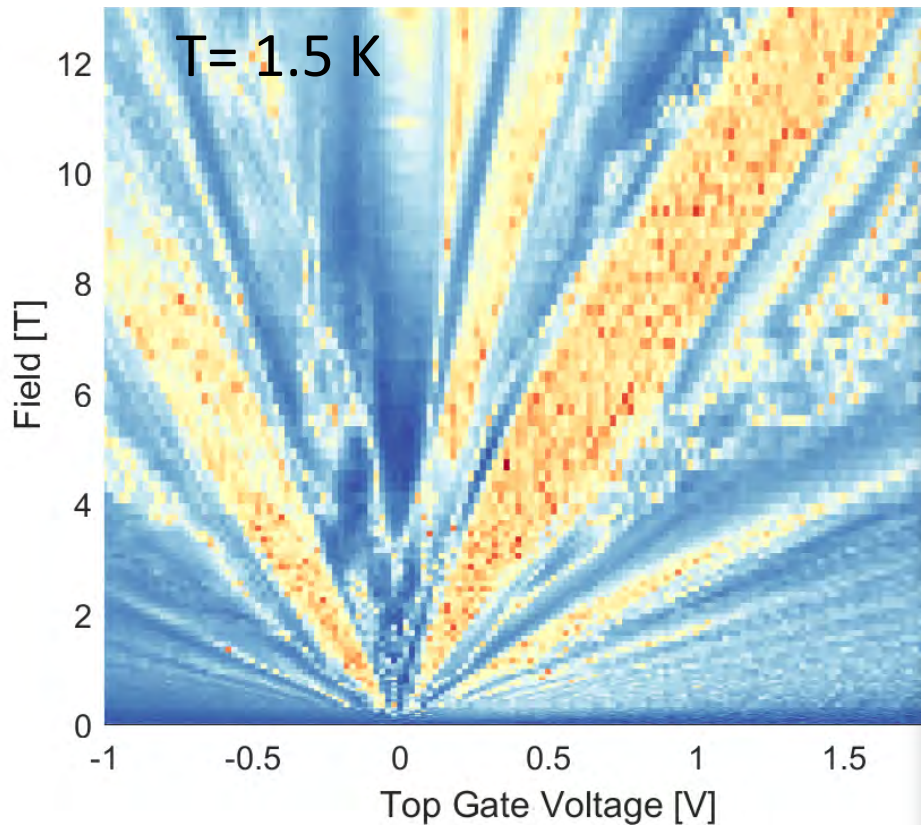
Charged current: $J = J_e + J_h$

Neutral current: $J_n = J_e - J_h$

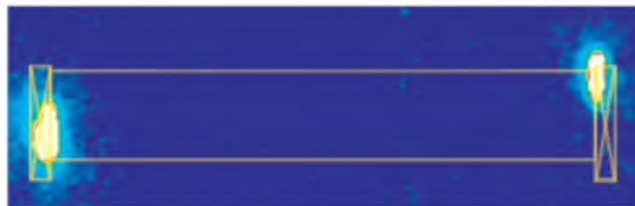
Corresponding conservative quantities by continuity equation: Q, Q_n



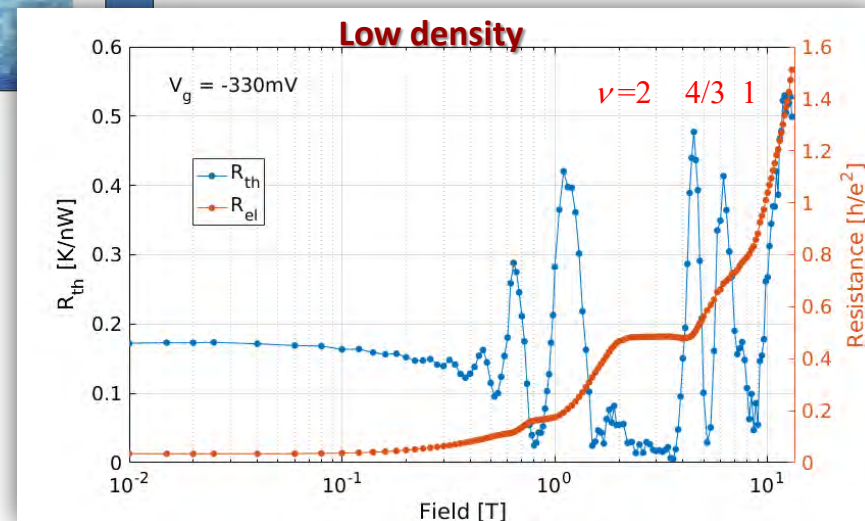
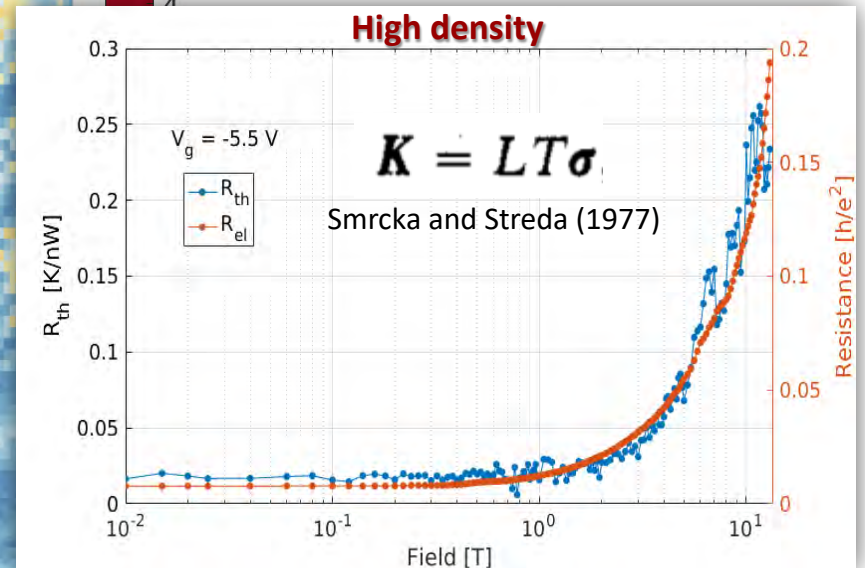
Magento-Thermal Transport Measurement



Hot spot formation in quantum Hall edge states



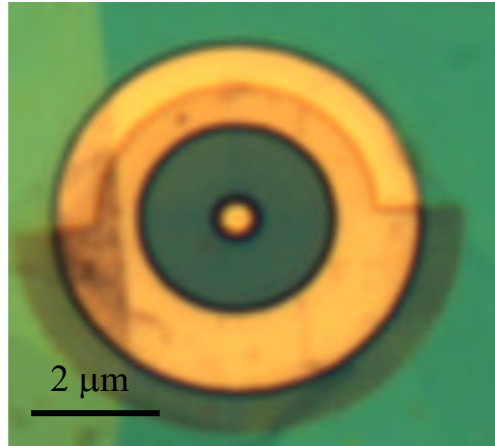
Ikushima et al (2007)



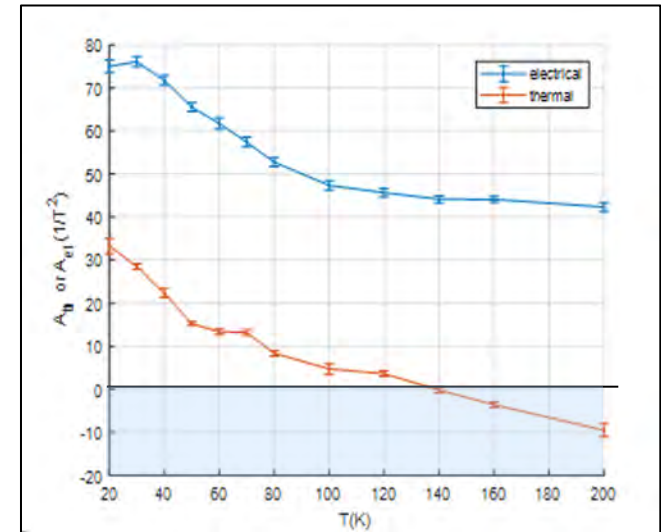
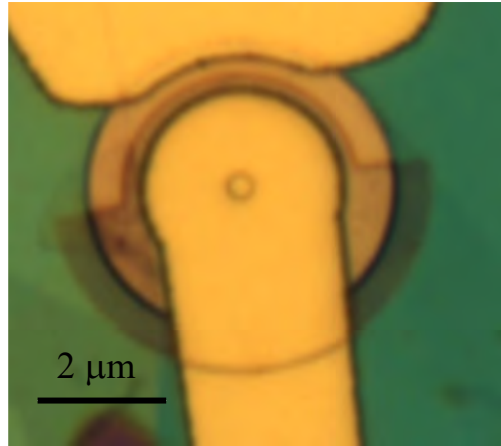
Crossno et al., unpublished

Magneto Thermal Transport in Corbino Device

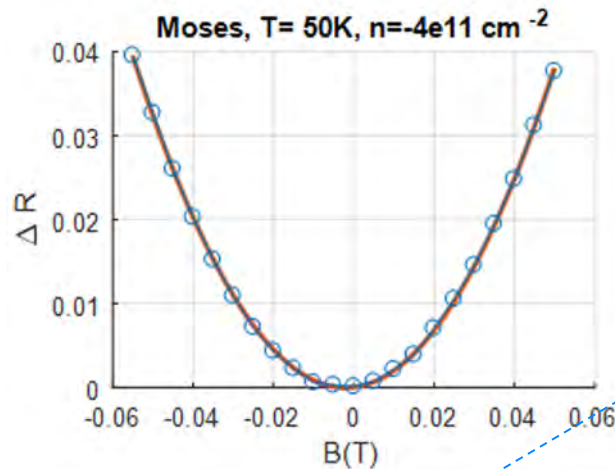
Corbino without bridge contact



Corbino with bridge contact



Normalized Magneto-Resistance

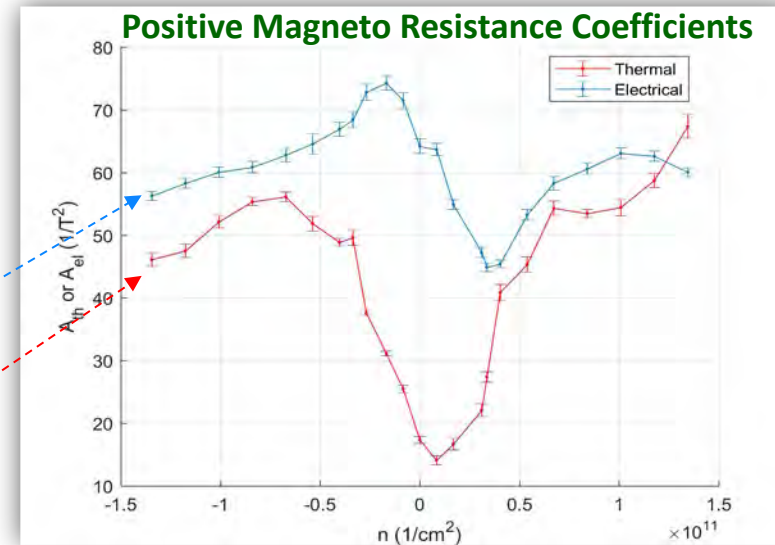


Electrical

$$\Delta R = \frac{R(B)}{R(0)} - 1 = A_{el} \cdot B^2$$

Thermal

$$\Delta R_{th} = \frac{R_{th}(B)}{R_{th}(0)} - 1 = A_{th} \cdot B^2$$

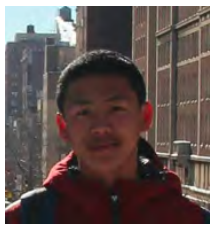


What can we extract viscosity from A_{el} and A_{th} ?

Magneto-Exciton Condensation in quantum Hall Graphene Double Layers



Xiaomeng Liu



Zeyu Hao



Jia Li.



Cory Dean.



Jim Hone



T. Taniguchi, K. Watanabe



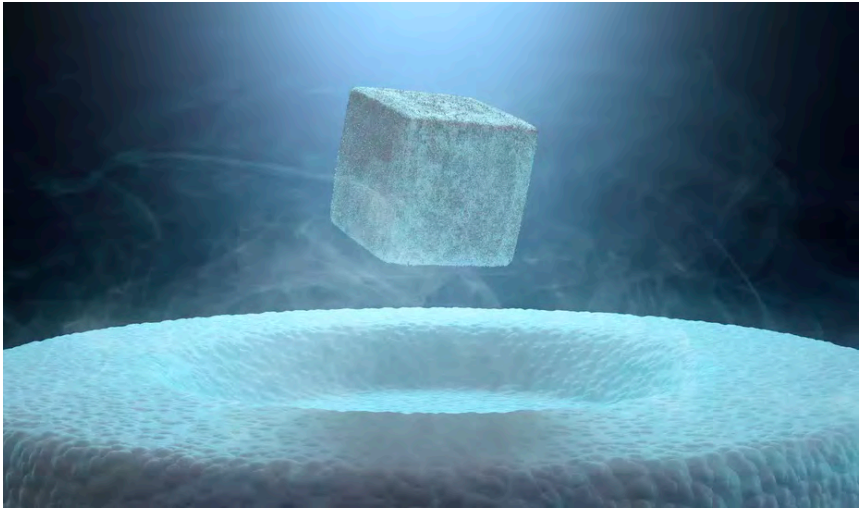
Bert Halperin

Quantum Hall Drag of Exciton Condensate in Graphene
X. Liu, K. Watanabe, T. Taniguchi, B. I. Halperin, P. Kim
Nature Physics **13**, 746–750 (2017)

Interlayer fractional quantum Hall effect in a coupled graphene double-layer
X. Liu, Z. Hao, K. Watanabe, T. Taniguchi, B. Halperin, P. Kim
Nature Physics **15**, 893–897 (2019)

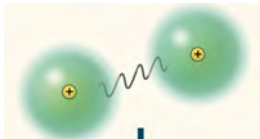
Crossover between Strongly-coupled and Weakly-coupled Exciton Superfluids
X. Liu¹, J.I.A Li, K. Watanabe, T. Taniguchi, J. Hone, B. I. Halperin, C.R. Dean, and P. Kim
in preparation

Superconductor and Superfluid

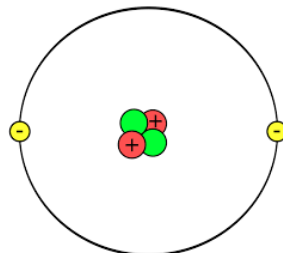


Superconductor: magnetic levitation

Composite bosons



Cooper pair



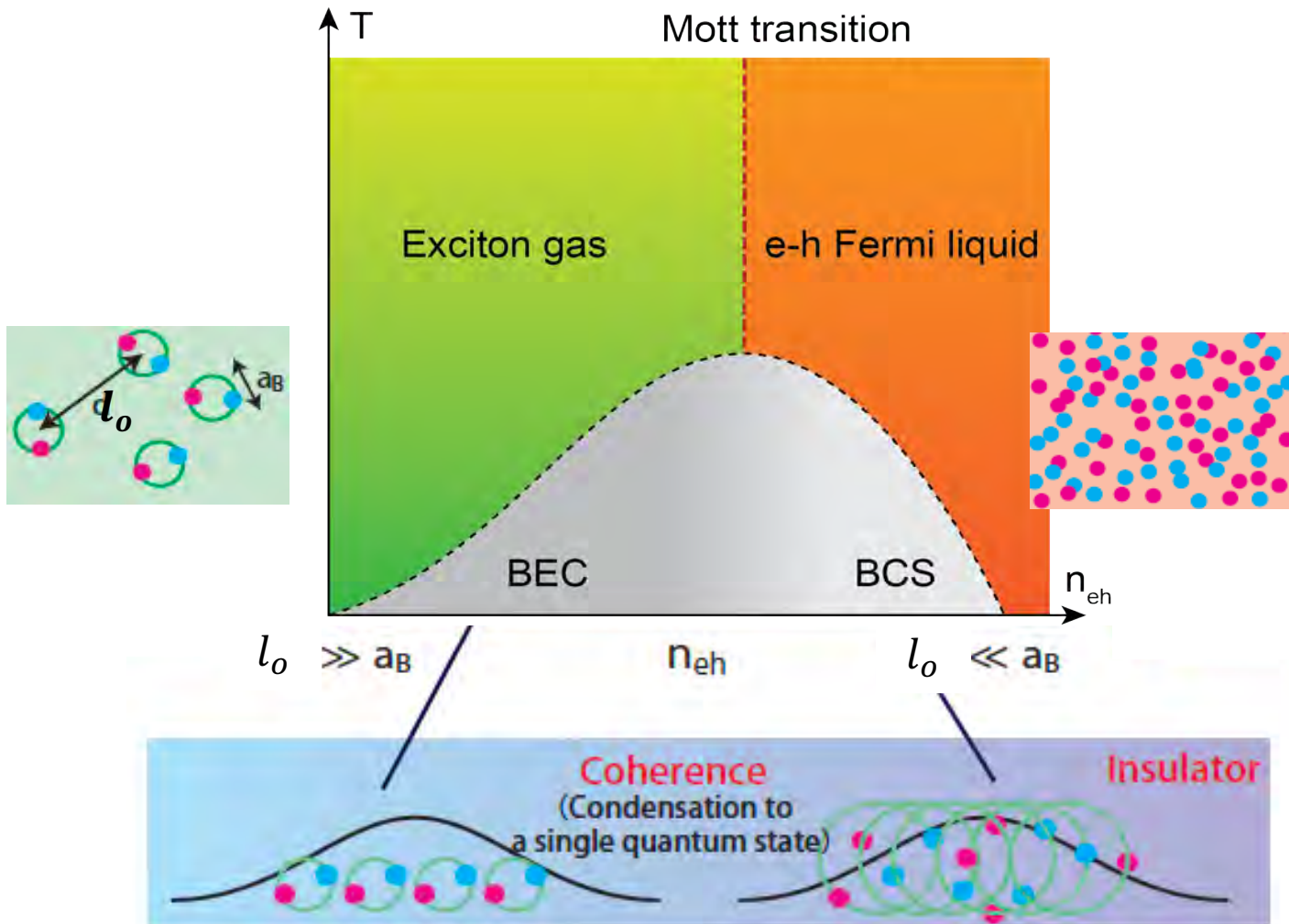
${}^4\text{He}$



Superfluid ${}^4\text{He}$: fountain effect

Exciton/e-h Phase Diagram

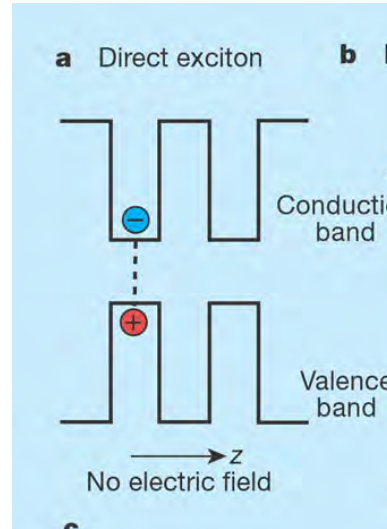
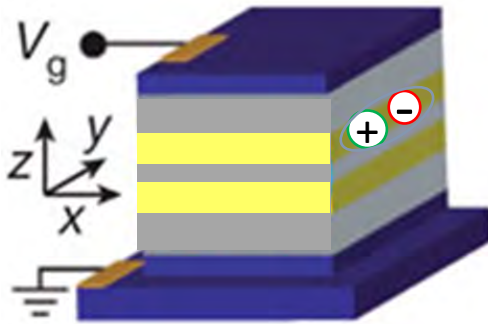
Schematic Meta Stable Phase Diagram of electron-hole in 3D



Excitons in semiconducting quantum wells

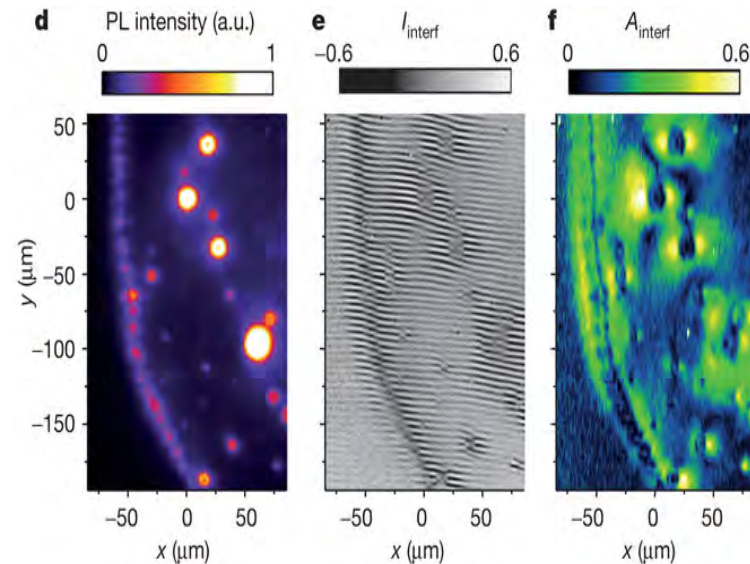
Direct and indirect excitons in semiconducting quantum wells

Semiconductor heterostructure



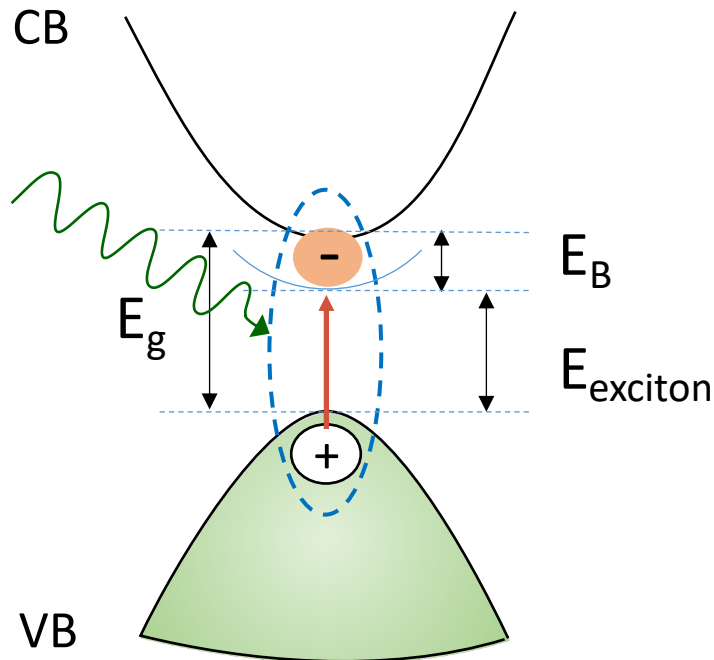
Ilias Perakis Nature (2002)

Spontaneous coherence
in cold interlayer exciton gas
formed in GaAs quantum wells



A. High, Nature 2012

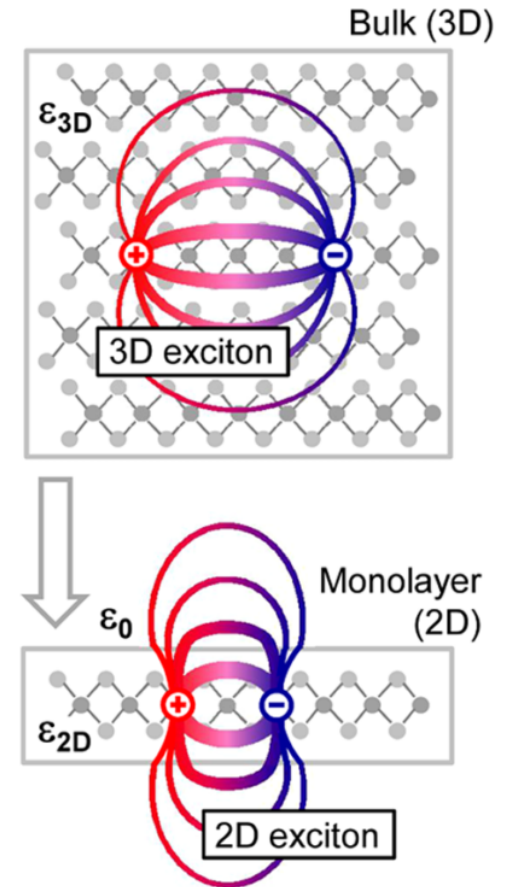
Excitons in 2D Materials



$$E_{\text{exciton}} = E_g - E_B$$

E_B = Exciton binding energy

E_g = Energy gap



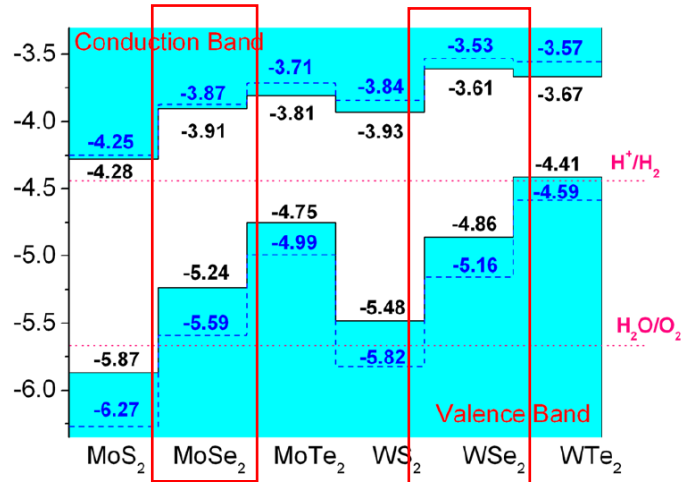
A. Chernikov *et al.* *Phys. Rev. Lett.*
113, 076802 (2014).

Exciton is a bound electron-hole pair.

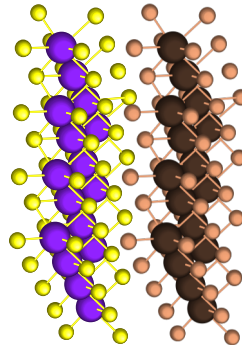
Exciton is strongly bound in 2D

Atomically Thin vdW p-n junction

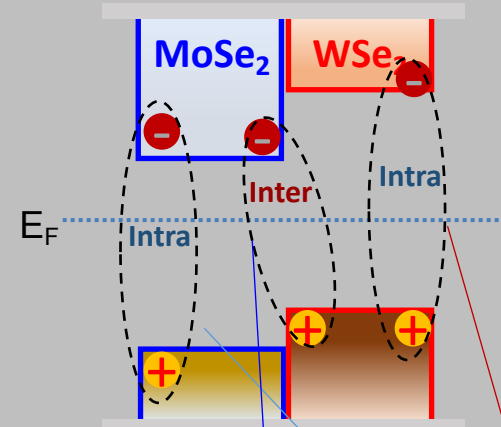
Band gaps and alignment of vdW semiconductors



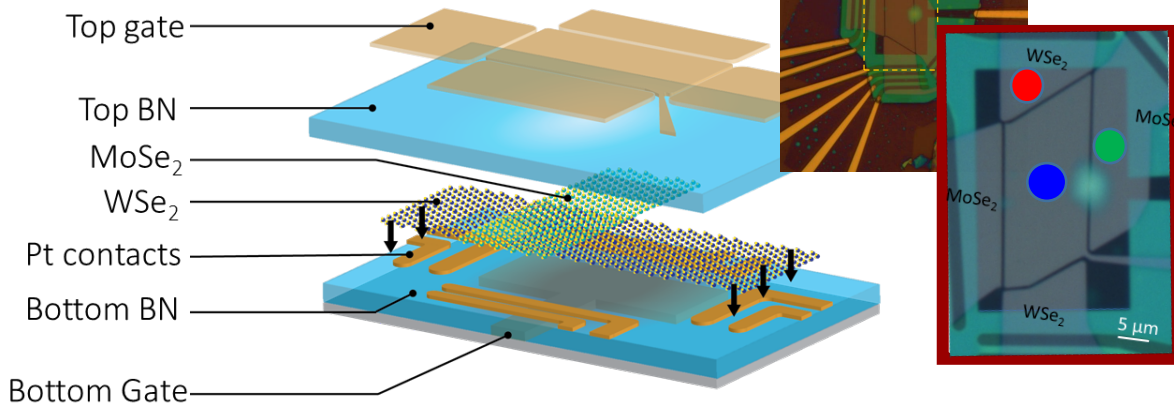
Appl. Phys. Lett. **102**, 012111 (2013)



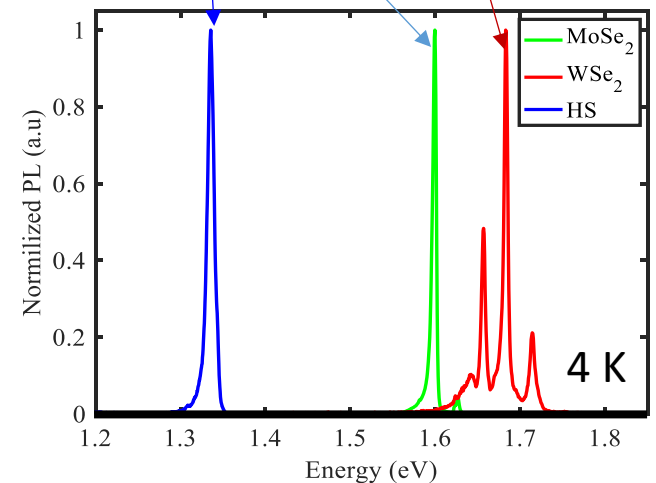
• Type II semiconductor heterostructures



Heterostructure Device and PL

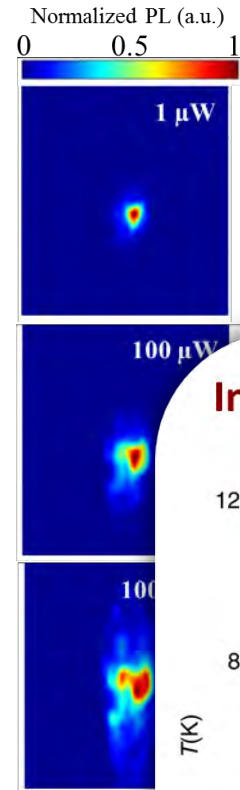
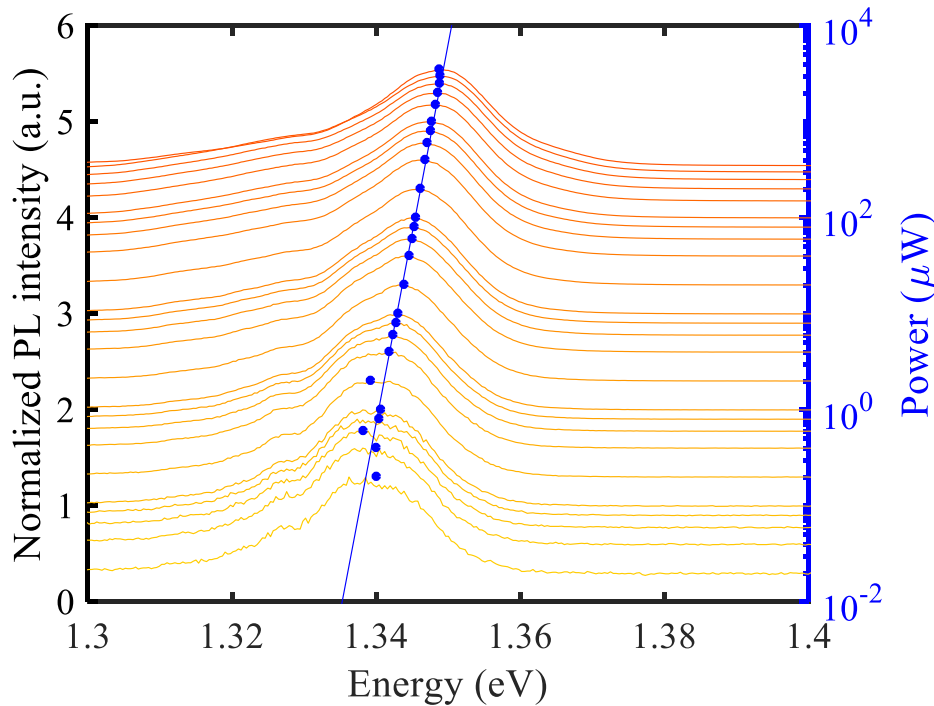


Photoluminescence



Toward Interlayer Exciton Condensation

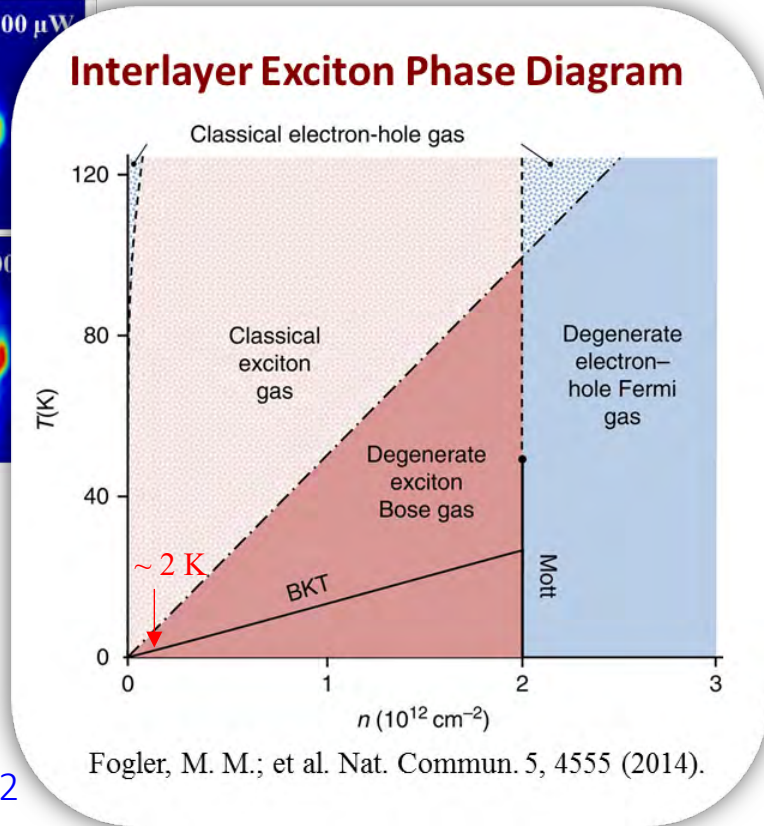
Laser power dependent PL



Blue shift due to the exciton-exciton interaction

$$\delta E = n_{eh} e^2 d / \epsilon$$

Estimated exciton density: $n_{IE} \sim 10^{11} \text{ cm}^{-2}$

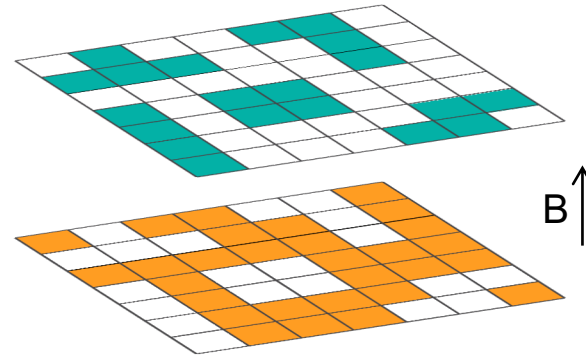
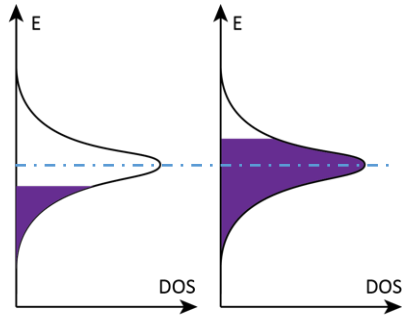


Fogler, M. M.; et al. Nat. Commun. 5, 4555 (2014).

Exciton condensation between Landau levels

Review: J. P. Eisenstein, Annu. Rev. Condens. Matter Phys. **5**, 159 (2014).

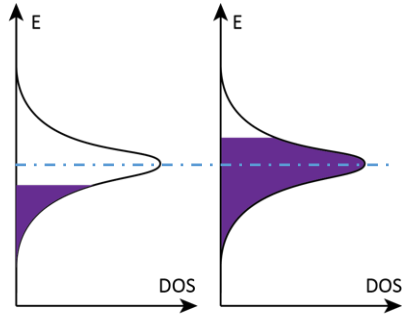
Two partially filled
Landau levels



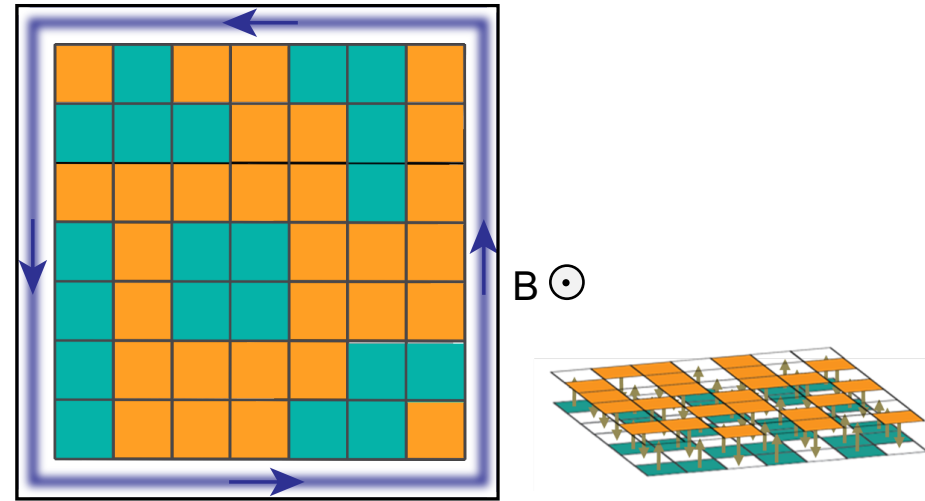
Exciton condensation between Landau levels

J. P. Eisenstein, Annu. Rev. Condens. Matter Phys. 5, 159 (2014).

Two partially filled Landau levels

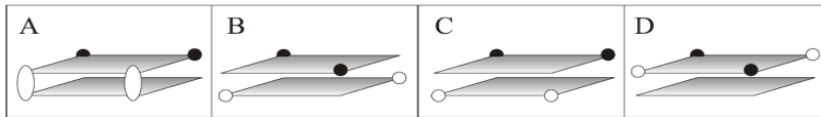


$$|\Psi\rangle = \prod_k \frac{1}{\sqrt{2}} (c_{k,T}^\dagger + e^{i\phi} c_{k,B}^\dagger) |0\rangle$$

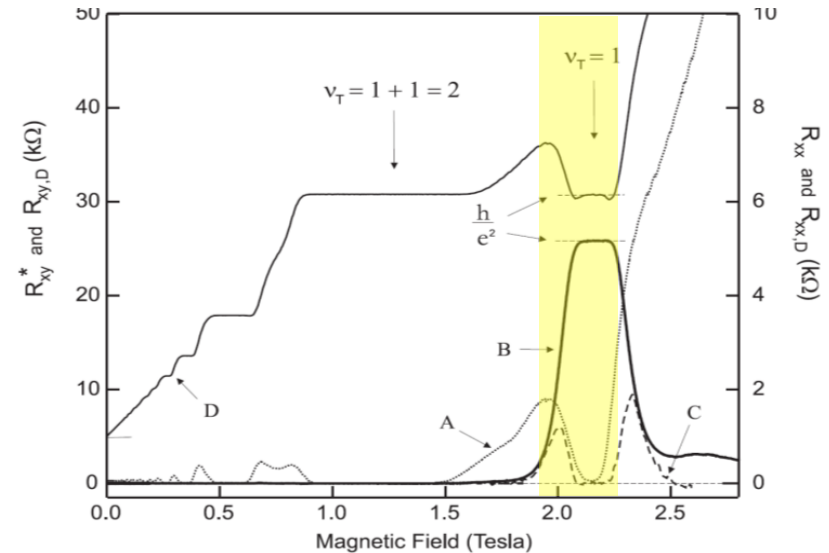


Total Landau level quantum Hall effect

GaAs Double Quantum Well

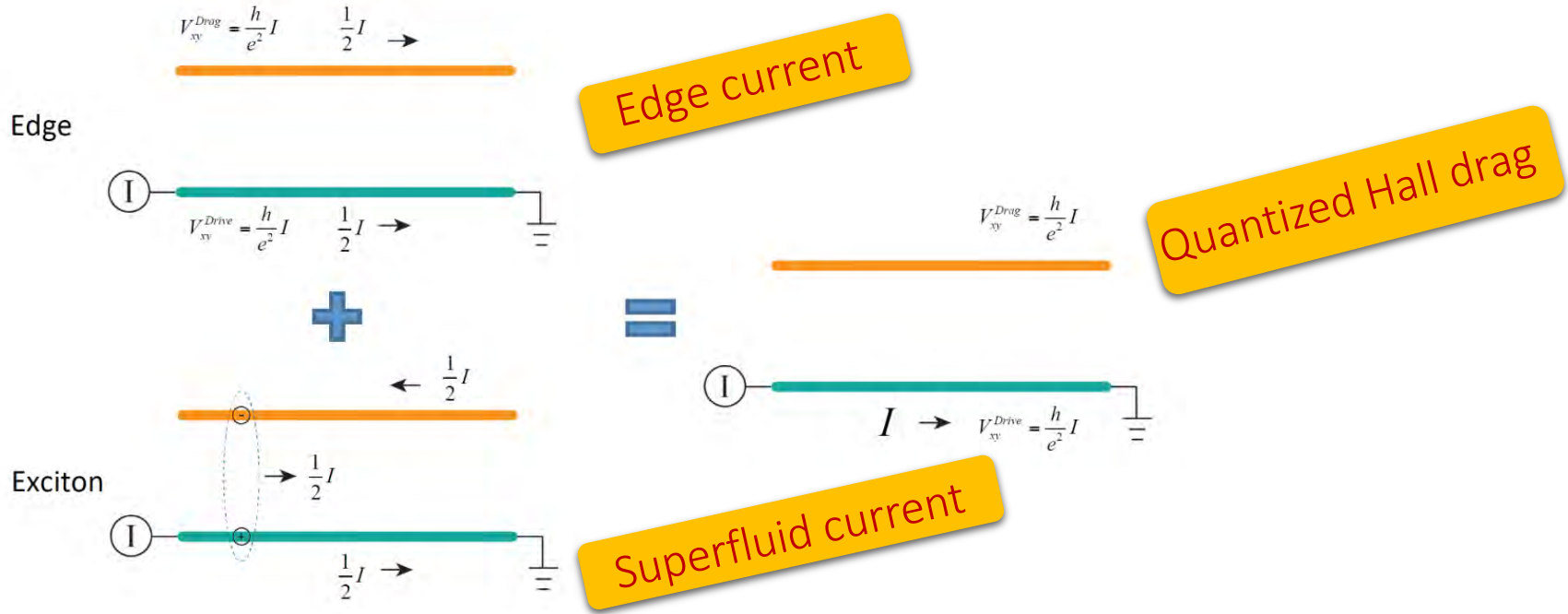


- Quantum Hall effect for two partially filled complementary LLs
- Quantized drag Hall

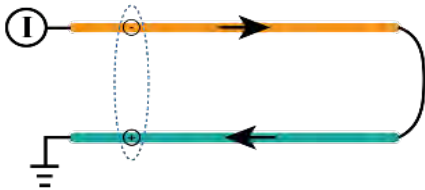


M. Kellogg, et. al, PRL (2002)

Exciton Current and Quantized Drag



Counter Flow Current

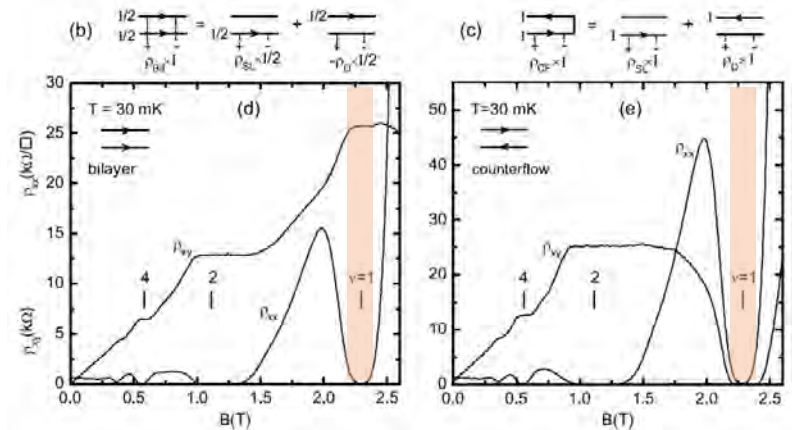


Dissipationless counter flow current flow:

$$R_{xx}^{CF} = \frac{V_{xx}}{I_{CF}} = 0$$

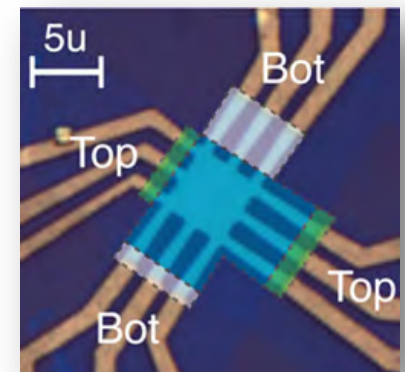
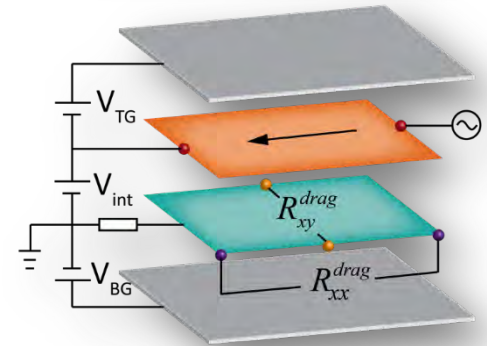
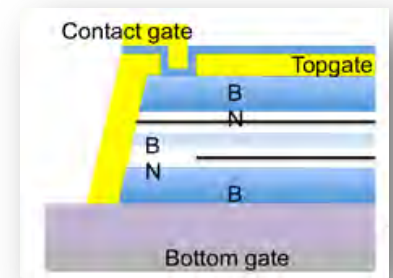
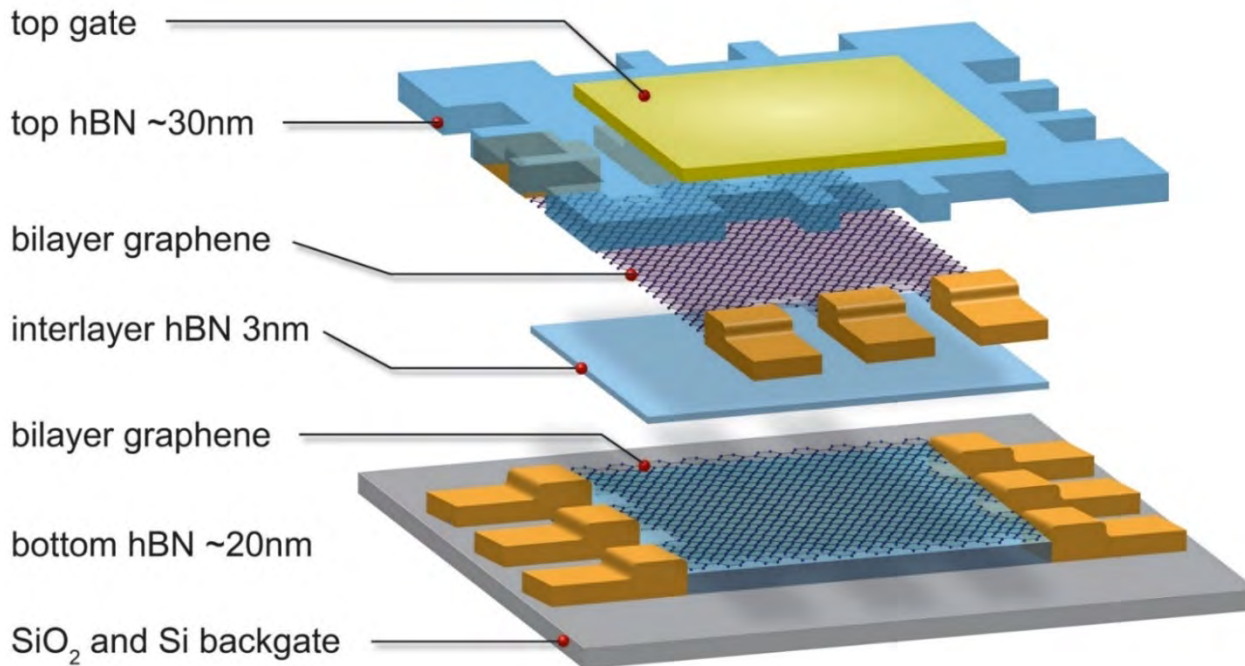
No net force on exciton:

$$R_{xy}^{CF} = \frac{V_{xy}}{I_{CF}} = 0$$

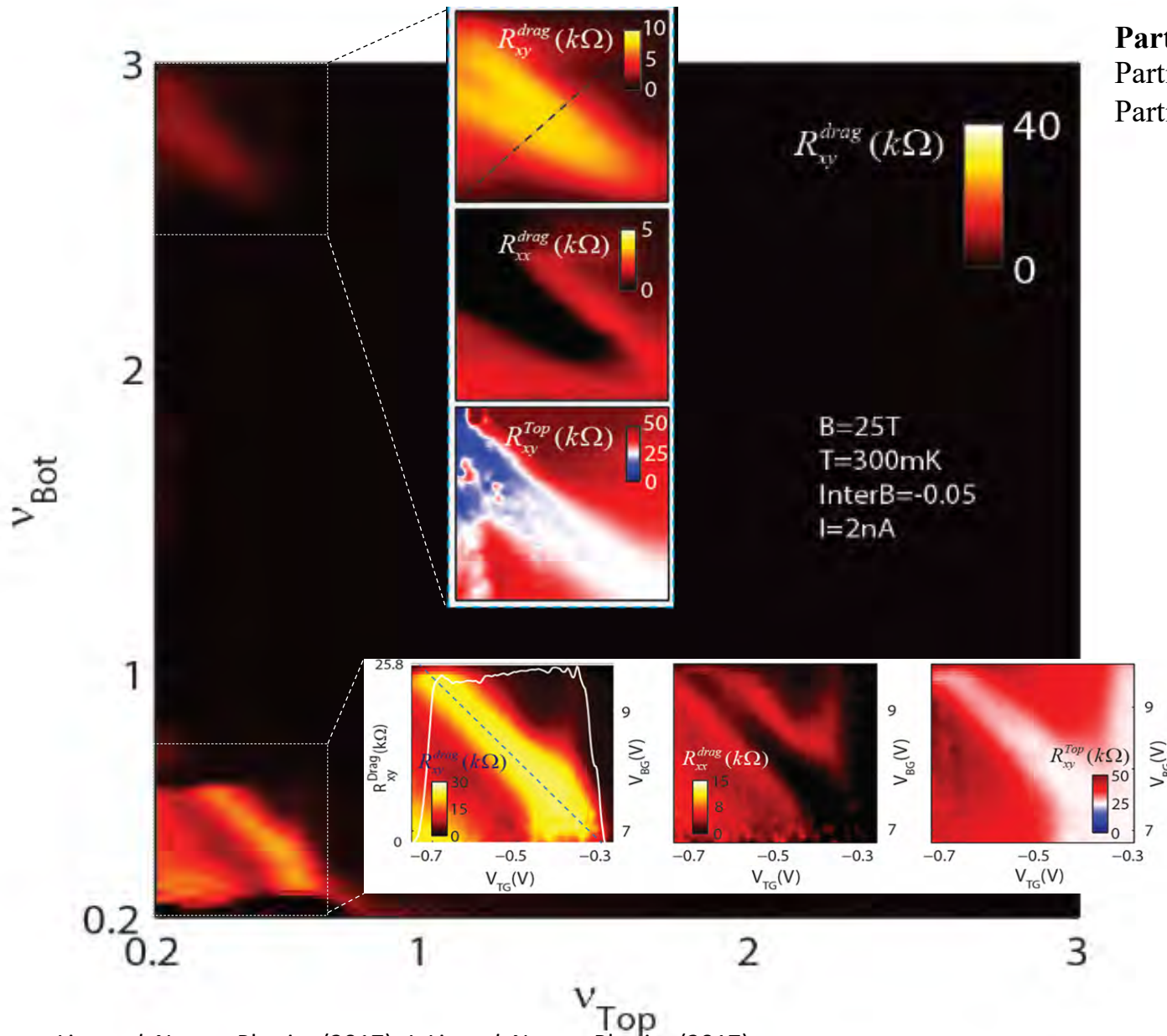


Double Graphene Layer Drag Device

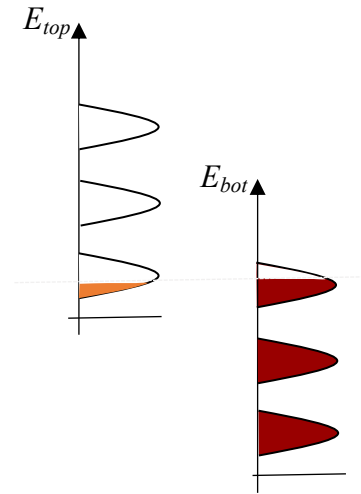
- Mobility $\sim 10^6$ cm²/Vsec
- hBN thickness $d = 3$ nm
- top and bottom gate
- contact gate
- interlayer bias



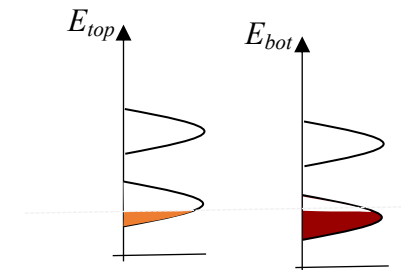
Quantized Hall Drag for $\nu_{tot} = 1$ and 3



Partial coherent exciton current:
 Partially filled $N_{top}=1$
 Partially filled $N_{bot}=3$

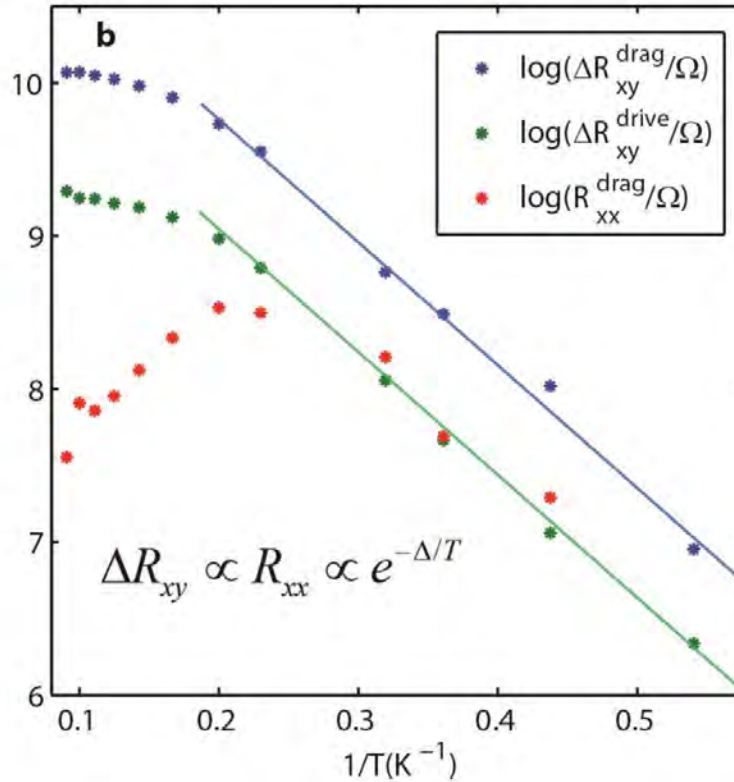
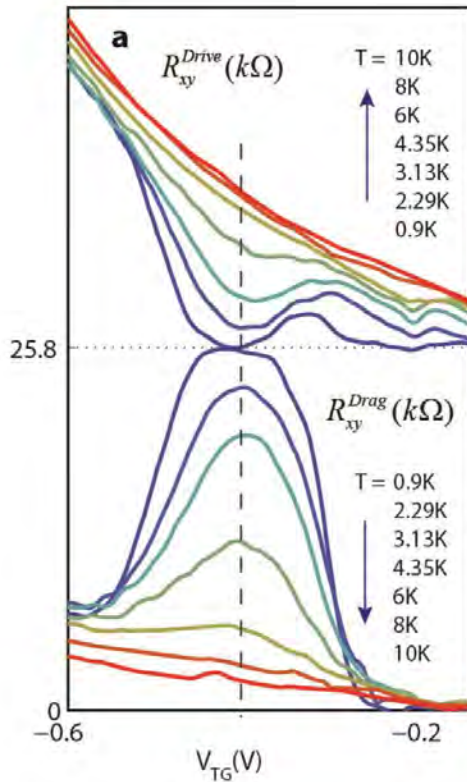


Coherent exciton current:
 Partially filled $N_{top}=1$
 Partially filled $N_{bot}=1$

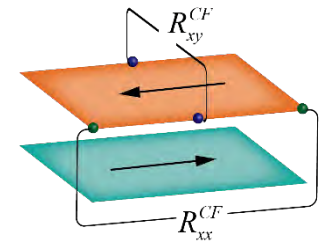


Exciton BEC Energy Scale and Counter Flow

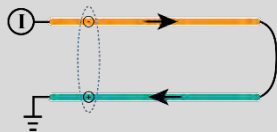
X. Liu *et al*, J. Li *et al*, Nature Physics (2017)



$\Delta \sim 8 \text{ K.}$



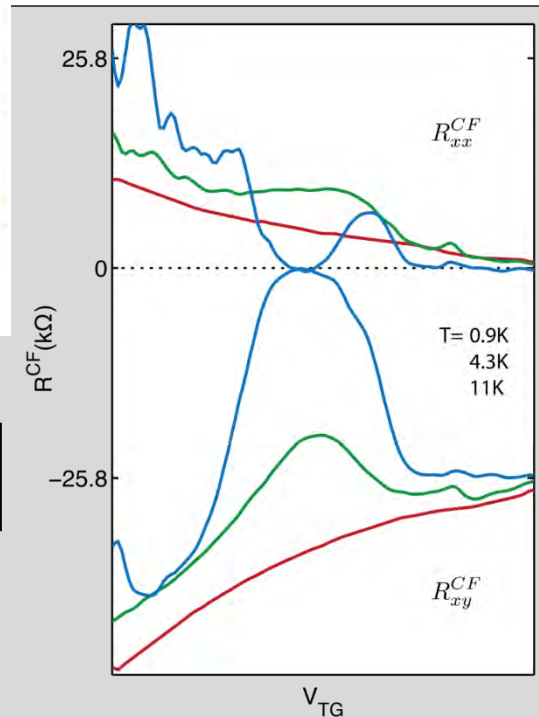
Superfluidic Counter flow



$$\begin{bmatrix} V_1 \\ V_2 \end{bmatrix} = \begin{bmatrix} R_{11} & R_{12} \\ R_{21} & R_{22} \end{bmatrix} \times \begin{bmatrix} I_1 \\ I_2 \end{bmatrix}$$

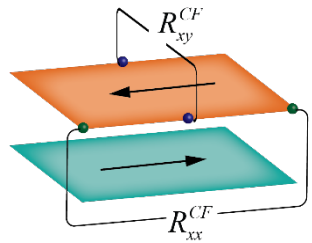
$$V_{top}^{CF} = R_{top}I - R_{drag}I$$

$$V_{bot}^{CF} = R_{drag}I - R_{bot}I$$

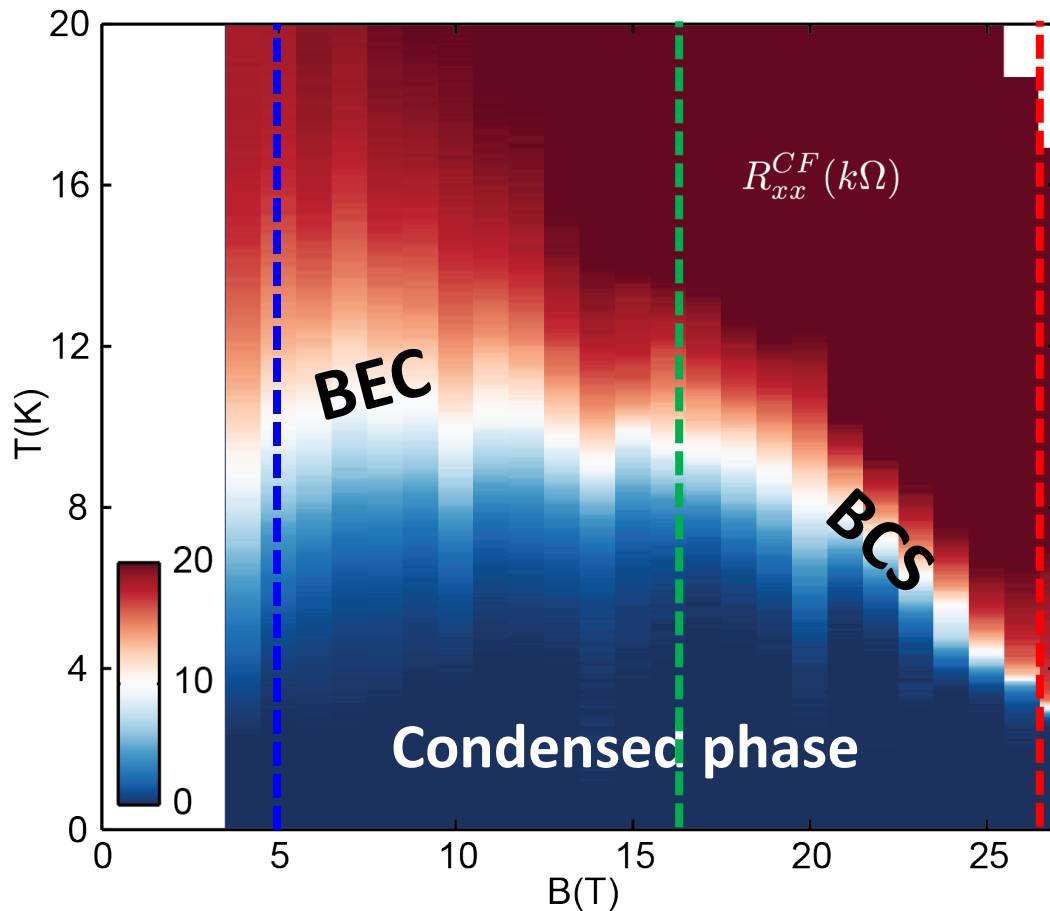


Counter-Flow Resistance of $\nu_{tot} = -1$

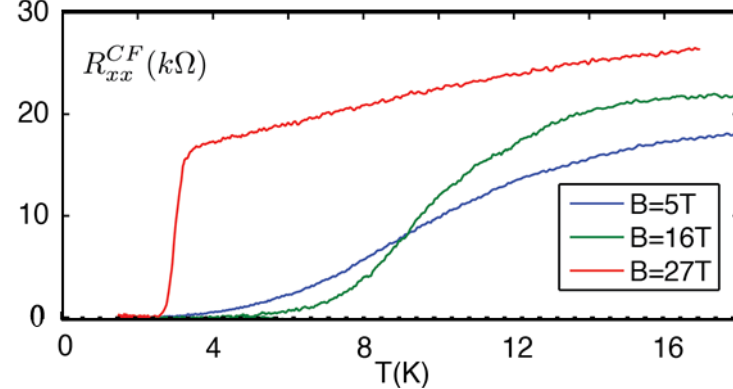
Xiaomeng Liu *et al*, unpublished (collaboration with Dean group)



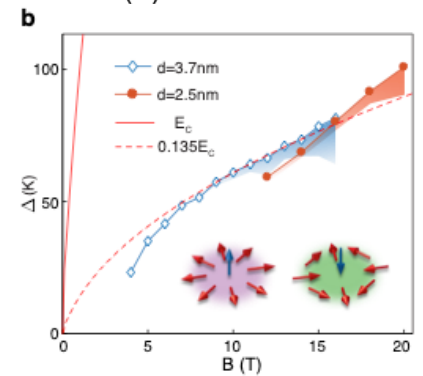
R_{xx}^{CF} (keeping $\nu_{tot} = -1$)



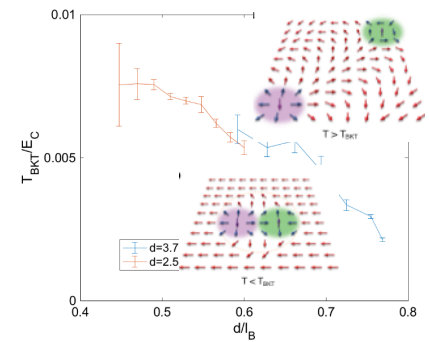
Temperature Dependence



BEC

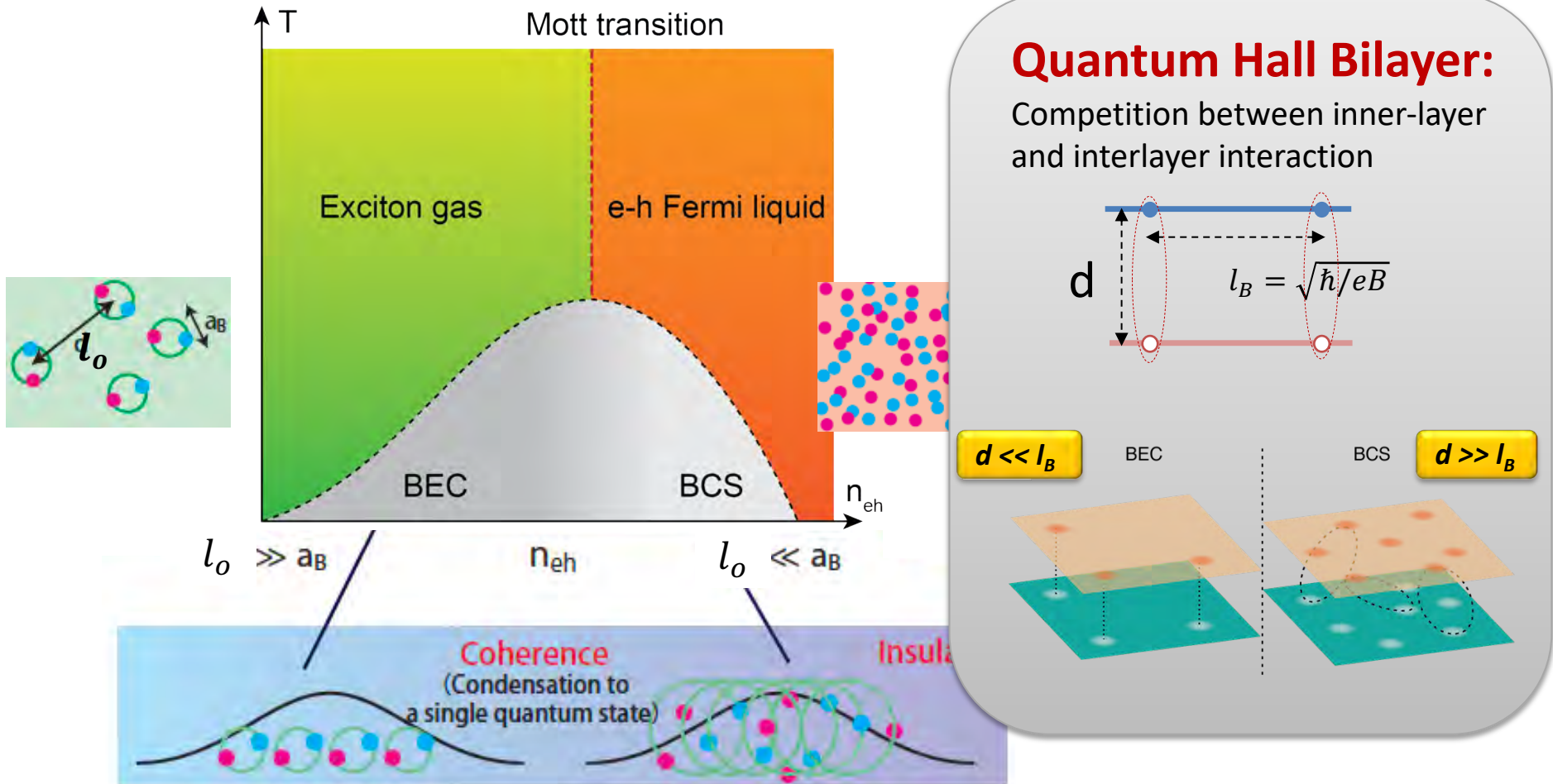


BCS



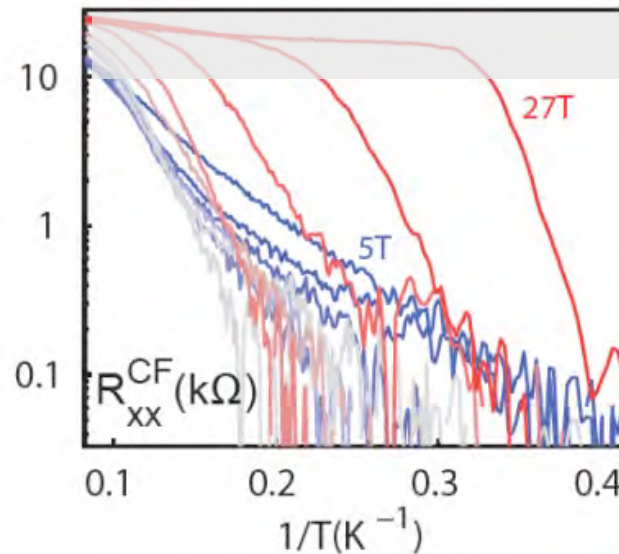
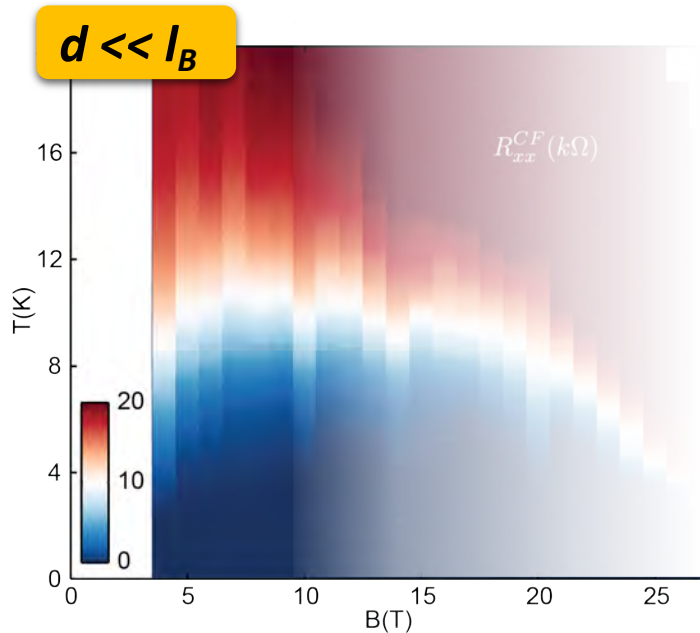
Exciton/e-h Phase Diagram

Schematic Meta Stable Phase Diagram of electron-hole in 3D



Activation Gap at the BEC Limit

Xiaomeng Liu *et al*, unpublished (collaboration with Dean group)



Activating behaviors

2D XY Ground State:

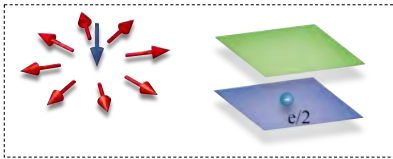
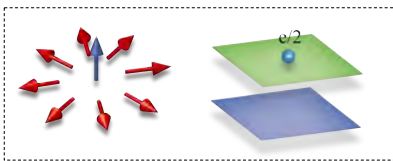
→ Anisotropic SU(2)

$$|\Psi\rangle = \prod_k \frac{1}{\sqrt{2}} (c_{k,T}^\dagger + e^{i\phi} c_{k,B}^\dagger) |0\rangle$$

$$|\psi\rangle = \prod_k (\cos\theta c_{k,T}^\dagger + e^{i\phi} \sin\theta c_{k,B}^\dagger) |0\rangle$$

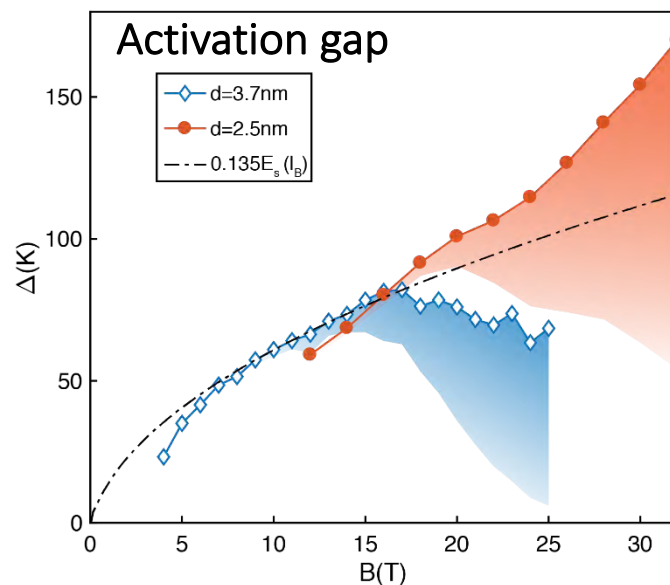
meron-antimeron pair, each carrying $e/2$ charge on one graphene layer.

Low Energy Excitation



$$E_{m-am} = \sqrt{\pi/32} \frac{e^2}{\epsilon l_B} \sim 0.31 \frac{e^2}{\epsilon l_B}$$

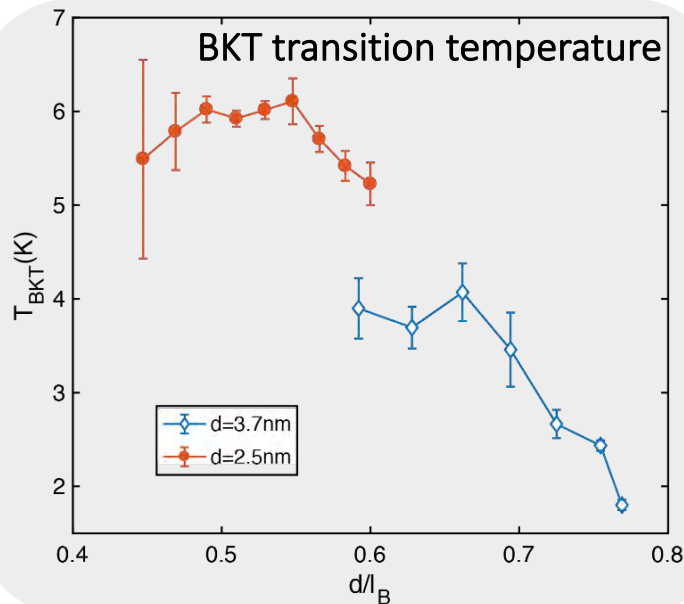
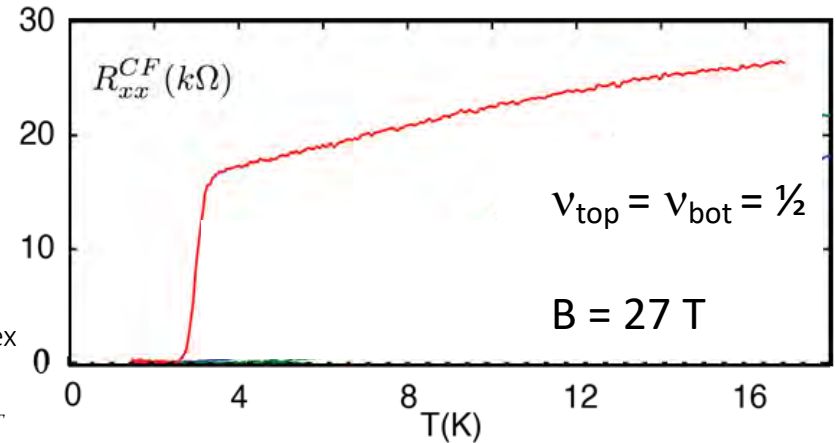
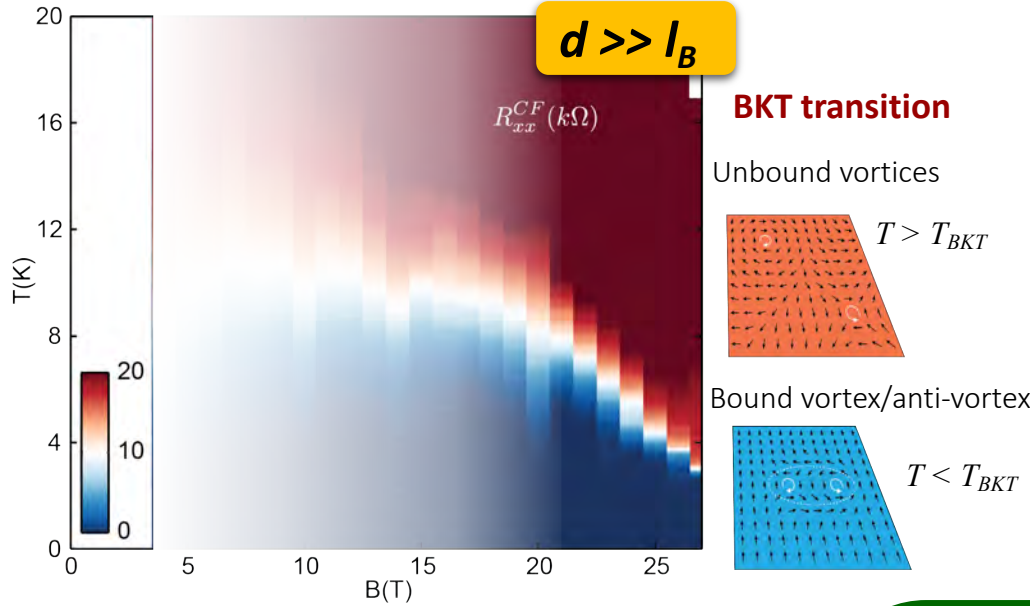
Activation gap



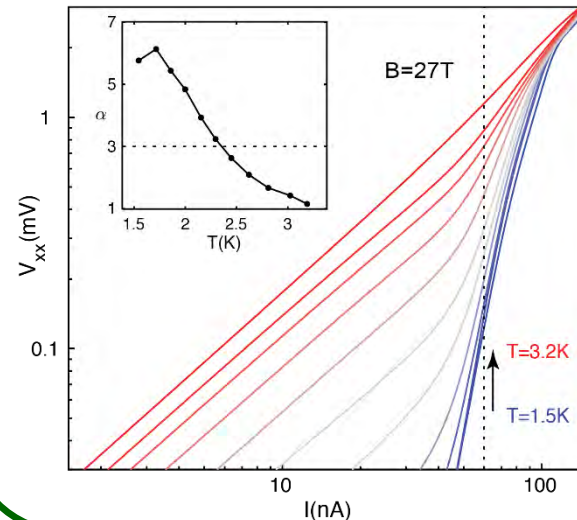
$$E_S = 0.135 \frac{e^2}{\epsilon l_B}$$

BKT Transition at the BCS Limit

Xiaomeng Liu *et al*, unpublished (collaboration with Dean group)



Counter Flow I-V Characteristic



IV curves exhibit power law

$T < T_{KT}: V \propto I^\alpha,$

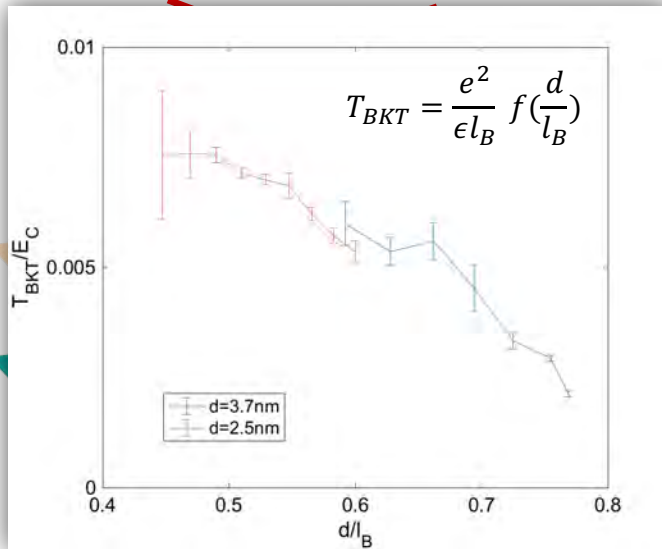
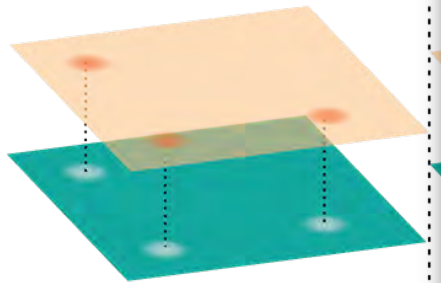
$$\alpha = 1 + 2 \frac{T_{KT}}{T}$$

$T > T_{KT}: V \propto I$

BCS-BEC Crossover in Magnetoexciton Condensate

$d \ll l_B$

BEC



Ground States

- $d \ll l_B$: Halperin (111) state

$$|\Psi\rangle = \prod (z_i - z_j)(w_i - w_j)(z_i - w_j) \times e^{-\frac{1}{4}(\sum |z_i|^2 + \sum |w_i|^2)}$$

- $d \gg l_B$
 : weakly coupled composite fermions

$$|\Psi\rangle = P_{LLL} \prod (z_i - z_j)^2 (w_i - w_j)^2 \Psi(k_{F,T}, k_{F,B})$$

- $d \sim l_B$: many proposals

N. E. Bonesteel, et al., PRL 77, 3009 (1996)

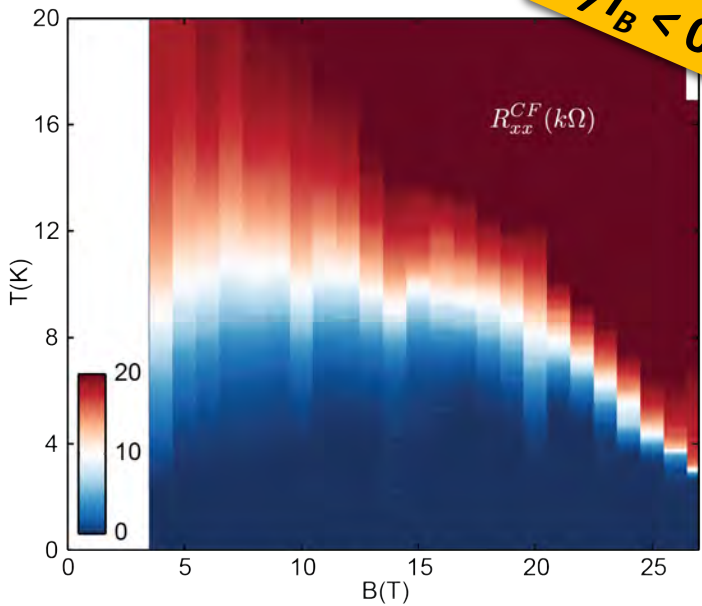
J. Alicea, et al., PRL 103, 256403 (2009).

G. Moller, et al., PRB 79, 125106 (2009)

I. Sodemann, et al., PRB 95, 085135 (2017)

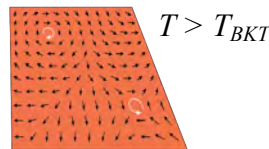
...

$d/l_B < 0.8$

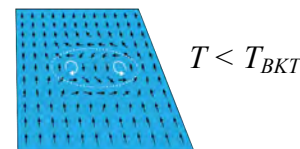


BKT transition

Unbound vortices

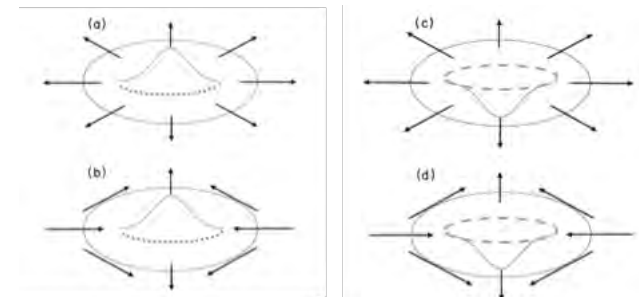


Bound vortex/anti-vortex



Topological defects:

vorticity and fractionalized charges

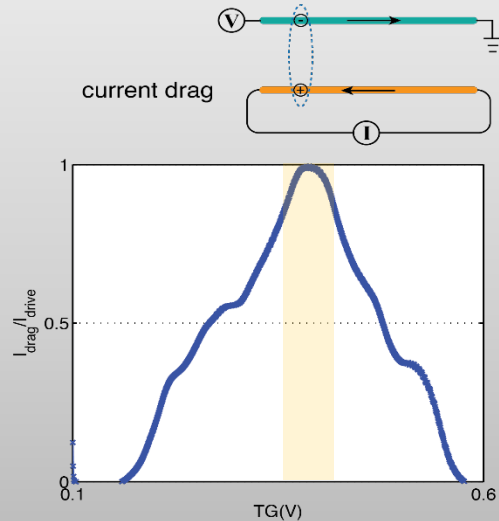


K. Moon, et al., PRB 51, 5183 (1995)

Magneto Exciton Insulator: $\nu_{tot}=0$

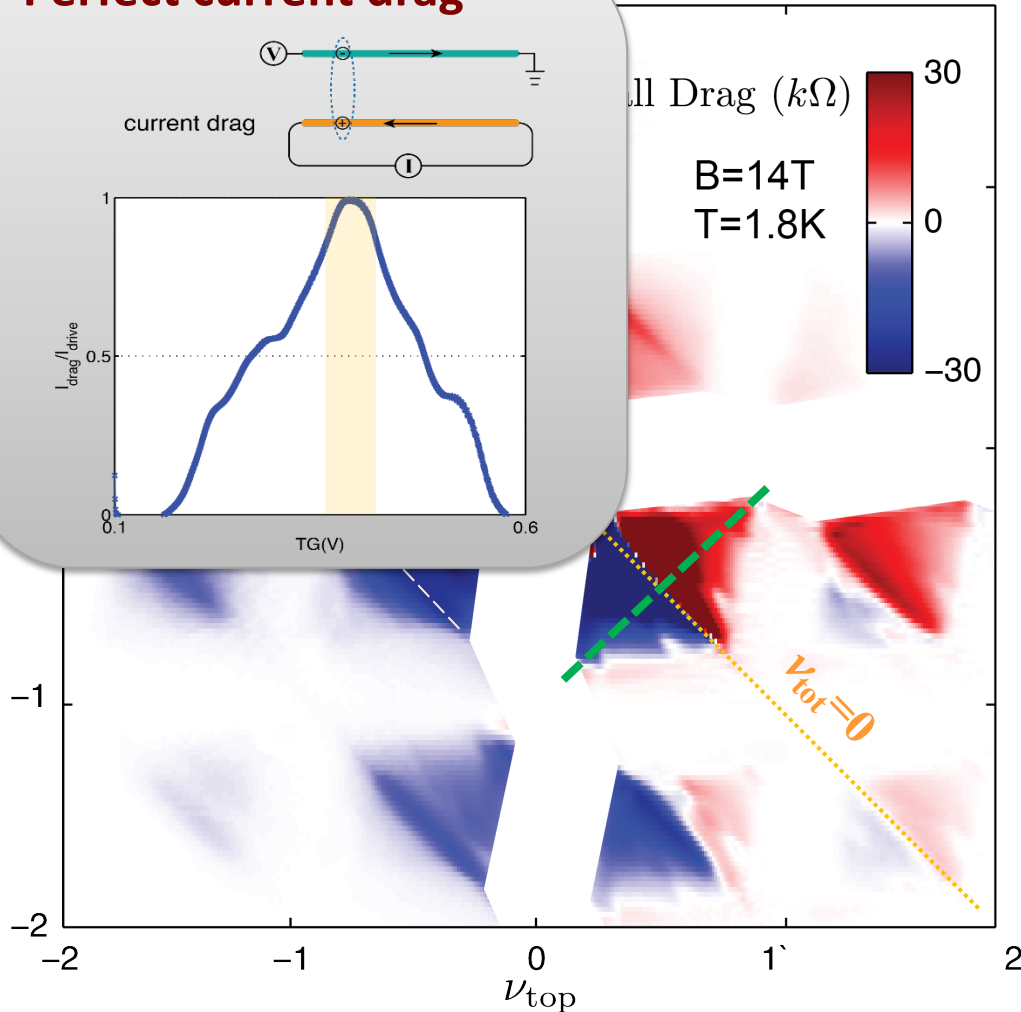
Monlayer/hBN/Monolayer

Perfect current drag

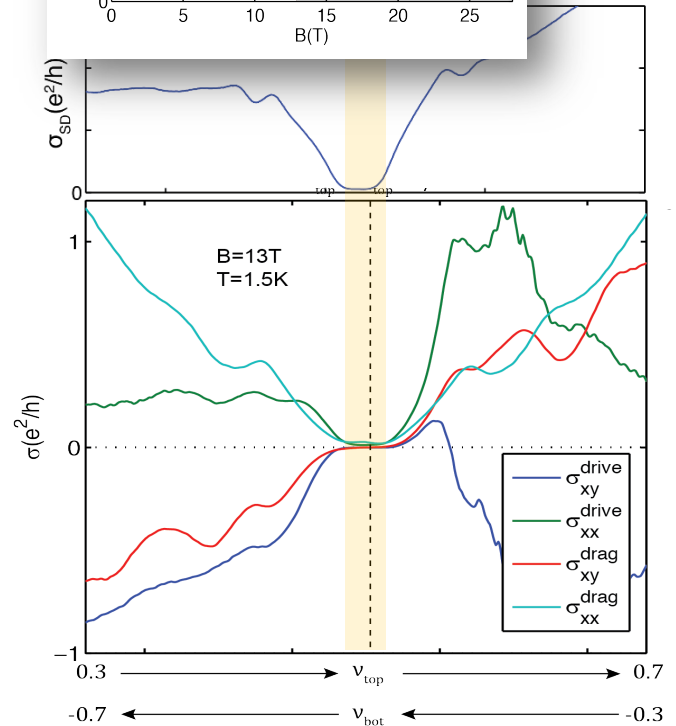
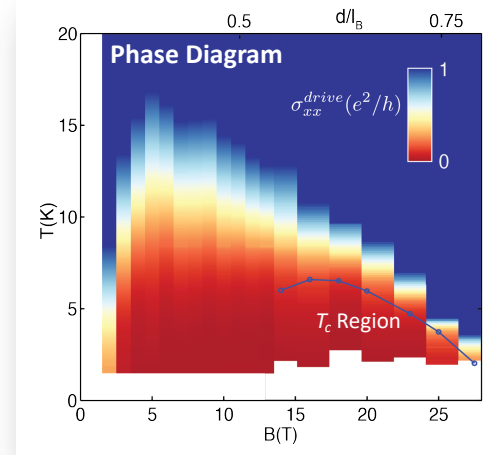


Current Drag ($k\Omega$)

B=14T
T=1.8K



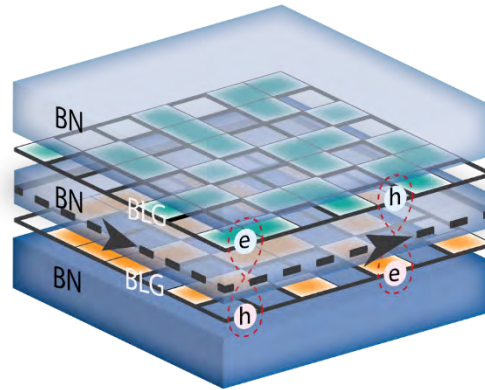
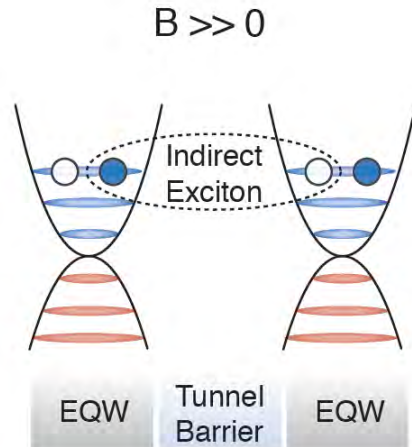
$\nu_{tot}=0$



Exciton insulator!

Topological Insulating Exciton Condensation

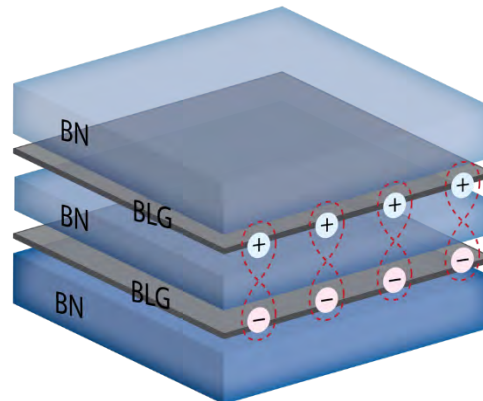
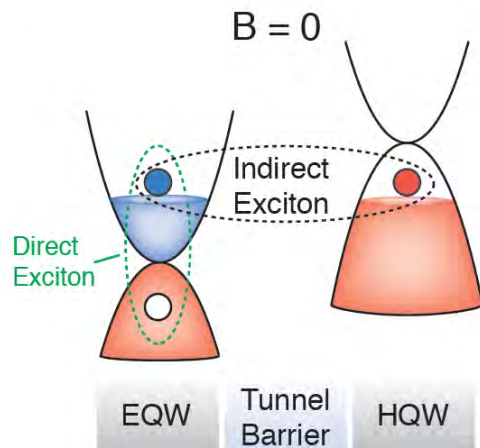
Exciton condensation between LL (topological exciton insulator)



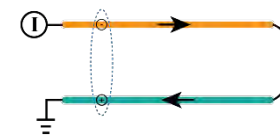
$$R_{xx}^{CF} = 0 \quad R_{xx}^{sym} = 0$$

$$R_{xy}^{CF} = 0 \quad R_{xy}^{sym} = \frac{h}{\nu_{tot} e^2}$$

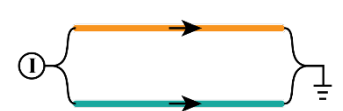
Exciton condensation (exciton insulator)



Counter Flow

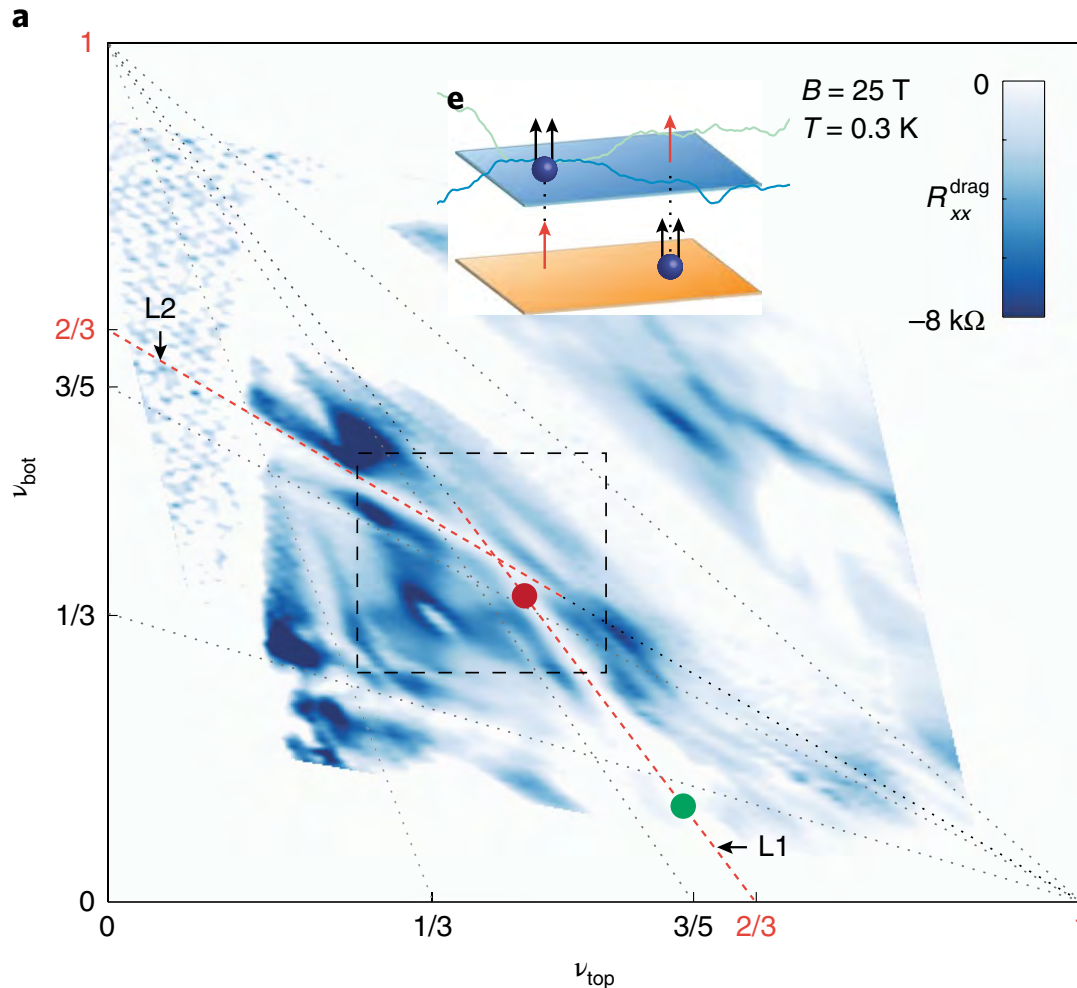


Symmetric Flow

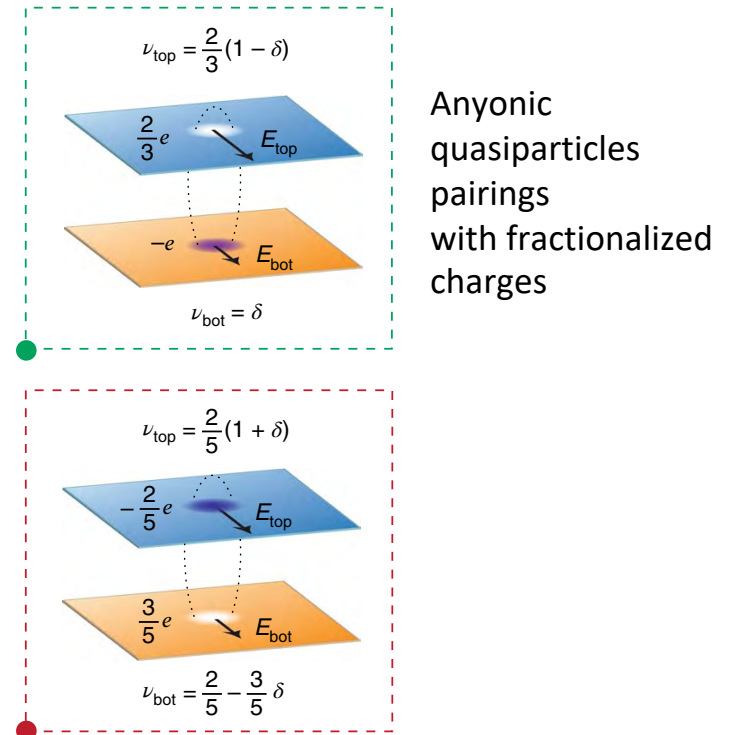


$$R_{CF} = 0 \quad R_{sym} = \infty$$

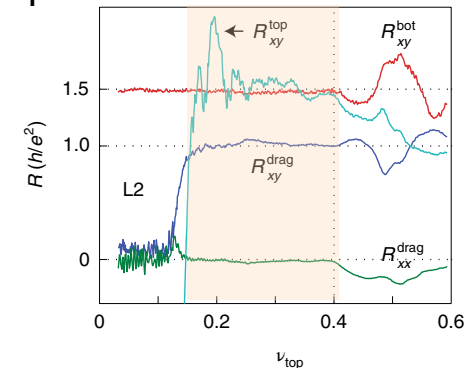
Anyon Pairing Across vdW Gap



Interlayer composite fermion pairing



f Semiquantization of drag Hall



Ferromagnetic Superconductivity in Twisted Double Bilayer Graphene



Xiaomeng Liu



Zeyu Hao



Ashvin Vishwanath



Jong Yeon Lee



Eslam khalaf



T. Taniguchi, K. Watanabe

Spin-polarized Correlated Insulator and Superconductor in Twisted Double Bilayer Graphene
X. Liu, Z. Hao, E. Khalaf, J. Y. Lee, K. Watanabe, T. Taniguchi, A. Vishwanath, P. Kim
arXiv:1903.08130, *submitted*

Graphene

Dirac Fermions

Quantum Hall Effect

Klein Tunneling

Fractional Quantum Effect

Fractal Quantum Hall Effect

Hydrodynamics

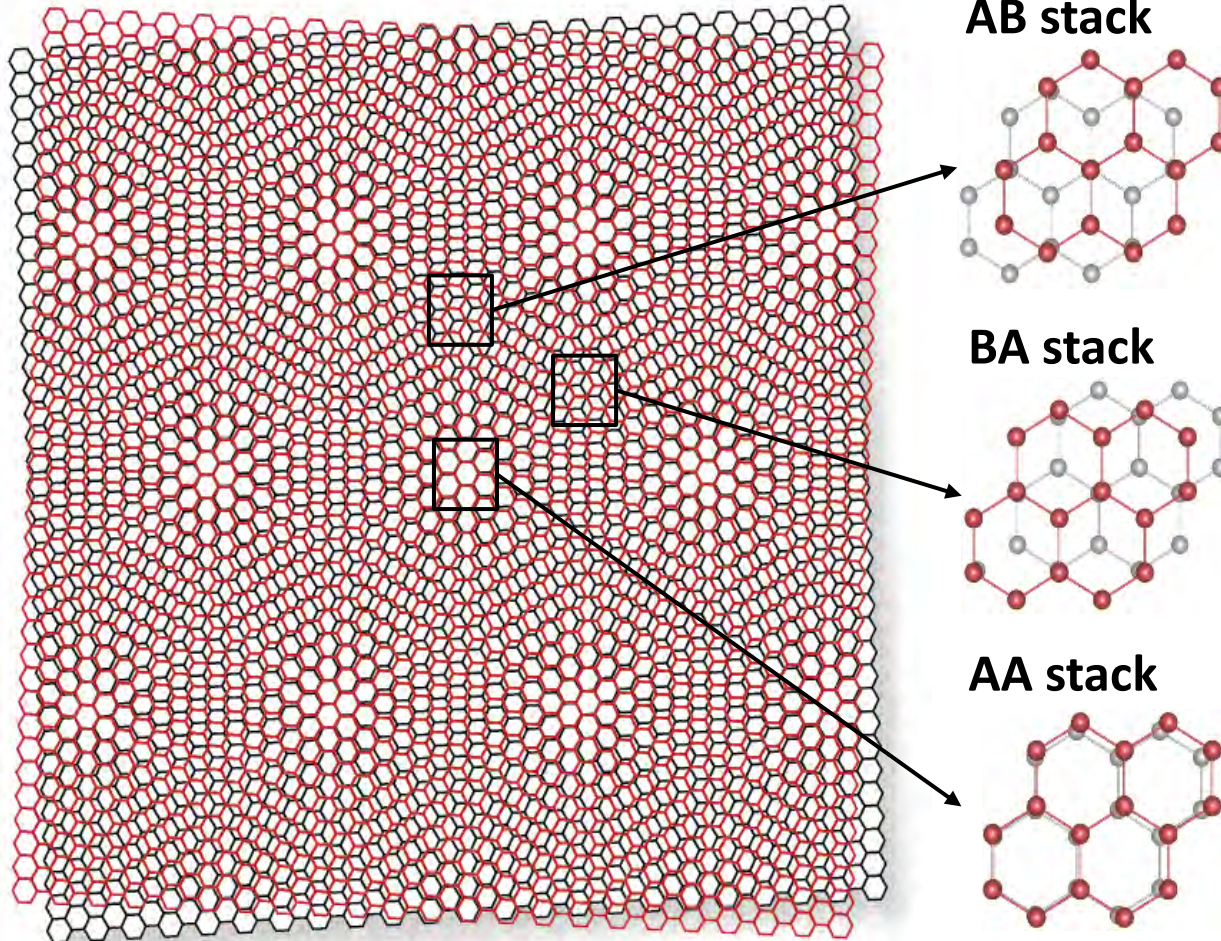
⋮

Superconductivity ?

Magnetism ?

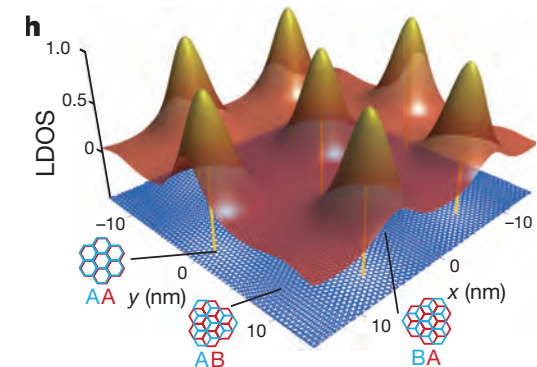
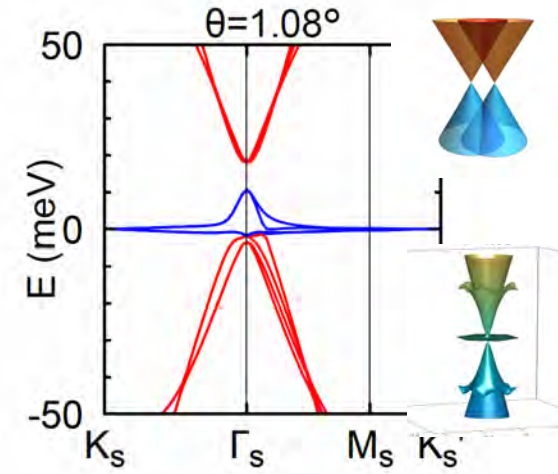
since 2004

Twisted Graphene Bilayer: Magic Angle



Moiré Structure in Twisted Graphene on Graphene

Special 'magic' angle

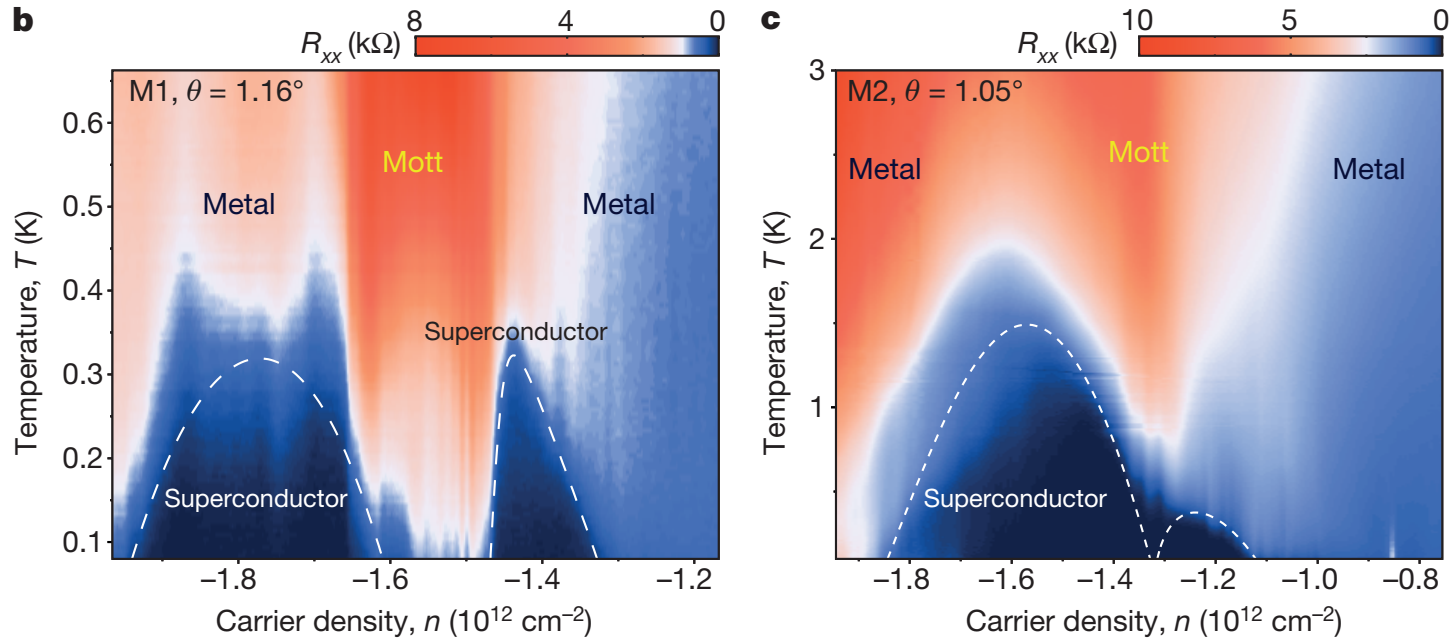


Localized electron wave function at AA sites

Bistritzer & MacDonald, PNAS (2011)

S. Fang, E. Kaxiras. *PRB* 93, 235153 (2016)

Superconductivity of Magic Angle TBG



Mott Insulator
&
Superconductors

Y. Cao et al. Nature (2018) x 2

Followed by:

Yankowitz et. al., *Science* 363 (2018): pressure tunable superconductivity

Chen et. al. *Nature* (2019): trilayer graphene/hBN

Lu et. al. *Nature* (2019): superconductivity and orbital magnet in magic angle graphene

• • •

Ferromagnetic Superconductors

Superconductivity on the border of itinerant-electron ferromagnetism in UGe_2

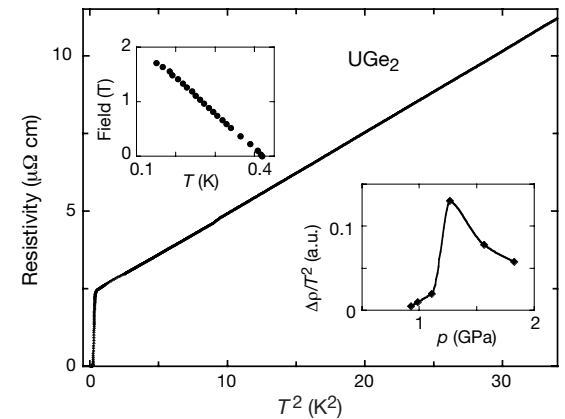
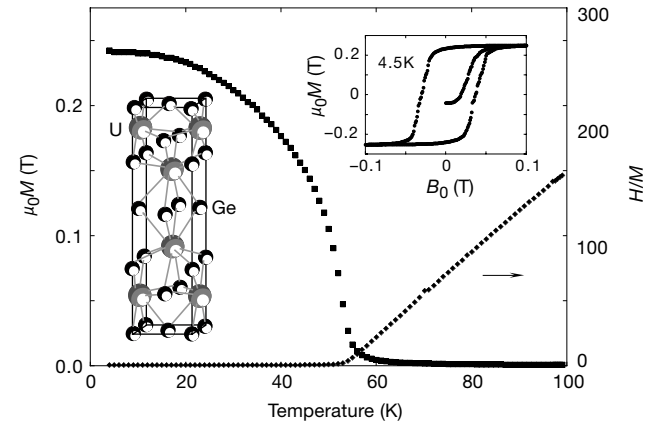
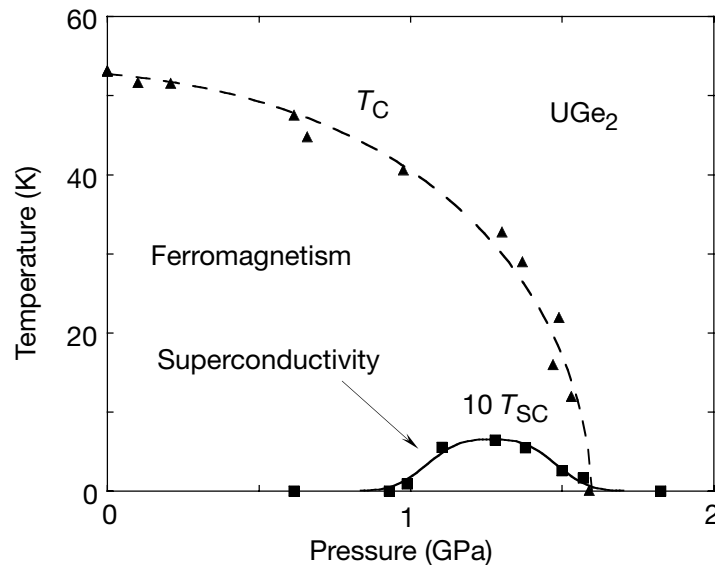
S. S. Saxena^{*†‡}, P. Agarwal^{*}, K. Ahilan^{*}, F. M. Grosche^{*‡}, R. K. W. Haselwimmer^{*}, M. J. Steiner^{*}, E. Pugh^{*}, I. R. Walker^{*}, S. R. Julian^{*}, P. Monthoux^{*}, G. G. Lonzarich^{*}, A. Huxley[§], I. Sheikin[§], D. Braithwaite[§] & J. Flouquet[§]

^{*} Department of Physics, Cavendish Laboratory, University of Cambridge, Madingley Road, Cambridge CB3 0HE, UK

[†] Materials Science Centre, University of Groningen, Nijenborgh 4, 9747AG, The Netherlands

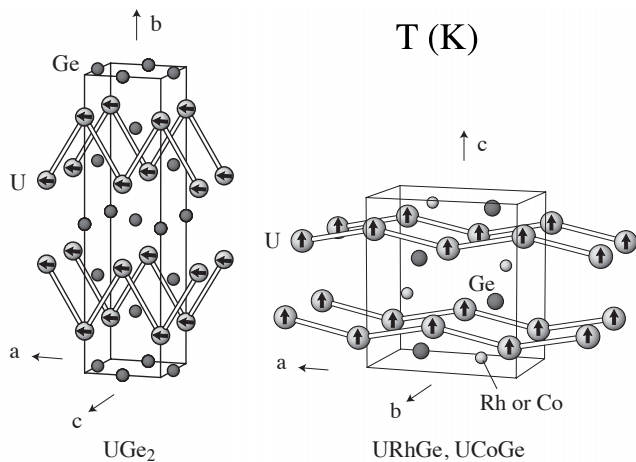
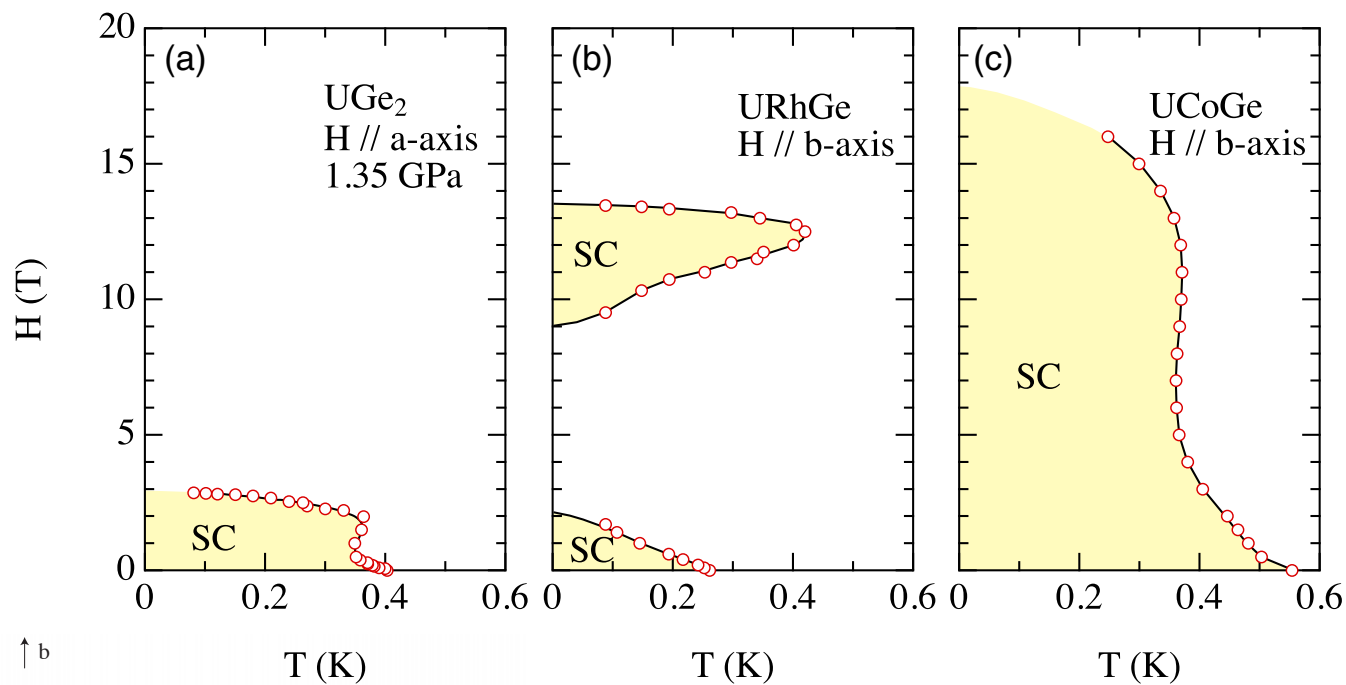
[§] Département de Recherche Fondamentale sur la Matière condensée - SPSMS, CEA Grenoble, 17 Av. des Martyrs, Grenoble 38054, France

NATURE | VOL 406 | 10 AUGUST 2000 |



Followed by URhGe (Aoki et al., 2001)
UCoGe (Huy et al., 2007)

Ferromagnetic Superconductors: H_c versus T



Magnetic field along the hard axis of ferromagnet.

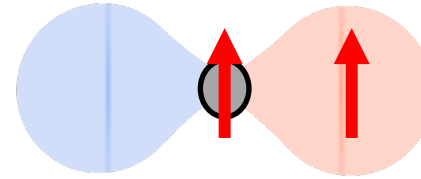
H_c exceeds the Pauli limit ($\sim 1.85 T_c$ [T/K])

Equal-Spin p-wave Pairing: Superfluid ^3He A phase

A. J. Leggett (1972)

A-phase Superfluid ^3He

$$\Psi_{\text{pair}}(\mathbf{r}) =$$



p-wave pairing

VOLUME 53, NUMBER 20

PHYSICAL REVIEW LETTERS

12 NOVEMBER 1984

Superfluid ^3He in High Magnetic Fields: The Phase Diagram

D. C. Sagan,^(a) P. G. N. deVegvar, E. Polturak,^(b) L. Friedman,^(c) S.-S. Yan^(d)
E. L. Ziercher, and D. M. Lee

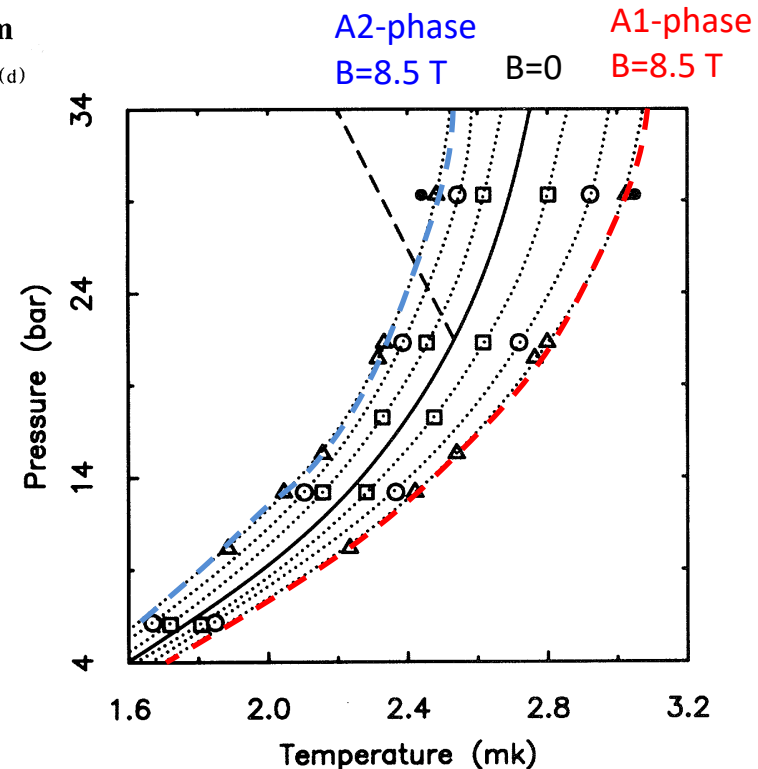
Laboratory of Atomic and Solid State Physics, Cornell University, Ithaca, New York 14853
(Received 30 July 1984)

▶ ↑↑ Cooper pairs condense at $T_c^{A_1} = T_c + \lambda^{A_1} B$

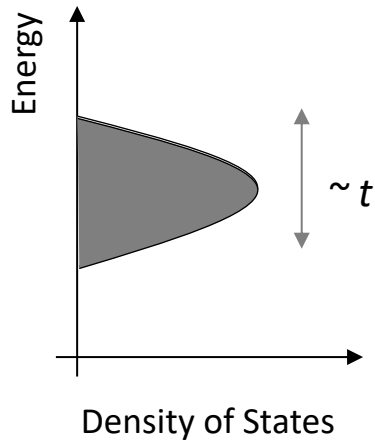
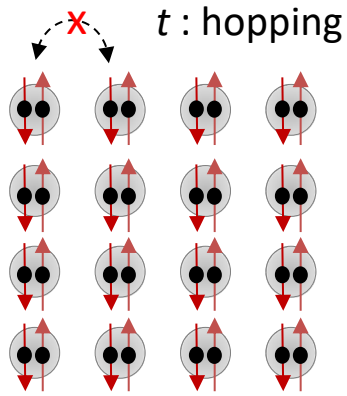
▶ ↓↓ Cooper pairs condense at $T_c^{A_2} = T_c - \lambda^{A_2} B$

$$\lambda^{A_1} \approx \left| \frac{\gamma \hbar}{2} \right| \left(\frac{k_B T_c}{E_f} \right)$$

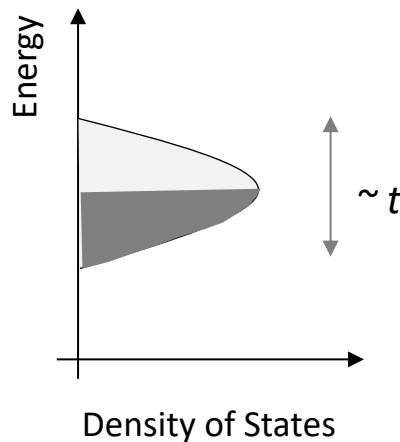
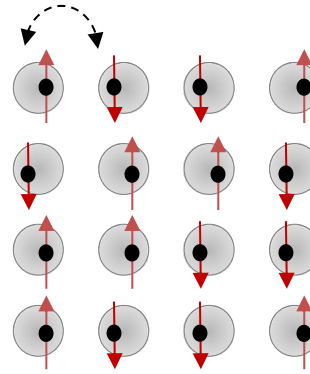
Ambegaokar and Mermin (1973)



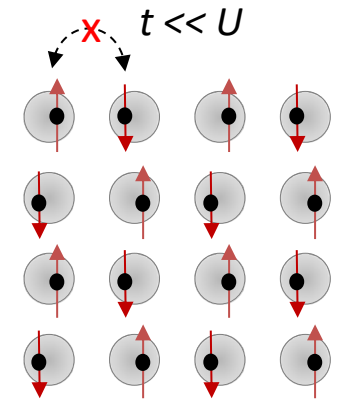
Mott Insulator



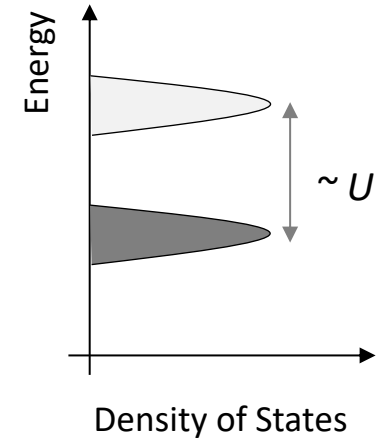
Insulator



Conductor



U : Coulomb interaction



Mott Insulator

Mott Insulator and Magnetism

The Mott insulators can further be correlated, considering the exchange interaction of localized electrons.

Anti-Ferromagnetic Mott Insulators are more common, as tightly localized electrons/holes prefer for anti-ferromagnetic spin coupling with neighbors.

However, ferromagnetic Mott Insulators are also possible for more extended Wannier orbitals.

Examples: YTiO_3 , $\text{Lu}_2\text{V}_2\text{O}_7$, $\text{Ba}_2\text{NaOsO}_6$...

PRL 99, 016404 (2007)

PHYSICAL REVIEW LETTERS

week ending
6 JULY 2007

Ferromagnetism in the Mott Insulator $\text{Ba}_2\text{NaOsO}_6$

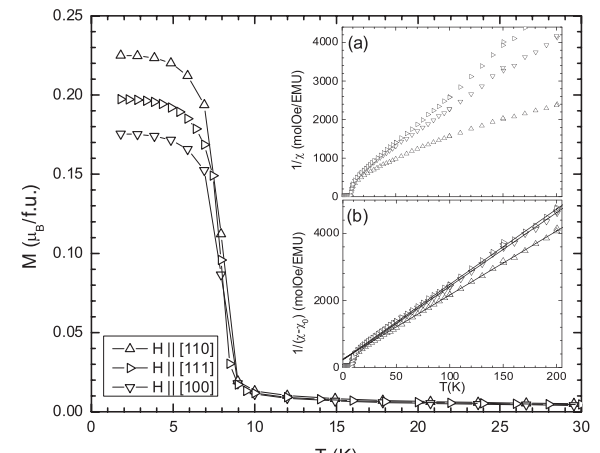
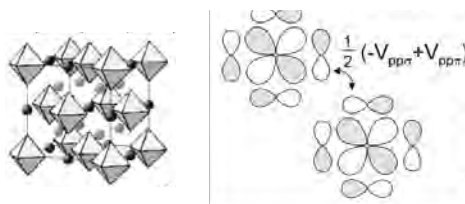
A. S. Erickson,¹ S. Misra,² G. J. Miller,² R. R. Gupta,³ Z. Schlesinger,³ W. A. Harrison,¹ J. M. Kim,¹ and I. R. Fisher¹

¹Department of Applied Physics and Geballe Laboratory for Advanced Materials, Stanford University, California 94305, USA

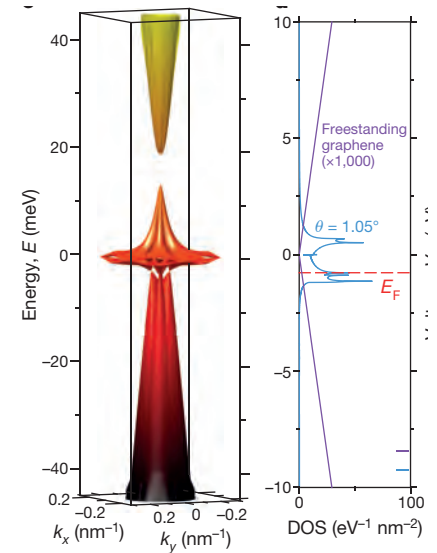
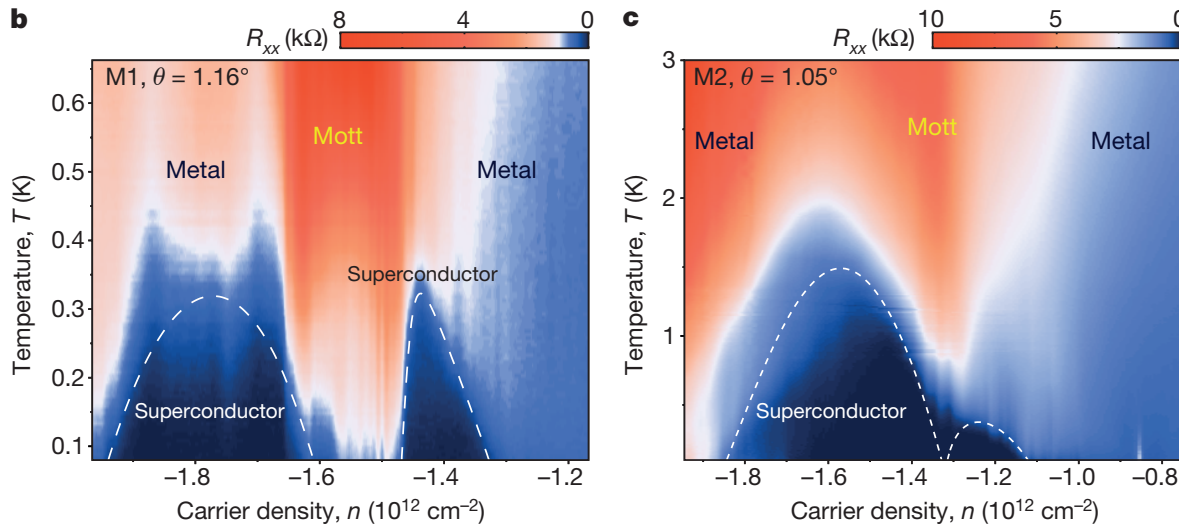
²Department of Chemistry and Ames Laboratory, Iowa State University, Ames, Iowa 50011-2300, USA

³Department of Physics, University of California, Santa Cruz, California 95064, USA

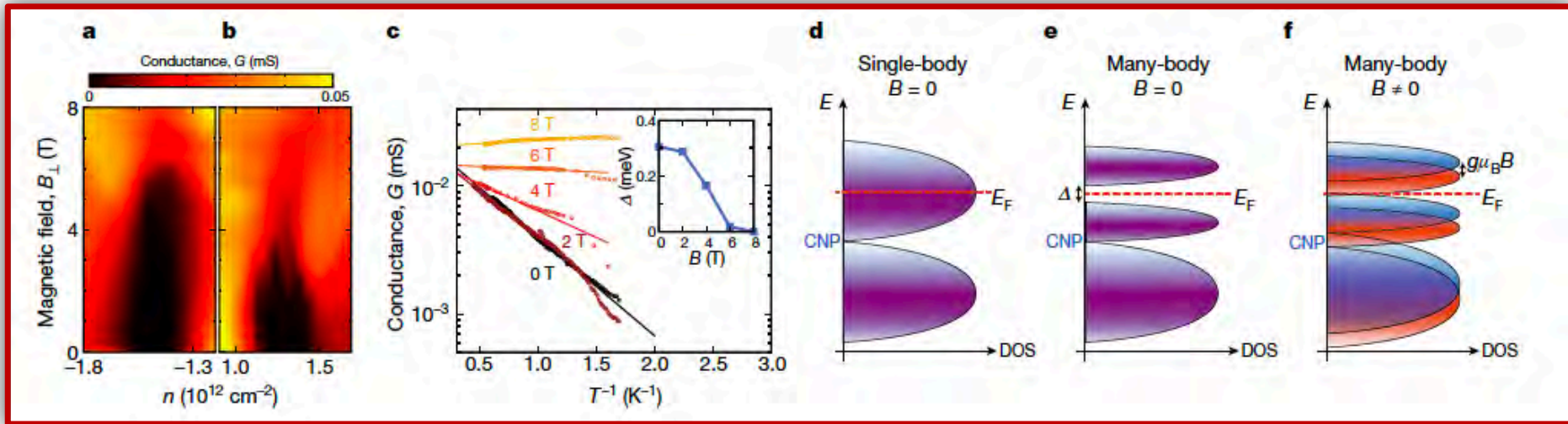
(Received 29 September 2006; published 6 July 2007)



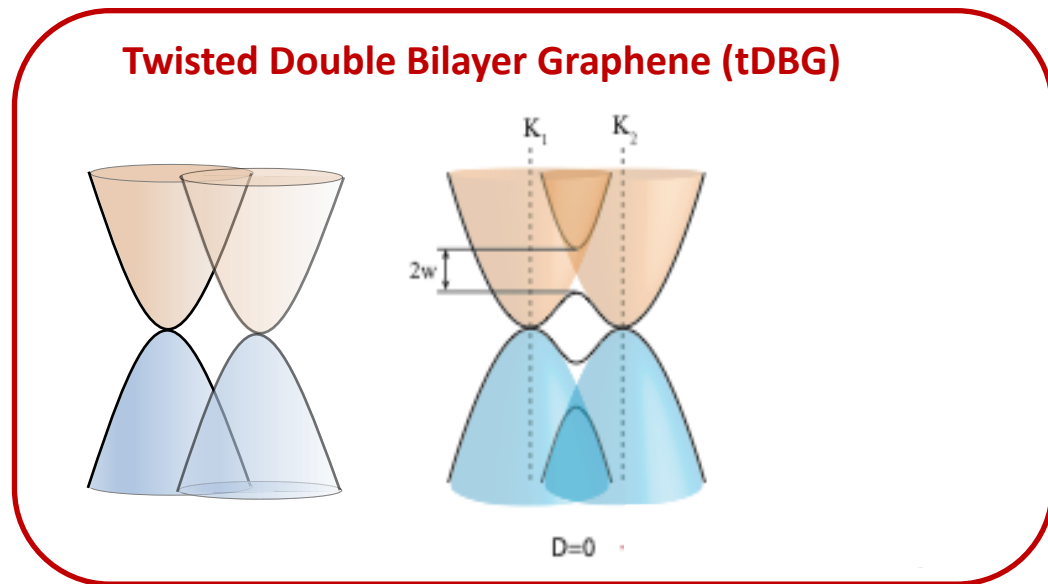
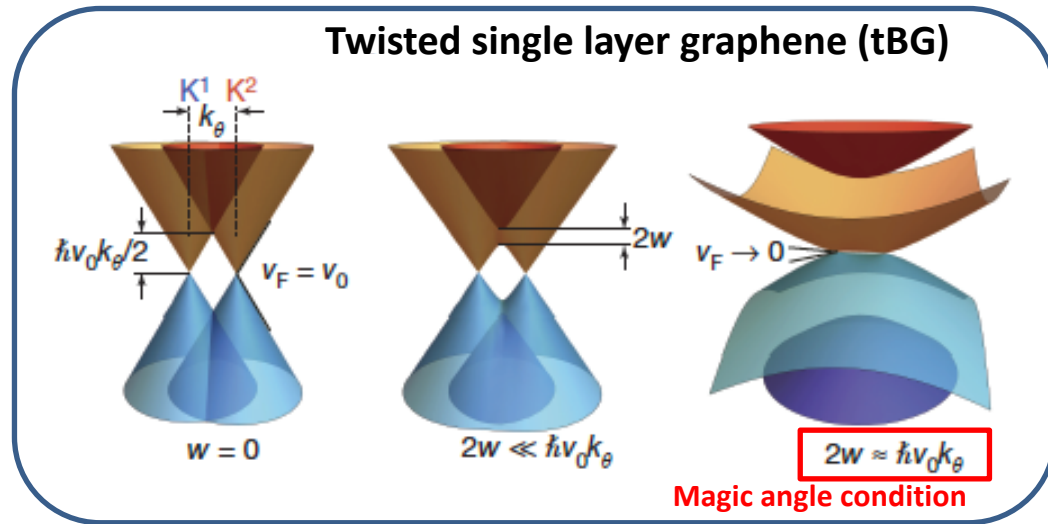
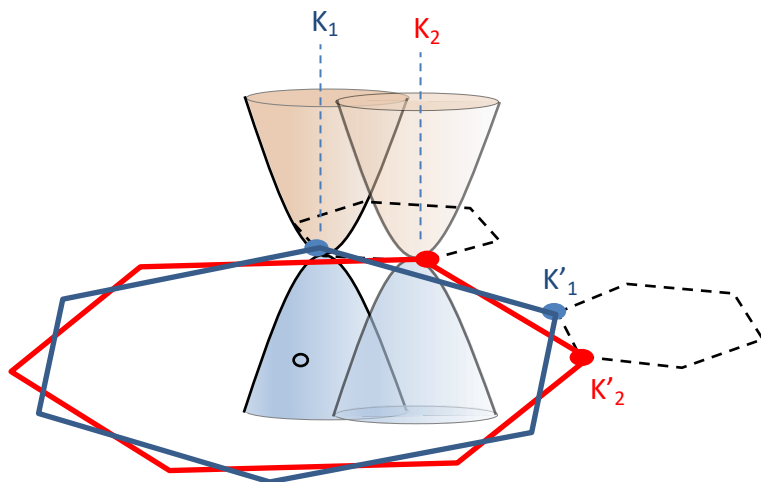
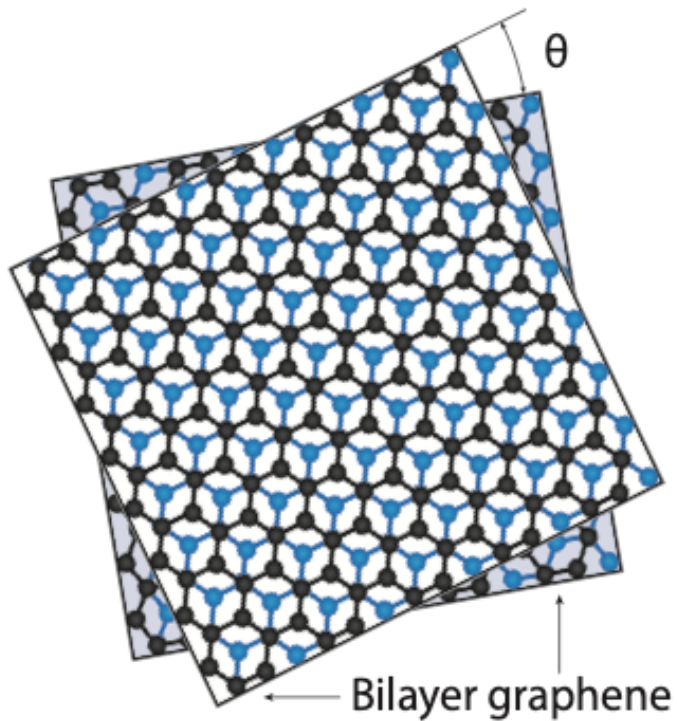
Correlated Quantum State in Twisted Graphene Bilayer



Spin unpolarized Mott Insulators (?)



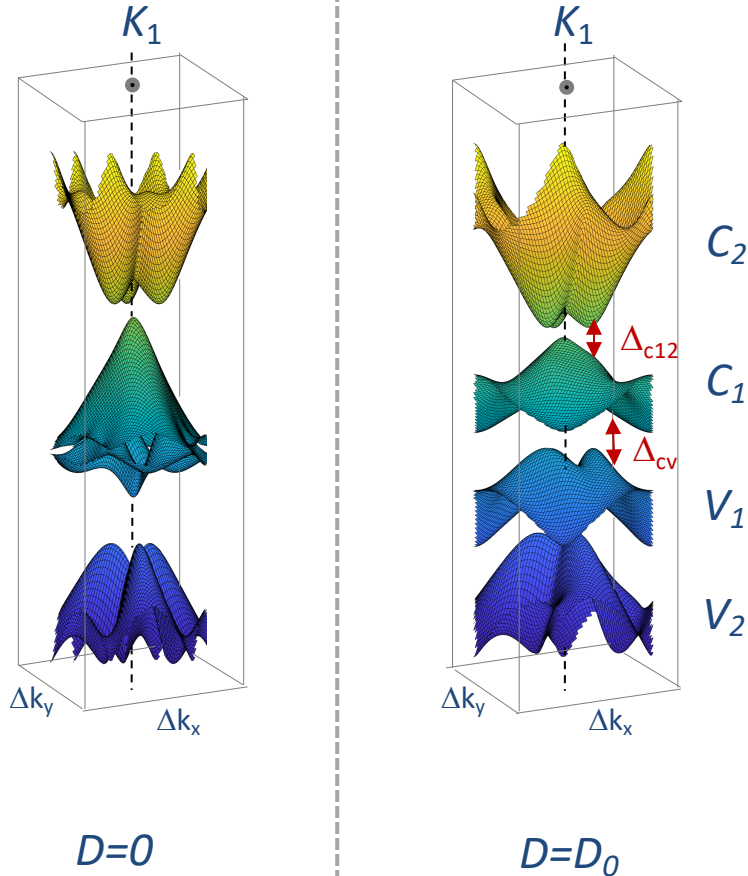
Twisted Double Bilayer Graphene



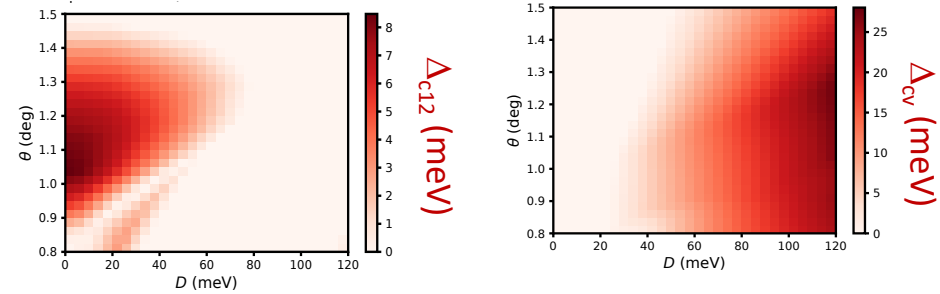
Gate tunable flat bands, no exact angle control needed!

Twisted Double Bilayer Graphene: Tunability

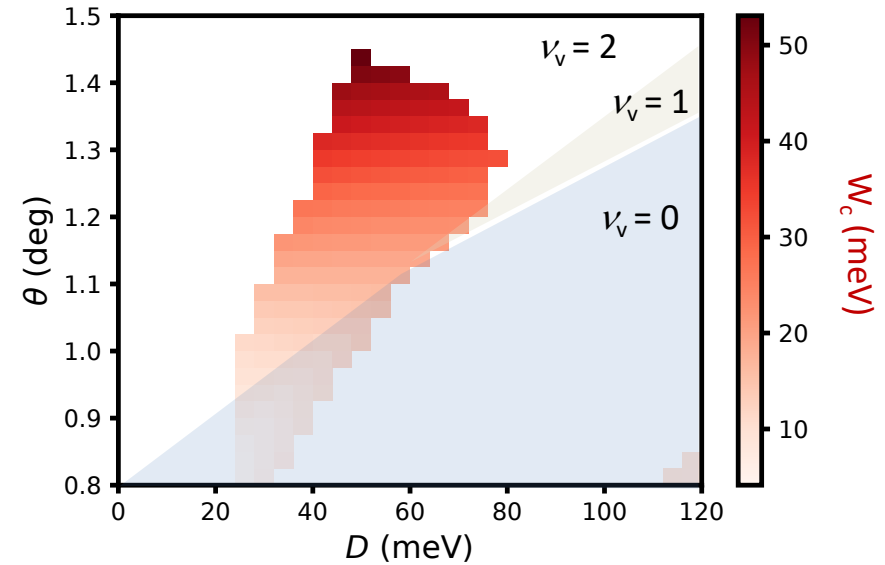
Tight binding with effective Wannier orbits



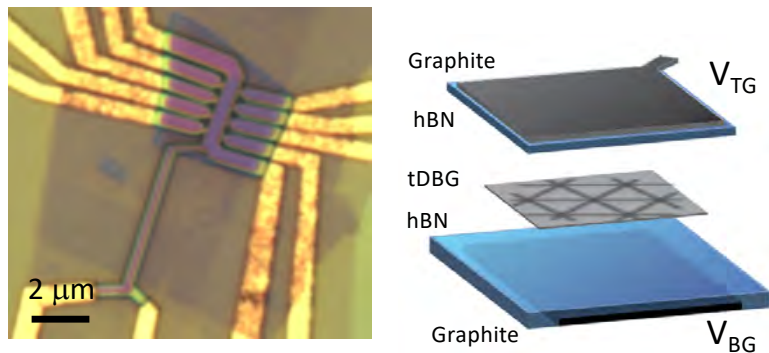
Band Gaps



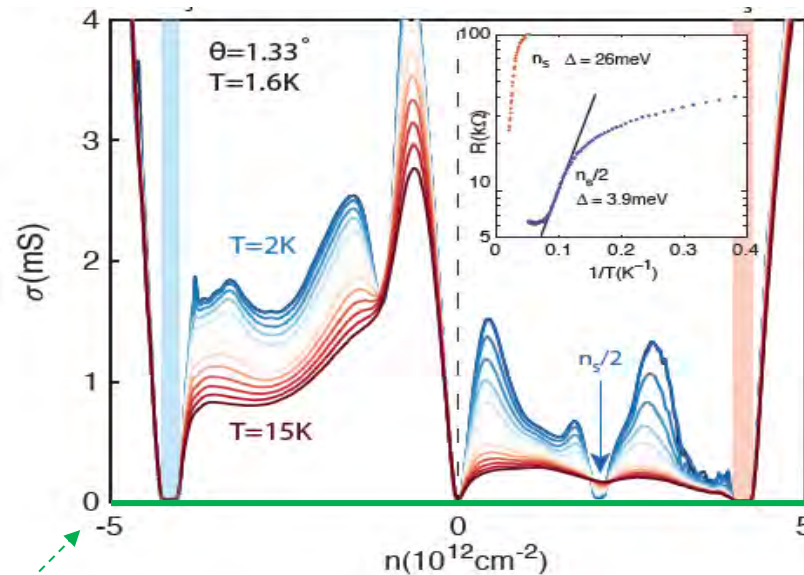
Isolated Conduction band width



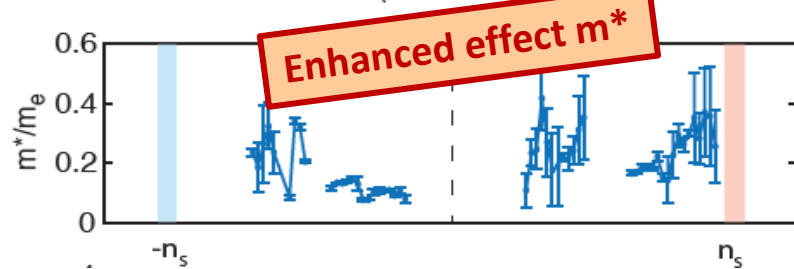
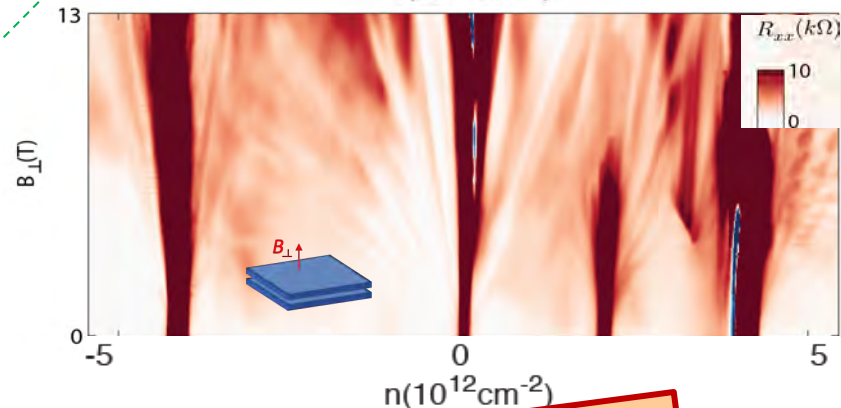
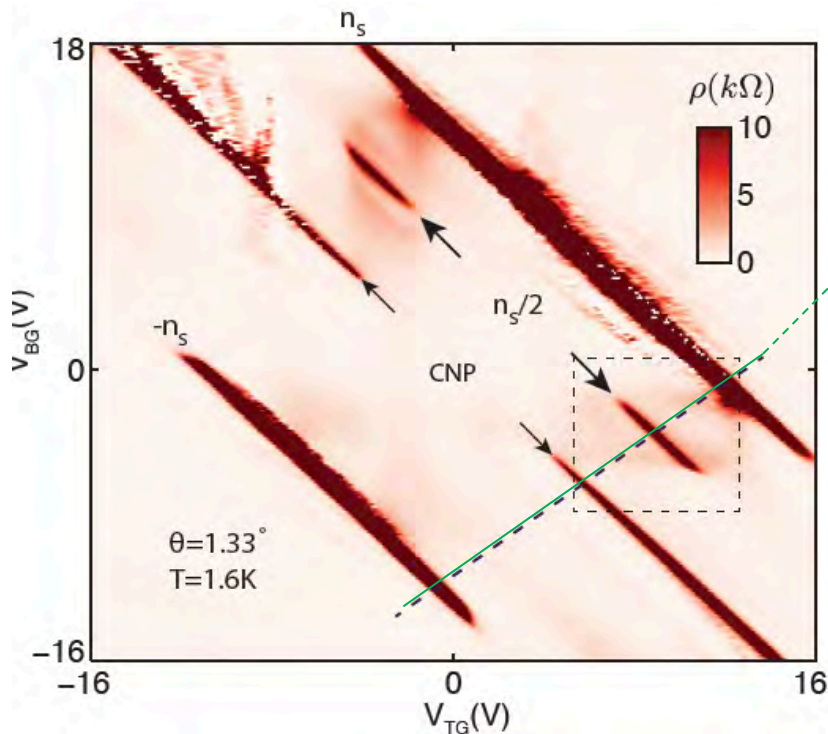
Mott Insulators in tDBG: $\theta = 1.33^\circ$



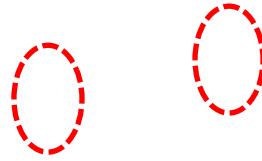
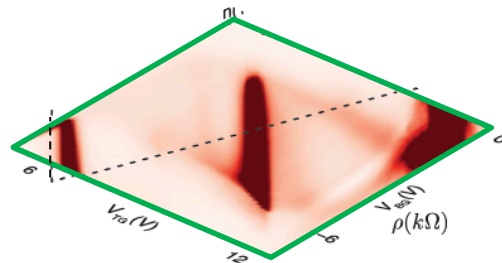
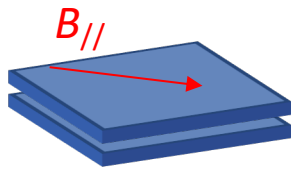
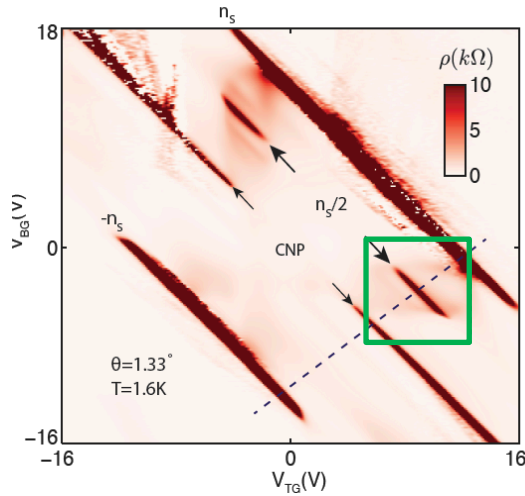
Temperature dependent 2-p conductance



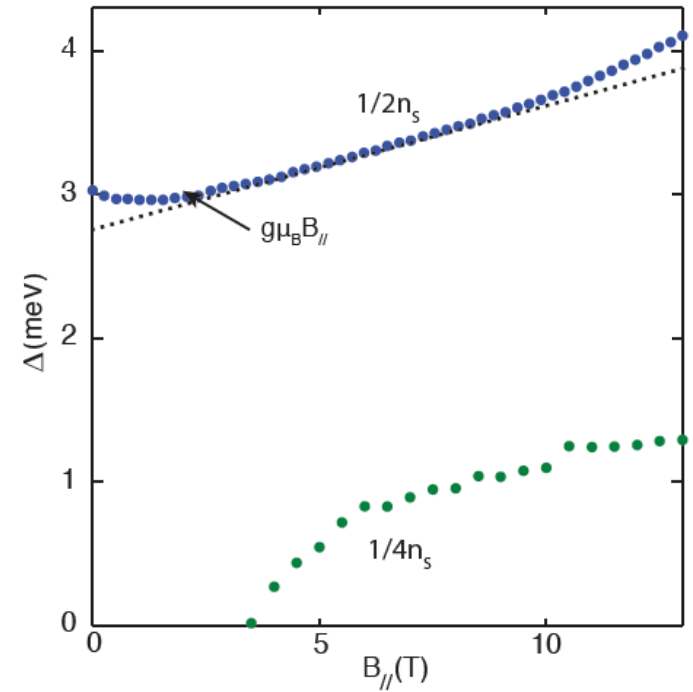
Top and bottom Gate dependent 4-terminal ρ



Ferromagnetic Mott Insulators in tDBG $\theta = 1.33^\circ$



- $n_s/4$ & $3n_s/4$ gaps appear at finite $B_{||}$
- $n_s/2$ states become stronger

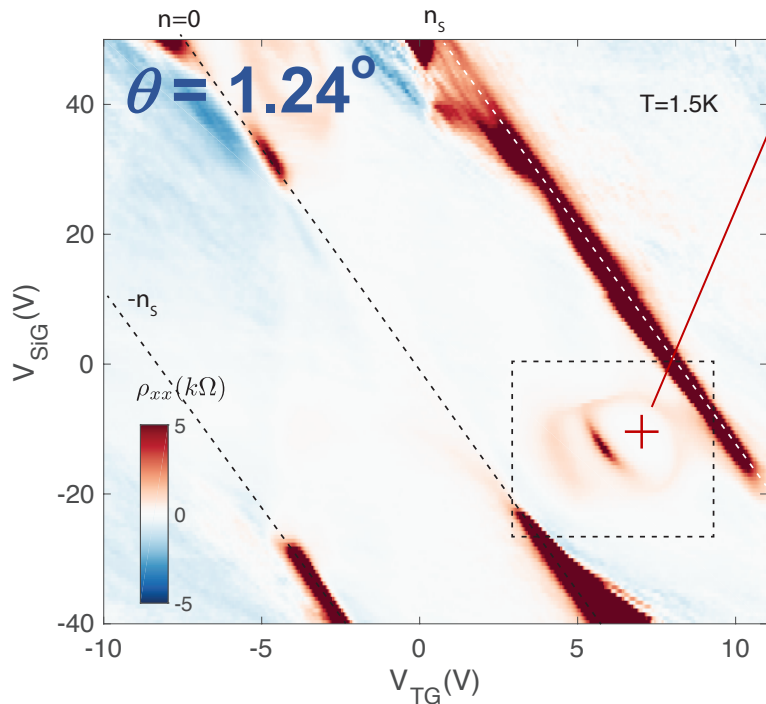
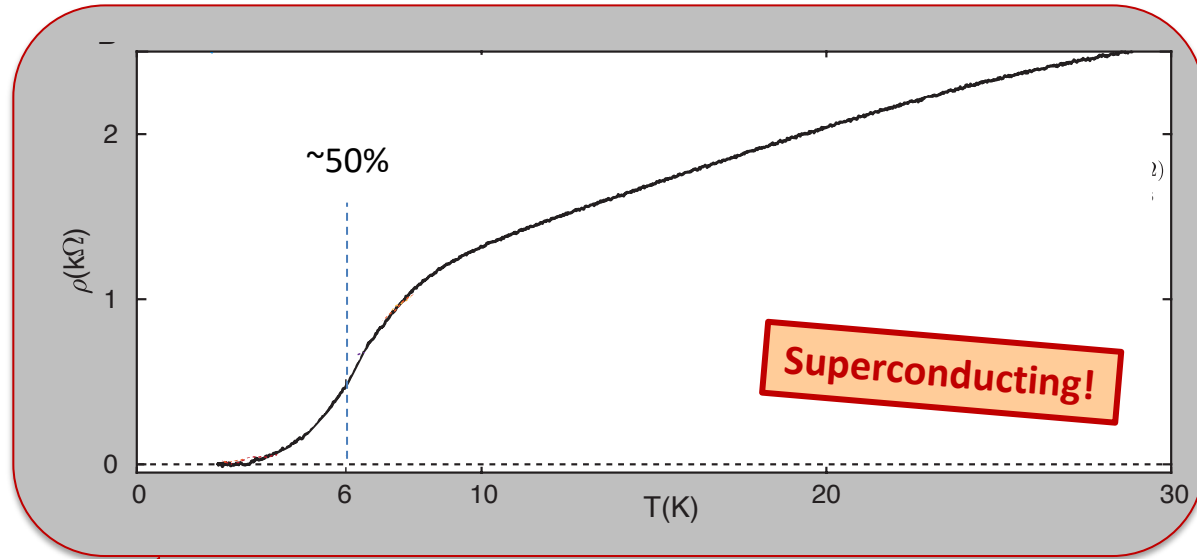
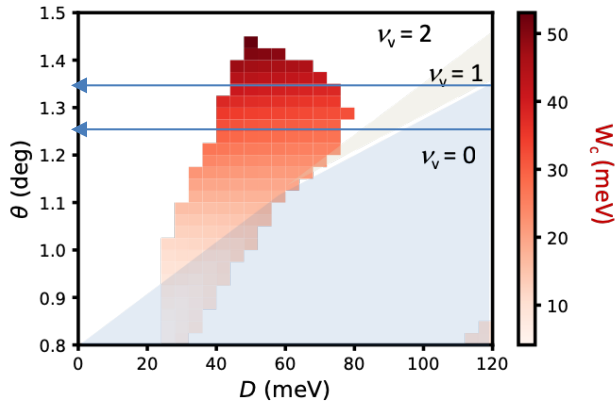


- Gap increases with $B_{||}$
- $g \approx 2$

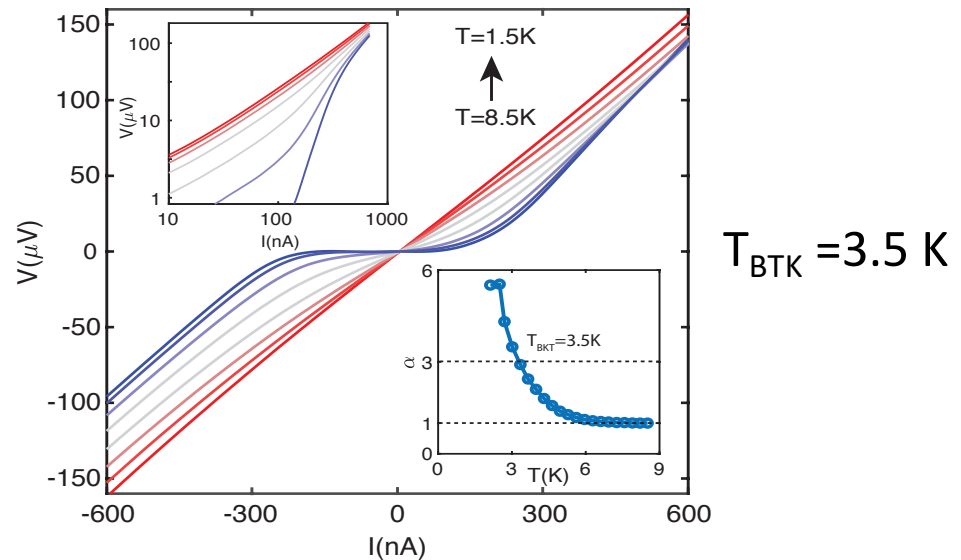
Spin polarized Mott State!

Superconductivity in tDBG

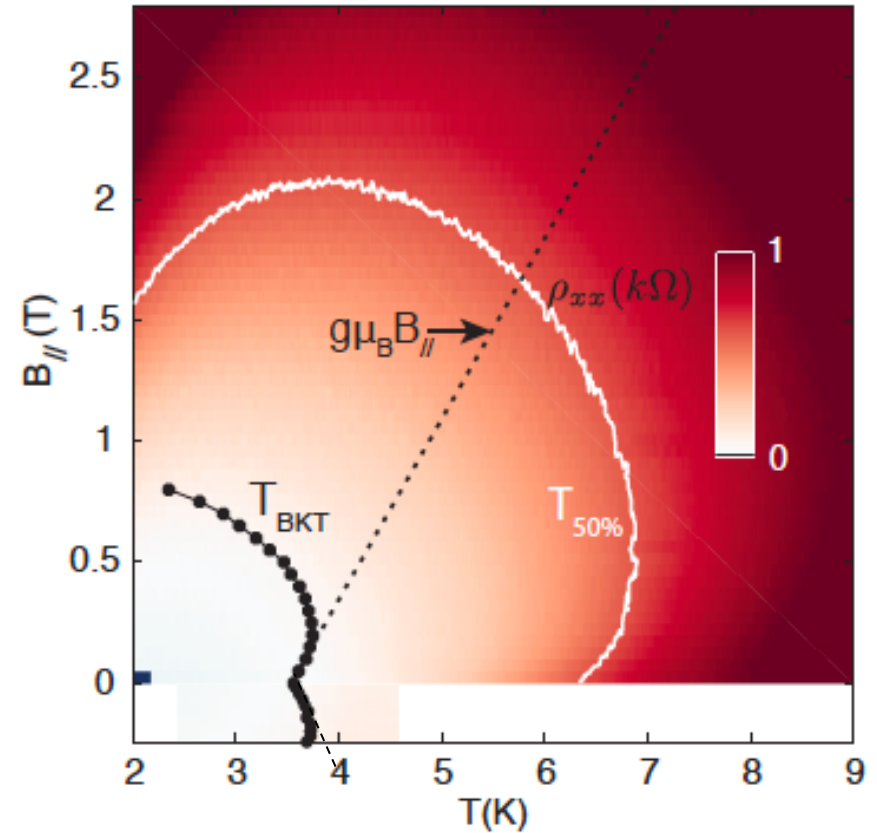
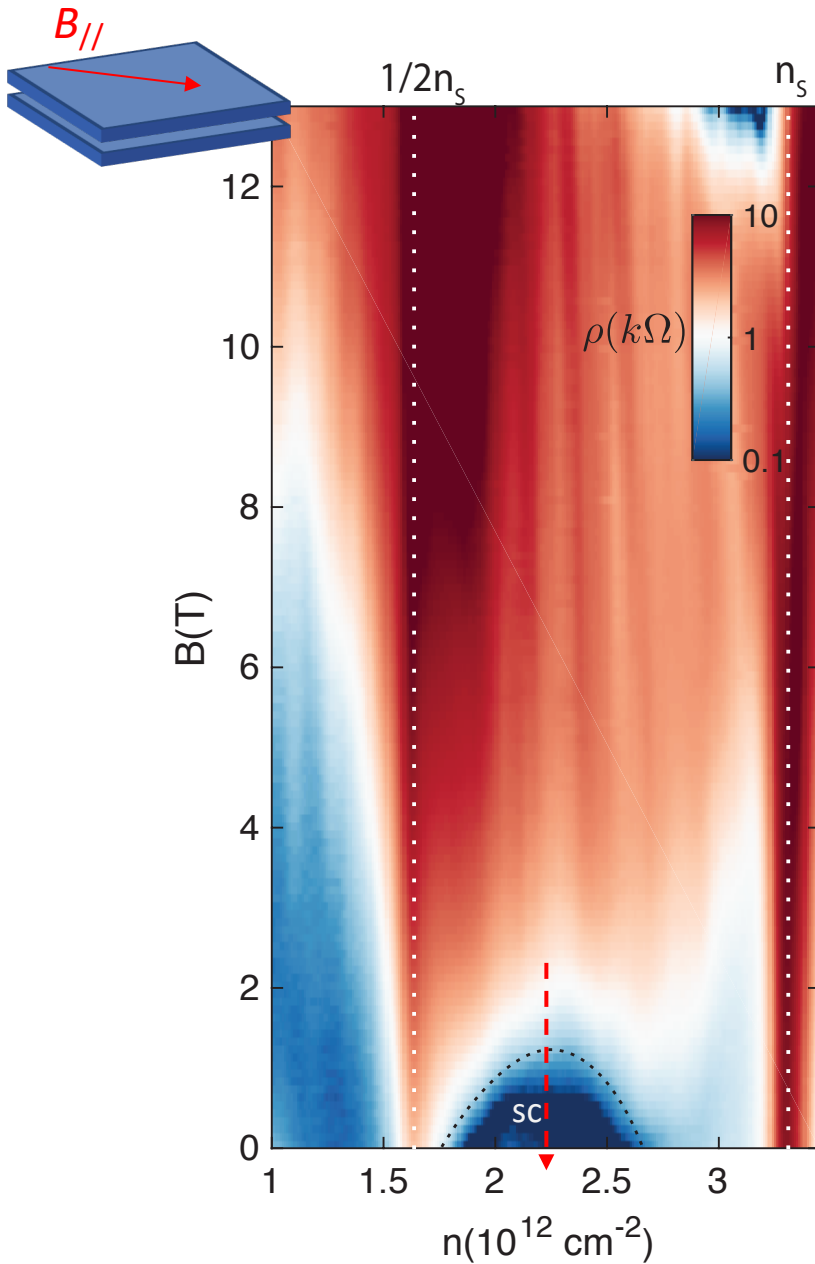
Isolated Conduction band width



I-V characteristics: BTK Transition



Parallel Magnetic Field Dependent SC



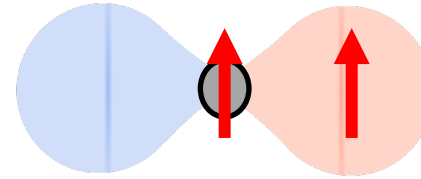
Superconducting state is enhanced by low magnetic field!

Equal-Spin p-wave Pairing: Superfluid ^3He A phase

A. J. Leggett (1972)

A-phase Superfluid ^3He

$$\Psi_{\text{pair}}(\mathbf{r}) =$$



p-wave pairing

VOLUME 53, NUMBER 20

PHYSICAL REVIEW LETTERS

12 NOVEMBER 1984

Superfluid ^3He in High Magnetic Fields: The Phase Diagram

D. C. Sagan,^(a) P. G. N. deVegvar, E. Polturak,^(b) L. Friedman,^(c) S.-S. Yan^(d)
E. L. Ziercher, and D. M. Lee

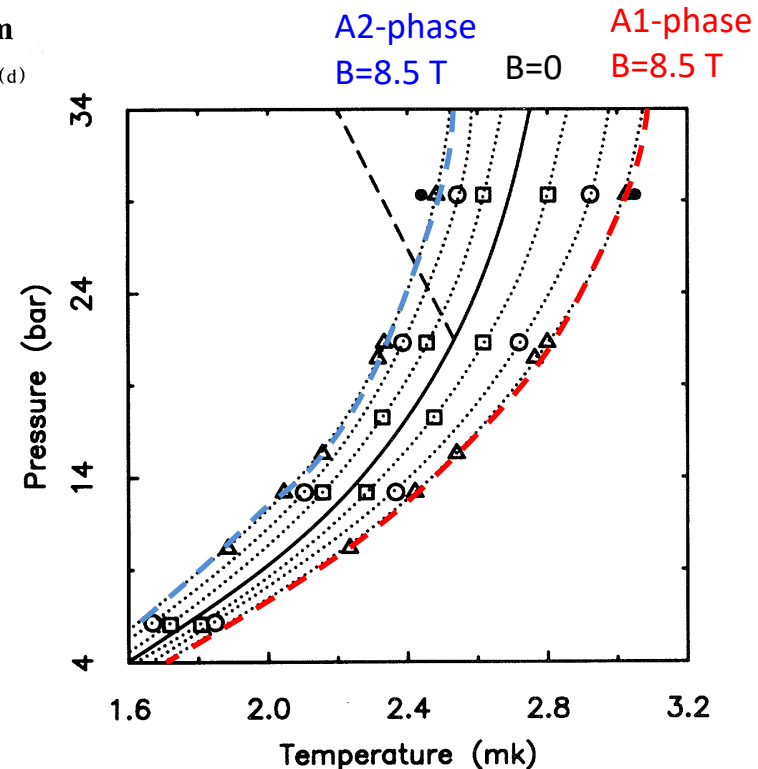
Laboratory of Atomic and Solid State Physics, Cornell University, Ithaca, New York 14853
(Received 30 July 1984)

▶ $\uparrow\uparrow$ Cooper pairs condense at $T_c^{A_1} = T_c + \lambda^{A_1} B$

▶ $\downarrow\downarrow$ Cooper pairs condense at $T_c^{A_2} = T_c - \lambda^{A_2} B$

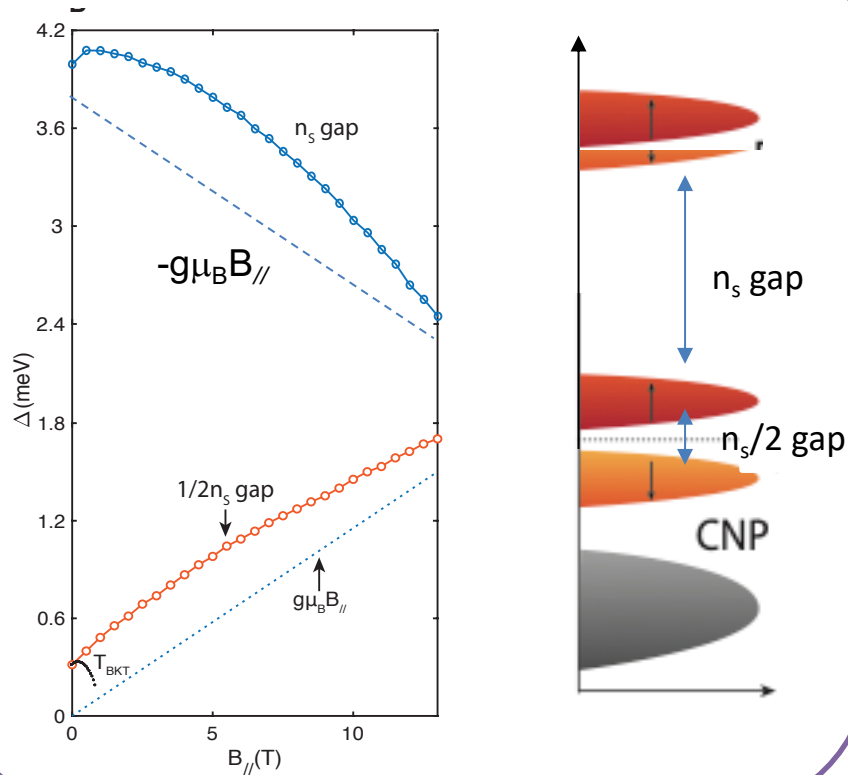
$$\lambda^{A_1} \approx \left| \frac{\gamma \hbar}{2} \right| \left(\frac{k_B T_c}{E_f} \right)$$

Ambegaokar and Mermin (1973)

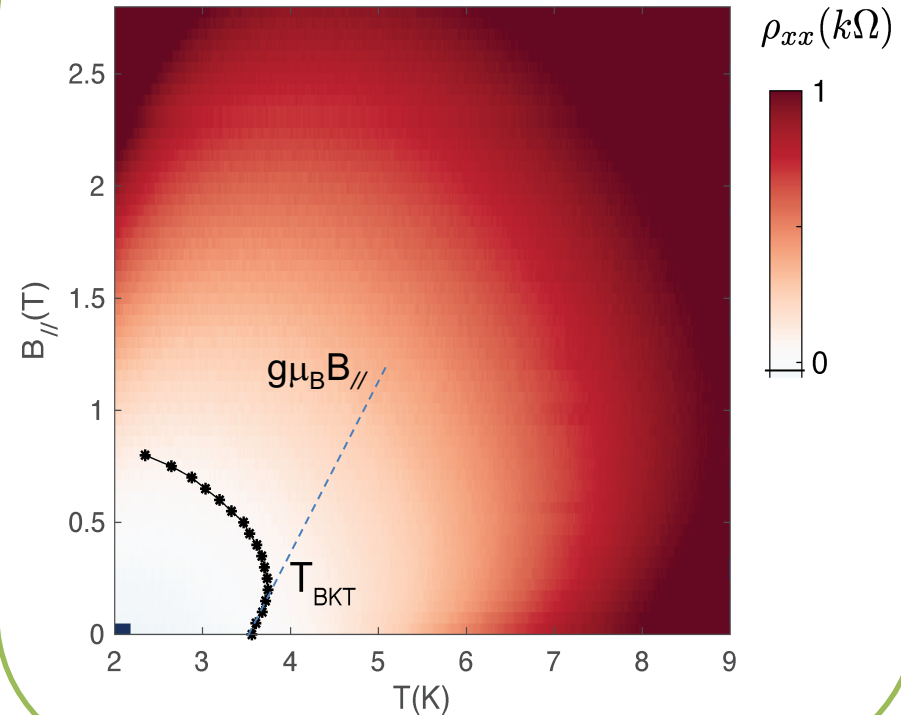


Ferromagnetic Superconductivity in tDBG

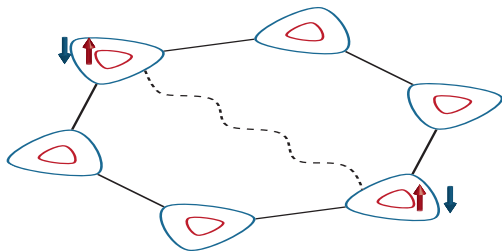
Spin-polarized Mott State



Spin-polarized SC State



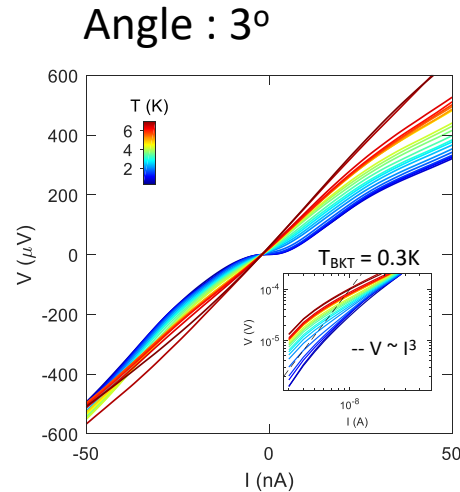
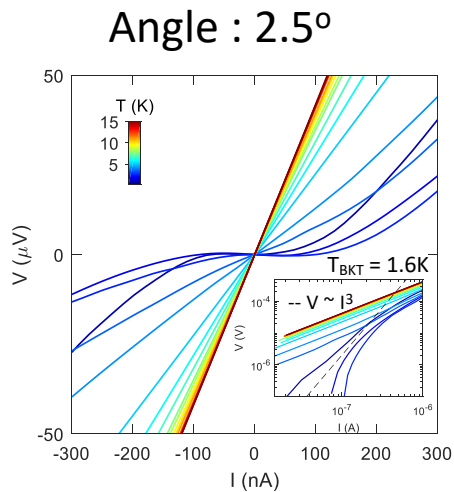
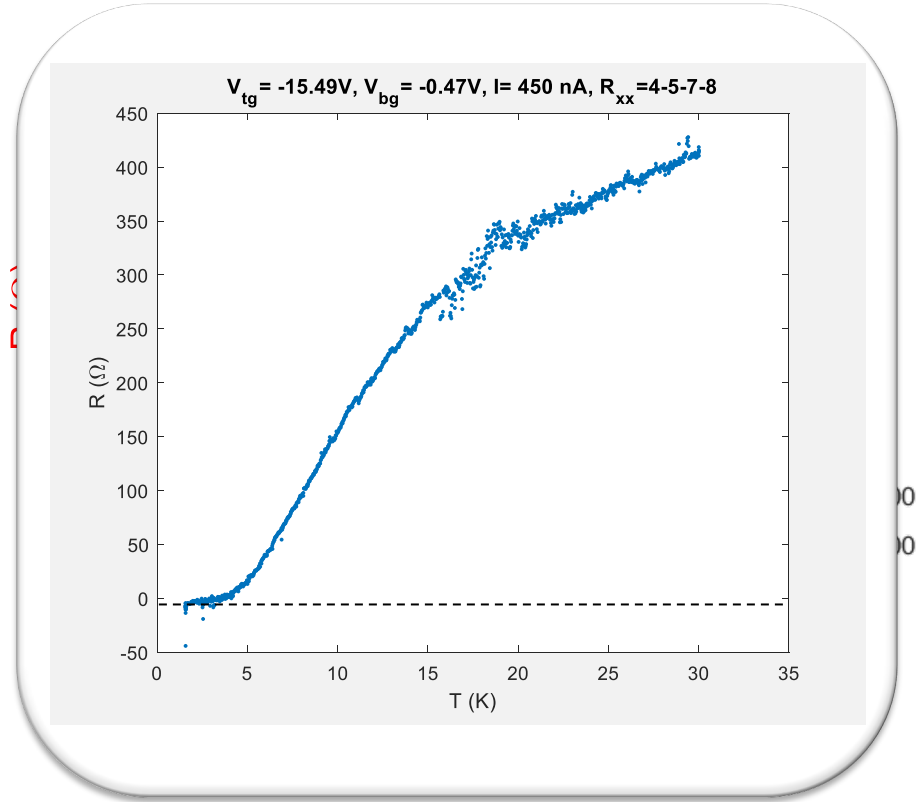
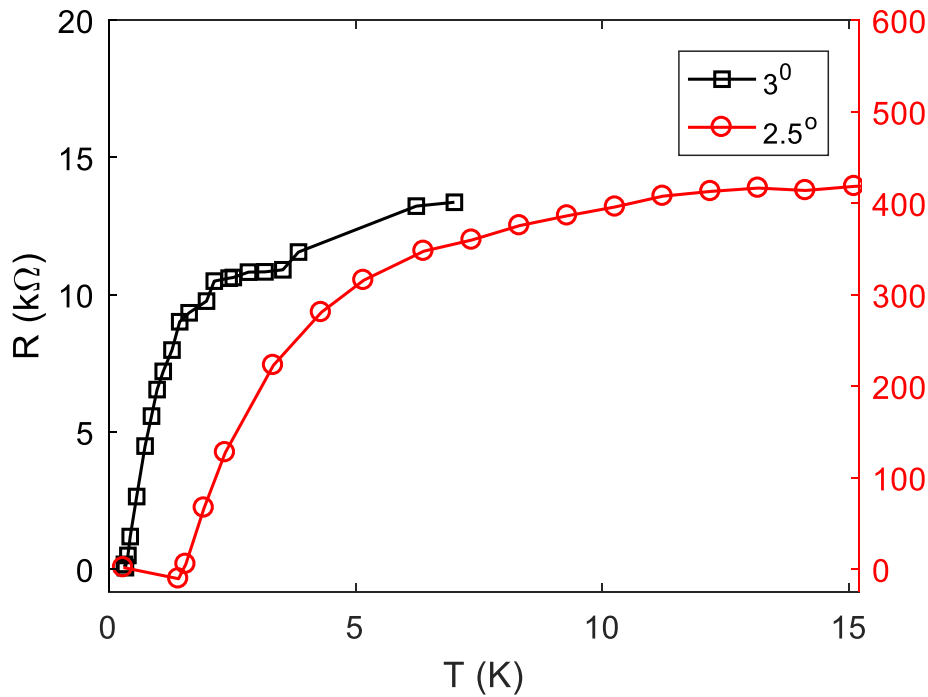
Cooper Pair: Spin triplet & Valley singlet



$$T_c(B) = T_c + aB - bB^2$$

$$a = 2\mu_B T_c \chi \frac{N'(\epsilon_F)}{N(\epsilon_F)} \ln \frac{\Lambda}{T_c}, \quad b = \frac{\mu_B^2}{T_c} \int_{\text{FS}} \sum_{\sigma=\pm} \frac{d\mathbf{k}}{\kappa} |\phi_{\mathbf{k}}|^2 (\hat{\mathbf{e}}_B \cdot \mathbf{g}_{\sigma,\mathbf{k}})^2$$

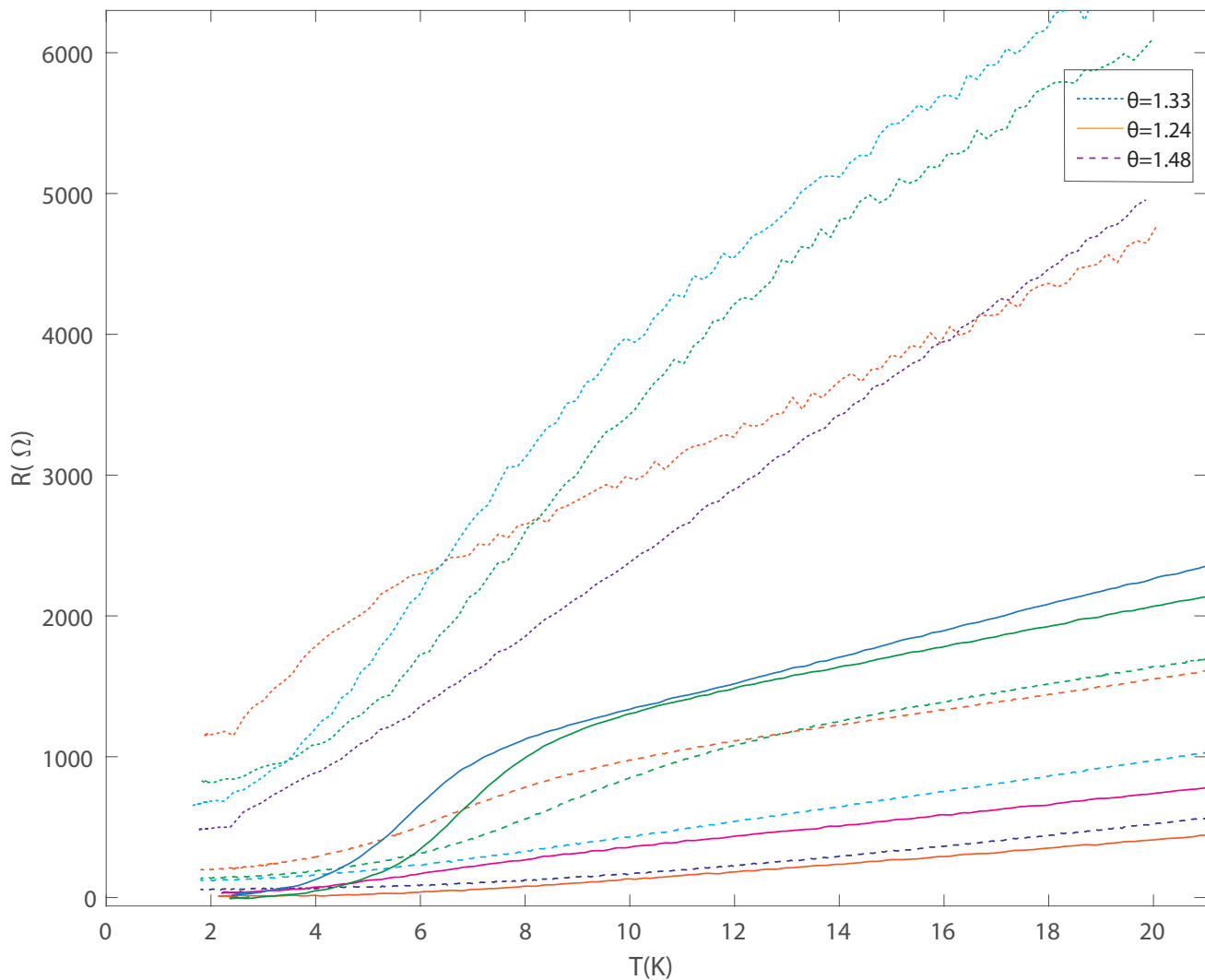
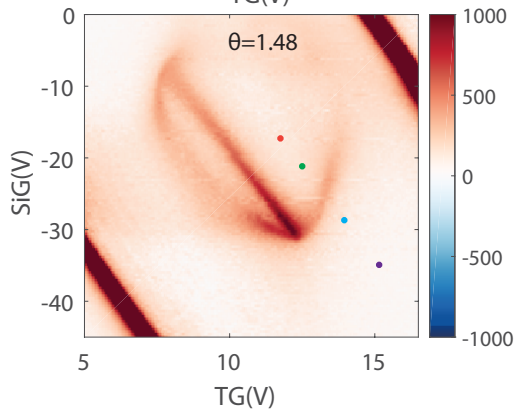
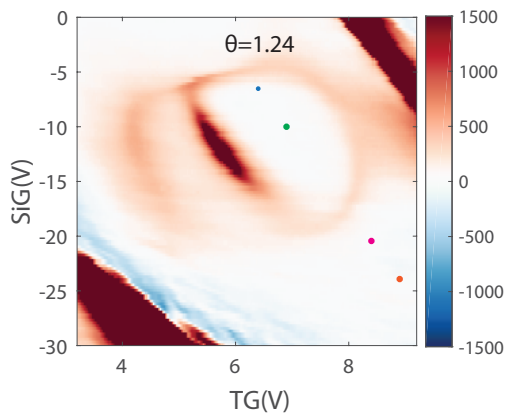
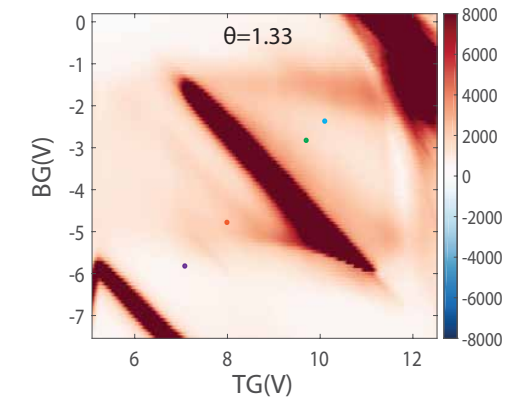
Superconducting Twisted bilayer WSe₂



~ 8 K
 Superconducting-like state $T_c \sim 0.3 - 3$ K
 has been realized in a wide angle range!

See also similar data in An *et al.*, arXiv:1907.03966

Superconducting Or Not Superconducting?

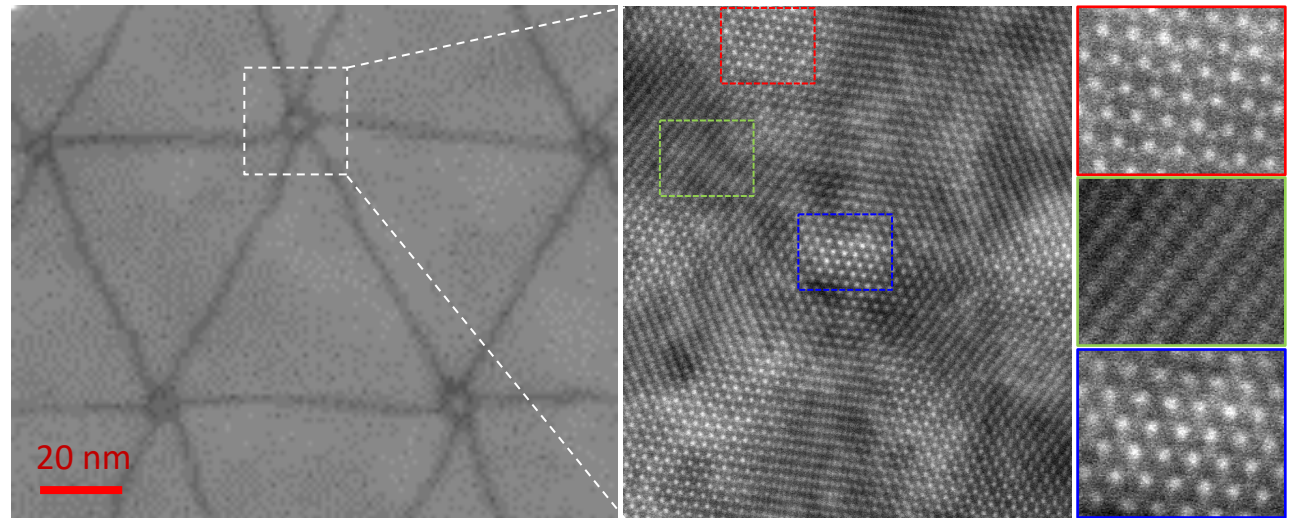


Atomic Registry in Domains and Boundaries

$\text{MoS}_2/\text{MoS}_2$

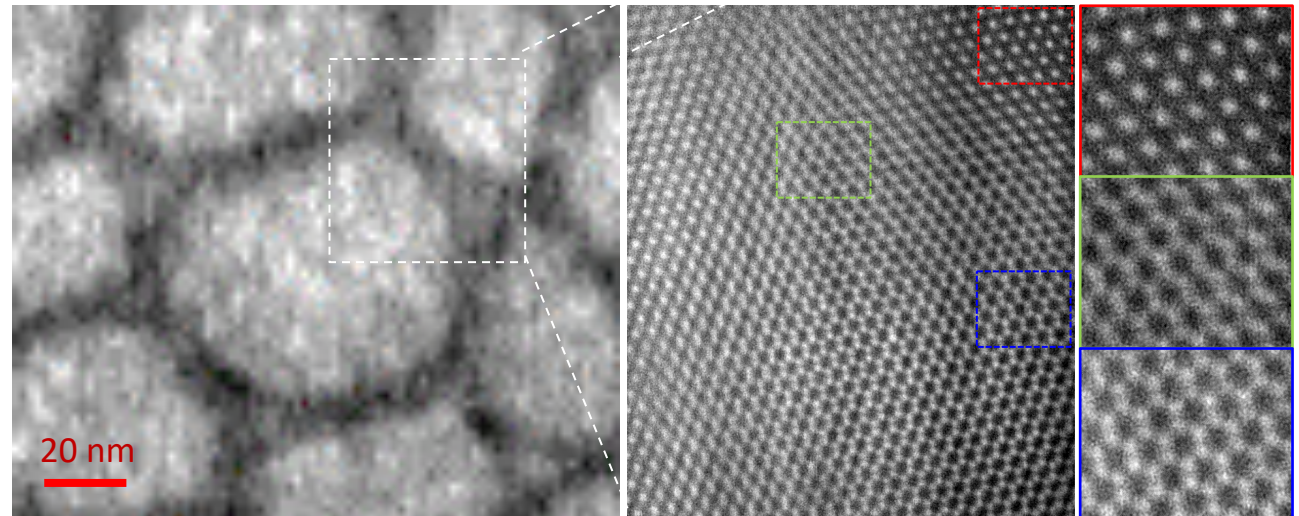
~ 0 degree

Circular AA domains where 6 domains (3 AB domains and 3 BA domains) meet each other



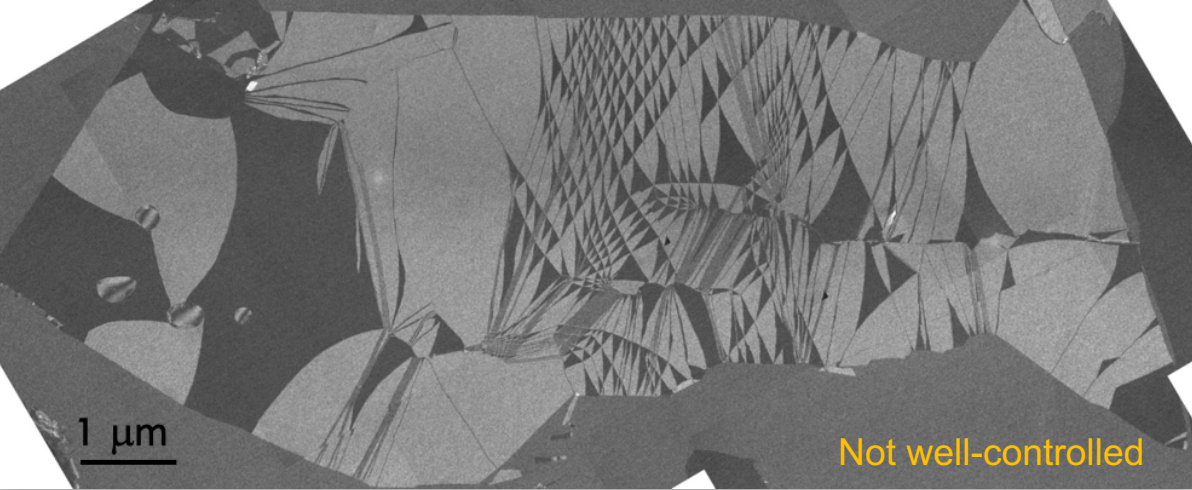
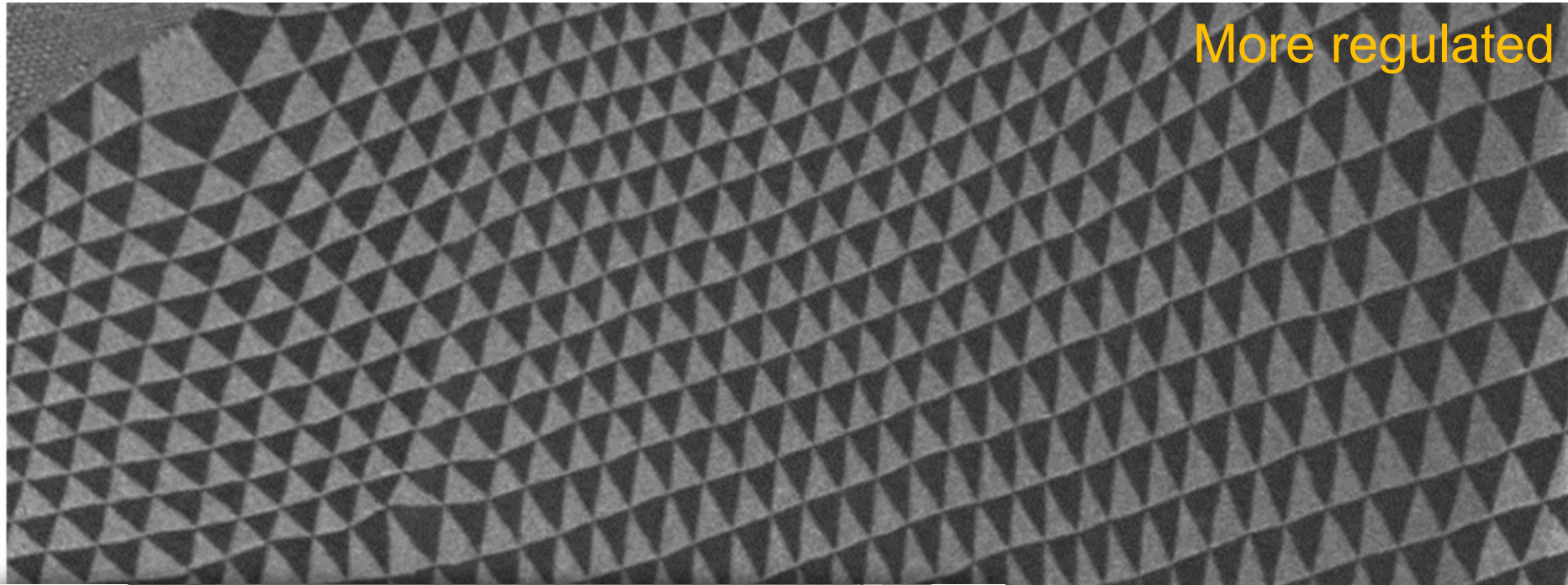
~ 180 degree

Triangular AB' and BA' domains where 3 domains (AA') meet each other.



Twisting Engineering of Moire Superlattice

Graphene/graphene 0.1-0.2deg



Summary and Outlook

- Spin polarized Mott gap state is realized in half-filled tDBL bands tuned by D .
- Quarter filled tDBT band can develop a spin polarized gap.
- Superconductivity appears near the half field states in 1.26 degree rotated tDBL.
- Superconductivity appeared in tDBL samples can be tuned by D and n .
- T_c enhanced with small in-plane magnetic fields.

Going Forward:

- What is the optimal T_c in tDBT?
- Will spin-polarized SC in tDBL exhibit topological superconductivity?